Master Thesis

ONE-LOOP AMPLITUDES IN PERTURBATIVE QUANTUM FIELD THEORY

Robbert Rietkerk

Supervisor: prof. dr. Eric Laenen

Nikhef Institute for Subatomic Physics

Institute for Theoretical Physics, Utrecht University

August 20, 2012

Thesis submitted for the degree of M.Sc.

Institute for Theoretical Physics, Utrecht University

Universiteit Utrecht

Nikhef Institute for Subatomic Physics

Abstract

We review methods for calculation of higher order corrections in perturbative quantum field theory. After laying the foundation with several traditional methods we turn to more recent developments. A particular method, proposed by Ossola, Papadopoulos and Pittau, reduces tensor integrals from one-loop diagrams with many external particles to known scalar integrals. This is achieved by a highly efficient algebraic algorithm, thereby opening the window to more precise predictions for collider processes. We describe the method and present an algebraic implementation in FORM.

In the field of soft corrections, some spectacular progress has been made as well. Processes can be calculated to all orders in perturbation theory through exponentiation of a certain set of diagrams. We investigate properties of such diagrams by applying the unitarity method.

Acknowledgements

I would like thank my supervisor professor Eric Laenen for guiding me on the journey that is called research. He inspires me with enthusiastic explanations and manages to ask just the right questions to push me forward.

Besides my supervisor, a number of other people also deserve thanks for their help. I thank Ioannis Malamos for giving me an introduction to his research and Domenico Bonocore for discussing topics of our mutual interest. I'm grateful to Jos Vermaseren and Jan Kuipers for answering my questions about FORM. Also Pierre Artoisenet and Damien George are much obliged for their readiness to help out with various problems. In particular I enjoyed discussions in front of the blackboard.

Thanks to Jory and Philipp for their companionship and help throughout the year and the rest of the theory group at Nikhef for providing such a pleasant environment. Also my fellow students in Utrecht provided enjoyable company, mostly during the first year of the masters. It has been great!

Finally, I thank my family for their love and support.

Contents

Chapter 1.

Introduction

One of the main quantities of interest in particle physics is the scattering cross-section, which describes the probability of interaction between particles. Quantum mechanics dictates that such probabilities are computed as squares of complex scattering amplitudes. Unfortunately not even the simplest scattering amplitude is known exact. Perturbation theory has become the established way to approximate results.

A beautiful tool in perturbation theory is the use of Feynman diagrams, a graphic visualization of terms in the series in powers of the coupling strength between interacting particles. The largest possible contribution to amplitudes come from tree diagrams. Higher order corrections are given by diagrams with loops.

While the computation of tree diagrams is well established, the one-loop diagrams are notoriously challenging. In the first place, loops give divergent contributions to the amplitude, which need to be properly handled by a renormalization procedure. It has first been shown to produce excellent results in the context of quantum electrodynamics. The correct prediction of the anomalous magnetic moment of the electron [1] is seen as one of the great successes of perturbation theory.

Quantum chromodynamics and the electroweak theory, on the other hand, give rise to much more diverse particle interactions. A big step forward was made in the late 1970s, when scalar integrals were computed for arbitrary masses [2] and non-scalar integrals were treated with Passarino-Veltman reduction [3].

In the mean time an alternative calculation method was constructed, which exploits unitarity of the scattering matrix [4]. This unitarity method allows to determine the absorptive (imaginary) part of an amplitude in a relatively simple manner. The dispersive (real) part of an amplitude can be reconstructed by means of dispersion relations [5].

Some processes, in particular many-particle scattering, remain highly challenging for practical reasons. The number of Feynman diagrams increases rapidly with the number of external particles, while the expressions for each of them become more and more lengthy.

One solution is to expand arbitrary one-loop integrals in terms of a basis of scalar one-loop integrals that are known analytically. The existence a finite basis is justified

by explicit tensor reduction and by the theorem that one needs up to four-point scalar integrals [6], directly related to the number of spacetime dimensions. The problem is then shifted to the determination of the coefficients in such an expansion.

The generalized unitarity method extracts these coefficients by cutting diagrams and relating their imaginary part to the discontinuities of scalar integrals from the basis [7]. Multiple cuttings are used to determine the coefficients of the box integrals efficiently. Massive virtual particles do pose a difficulty, although some special cases have been found [8].

The OPP reduction method is based on a similar expansion, but at the integrand level [9]. Determination of the coefficients is performed by evaluating the integrand at different loop momenta. In contrast to generalized unitarity, no information on the analytic structure of the amplitude is needed and it has no problem with massive particles. This feature makes a numerical implementation of the method feasible [10]. It has already been used to give next-to-leading order predictions for many-particle processes at colliders, such as the LHC [11].

In the area of soft corrections, exponentiation of amplitudes has been established in the eikonal approximation [12]. This powerful theorem allows the extraction of all-order information on the scattering amplitude from lower-order diagrams in the exponent. We investigate a way to quickly compute contributions to the exponent, making use of unitarity.

Chapter 2.

One-Loop Corrections

As we mentioned in the introduction, one-loop corrections in perturbation theory are not calculated without difficulties. Among them are the notorious divergences: infinite contributions to tree-level amplitudes.

In this chapter we show how to dimensionally regularize expressions in the context of quantum electrodynamics. The one-loop corrections to the three standard Feynman diagrams are the vacuum polarization, the electron self-energy and the vertex correction. We give the full results to these diagrams, including in particular the finite parts.

The last section focuses on the renormalization procedure, used to render the theory finite. In particular we introduce the renormalization constant Ward identities. Using our results for the one-loop corrections we show that QED is renormalizable to all orders.

2.1. Vacuum Polarization

The Lagrangian for QED is given by

$$\mathcal{L} = \bar{\psi}(i\not{\partial} - m)\psi - \tfrac{1}{4}(F_{\mu\nu})^2 - eA_\mu\bar{\psi}\gamma^\mu\psi - \tfrac{1}{2}\lambda(\partial_\mu A^\mu)^2\,. \tag{2.1}$$

This Lagrangian gives rise to three Feynman diagrams, namely the propagators for the electron and photon and the $e^+e^-\gamma$ vertex. We use the well-known Feynman rules used by Peskin and Schroeder in the Feynman gauge [13].

Let us turn to the quantum corrections. We start with the vacuum polarization diagram, see figure 2.1, which is given by

$$i\Pi^{\mu\nu}(k) = (-ie)^2(-1)\int\frac{d^dq}{(2\pi)^d}\mathrm{tr}\left[\gamma^\mu\frac{i(\not{q}+m)}{q^2-m^2+i\epsilon}\gamma^\nu\frac{i(\not{q}+\not{k}+m)}{(q+k)^2-m^2+i\epsilon}\right]. \tag{2.2}$$

Counting powers of the loop momentum, we find that it contains logarithmic and quadratic divergences. We shall assume for the moment that $k^2 < 4m^2$, so that the fermions in the loop are necessarily virtual. The final result can then be analytically continued to higher photon momenta, including the process of creating two real fermions.

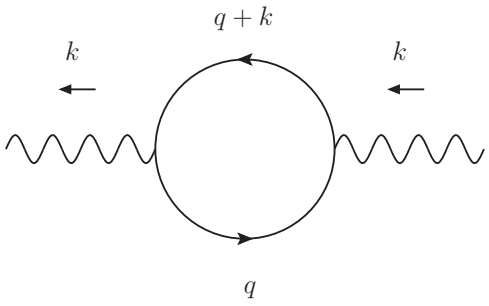

Figure 2.1.: Vacuum polarization: one-loop correction to the photon propagator.

Calculation of the integral over q is performed in several steps. First, one applies the Feynman parameter trick (A.28) to combine the two denominators. Next, one completes the square in the denominator, shifts the loop momentum to $l = q + xk$ and defines $M^2 = m^2 - x(1-x)k^2$. Taking the trace is done with the aid of (A.8)-(A.10). The result contains powers of the loop momentum in the numerator. Terms linear in l vanish according to (A.23), while terms containing $l^\mu l^\nu$ become proportional to $l^2\eta^{\mu\nu}$ after symmetric integration (A.24). The latter can be further simplified with (A.26). The result is remarkably simplified

$$i\Pi^{\mu\nu}(k) = -8e^2 \int_0^1 dx \int \frac{d^dl}{(2\pi)^d} \frac{k^2\eta^{\mu\nu} - k^\mu k^\nu}{(l^2 - M^2 + i\epsilon)^2} \,. \tag{2.3}$$

Let us separate the tensor structure from a scalar prefactor

$$i\Pi^{\mu\nu}(k) = i\Pi(k^2)(k^2\eta^{\mu\nu} - k^\mu k^\nu) \,, \tag{2.4}$$

thereby defining

$$\Pi(k^2) = 8ie^2 \int_0^1 dx\, x(1-x) \int \frac{d^dl}{(2\pi)^d} \frac{1}{(l^2 - M^2 + i\epsilon)^2} \,. \tag{2.5}$$

Observe that the vacuum polarization in this form explicitly satisfies $k_\mu \Pi^{\mu\nu} = 0$. Actually this must be true on general grounds. As a direct consequence of the gauge invariance of the Lagrangian there exists a Ward identity, which states that a general amplitude with an external photon carrying momentum k satisfies $k_\mu \mathcal{M}^\mu(k) = 0$.

The d-dimensional momentum integral in $\Pi(k^2)$ is standard and we plug in the result from (A.21), which is given in terms of $d = 4 - 2\,\varepsilon$. Also we substitute the fine-structure constant $\alpha = e^2/(4\pi)$.

$$\Pi(k^2) = -i\frac{\alpha}{3\pi}(\mu^2)^{-\,\varepsilon} \left[\frac{1}{\varepsilon} - \gamma + \int_0^1 dx\, 6x(x-1) \log\left(\frac{M^2}{4\pi\mu^2} \right) \right] \,. \tag{2.6}$$

Trivial integration over x-independent terms has been carried out. Let us remind that $M^2 = m^2 - x(1-x)k^2$. The factor $(\mu^2)^{-\,\varepsilon}$ serves to give the expression a correct mass

dimension away from $d = 4$. We have now found the correct pole structure of the first order vacuum polarization. What is left to do is to determine explicitly the finite part.

Feynman Parameter Integral

Consider the last term between the brackets in (2.6),

$$\int_0^1 dx\, 6x(x-1)\log\left(\frac{m^2 - x(1-x)k^2}{4\pi\mu^2}\right). \tag{2.7}$$

The integral is well defined because the argument of the logarithm is positive for all values of x thanks to our assumption $k^2 < 4m^2$. Let's define the ratio

$$r := \frac{k^2}{4m^2}, \tag{2.8}$$

and assume further that $r \neq 0$ so that the logarithm is x-dependent. The trivial case $r = 0$ will be treated separately. One way to solve the integral is to factorize the argument of the logarithm, split into a sum of logarithms, shift integration variable if necessary and finally apply partial integration to terms of the form $\int x^n \log(x)$.

Here we go. Factorizing the argument of the logarithm gives $k^2/(4\pi\mu^2) \cdot (x - x_+) \cdot (x - x_-)$, with $x_\pm = \frac{1}{2}(1 \pm \beta)$ and

$$\beta := \sqrt{1 - 1/r}\,. \tag{2.9}$$

Splitting the logarithm one obtains three terms. The first is simply $\log(4\pi\mu^2/k^2)$. The other two terms are

$$\begin{aligned}
&\int_0^1 dx\, 6x(x-1)\log(x - x_+) + \{x_+ \to x_-\} \\
&= \frac{5}{6} + 2x_+(1-x_+) - \log(1-x_+) + (3-2x_+)x_+^2 \log\left(\frac{1-x_+}{-x_+}\right) + \{x_+ \to x_-\} \\
&= \frac{5}{6} + 2x_+x_- - \log(x_-) + (1+2x_-)x_+^2 \log\left(\frac{-x_-}{x_+}\right) + \{x_+ \leftrightarrow x_-\} \\
&= \frac{5}{3} + 4x_+x_- - \log(x_+x_-) + [(1+2x_-)x_+^2 - (1+2x_+)x_-^2]\log\left(\frac{-x_-}{x_+}\right) \\
&= \frac{5}{3} + \frac{1}{r} + \log(4r) + \left(1 + \frac{1}{2r}\right)\beta \log\left(\frac{\beta-1}{\beta+1}\right).
\end{aligned} \tag{2.10}$$

In the second equality we made use of the observation that $1 - x_\pm = x_\mp$, meaning that $(1 - x_+) \to (1 - x_-)$ and $x_- \to x_+$ are equivalent substitutions.

In terms of r and β, the final result for the vacuum polarization is

$$\Pi(k^2) = -\frac{\alpha}{3\pi}(\mu^2)^{-\varepsilon}\left[\frac{1}{\varepsilon} - \gamma - \log\left(\frac{m^2}{4\pi\mu^2}\right) + \frac{5}{3} + \frac{1}{r} + \left(1+\frac{1}{2r}\right)\beta\,\log\left(\frac{\beta-1}{\beta+1}\right)\right]. \tag{2.11}$$

together with the tensor structure (2.4).

Analytic Continuation

The above solution was derived under the assumption $r < 1$ and $r \neq 0$. Therefor we must rederive a solution for a photon on mass shell and also see what happens for a photon with timelike or spacelike momentum. Moreover, we would also like to extend the solution to $r > 1$ in order to describe processes such as pair creation.

i) For $r = 0$ we must go back to the original Feynman parameter integral (2.7) and set $k^2 = 0$. The integral is then trivial and gives $-\log(m^2/(4\pi\mu^2))$, meaning that in this case we have only the first three terms of (2.11),

$$\Pi(0) = -\frac{\alpha}{3\pi}(\mu^2)^{-\varepsilon}\left[\frac{1}{\varepsilon} - \gamma - \log\left(\frac{m^2}{4\pi\mu^2}\right)\right]. \tag{2.12}$$

ii) For $0 < r < 1$ the argument of the logarithm becomes a complex number of unit norm $\exp(i\theta(r))$, with $\theta(r) = 2\arctan(\sqrt{r}/\sqrt{1-r}) = 2\arcsin(\sqrt{r})$. Both the square root β and logarithm become purely imaginary. Thus the last term in (2.11) remains real and is written as

$$-2\left(1+\frac{1}{2r}\right)\sqrt{\tfrac{1}{r}-1}\,\arcsin(\sqrt{r}) \quad \text{for } 0 < r < 1\,. \tag{2.13}$$

iii) For $r \geq 1$ the argument of the logarithm is negative and real, so it sits on a branch cut. Following the prescription (A.16) for analytic continuation we let $M^2 \to M^2 - i\epsilon$ and consequently $r \to r + i\epsilon$ (taking their definitions into account). This puts the logarithm just above the branch cut, which then contributes an additional $+i\pi$, making the last term equal to

$$\left(1+\frac{1}{2r}\right)\beta\left[\log\left(\frac{1-\beta}{1+\beta}\right) + i\pi\right] \quad \text{for } r \geq 1\,. \tag{2.14}$$

Only in this regime the vacuum polarization picks up an imaginary part. It happens because above the threshold $k^2 > 4m^2$ the photon can decay into a real electron-positron pair.

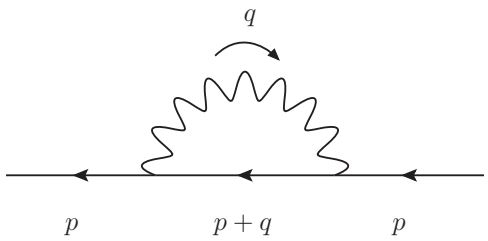

Figure 2.2.: Electron self-energy: one-loop correction to the electron propagator.

In conclusion, the vacuum polarization is given by

$$\Pi(k^2) = \Pi(0) - \frac{\alpha}{3\pi}(\mu^2)^{-\varepsilon}\left[\frac{5}{3} + \frac{1}{r} + \left(1 + \frac{1}{2r}\right)\beta\left(\log\left|\frac{\beta-1}{\beta+1}\right| + i\pi\theta(r-1)\right)\right] \quad (2.15)$$
$$\text{for} \quad r < 0,\ r \geq 1\,,$$

$$\Pi(k^2) = \Pi(0) - \frac{\alpha}{3\pi}(\mu^2)^{-\varepsilon}\left[\frac{5}{3} + \frac{1}{r} - 2\left(1 + \frac{1}{2r}\right)\sqrt{\tfrac{1}{r} - 1}\,\arcsin(\sqrt{r})\right] \quad (2.16)$$
$$\text{for} \quad 0 < r < 1\,.$$

Our result agrees with [14] upon translating $\varepsilon \to -\frac{1}{2}\varepsilon$, $\eta^{\mu\nu} \to -\eta^{\mu\nu}$ and $\gamma^\mu \to i\gamma^\mu$, and multiplying the whole diagram by i, to compensate for different normalization.

2.2. Electron Self-Energy

The electron self-energy diagram is shown in figure 2.2 and the corresponding expression is

$$-i\Sigma(p) = (-ie)^2 \int \frac{d^dq}{(2\pi)^d}\gamma^\mu \frac{i(\not{p} + \not{q} + m)}{(p+q)^2 - m^2 + i\epsilon}\gamma^\nu \frac{-i\eta_{\mu\nu}}{q^2 + i\epsilon}\,. \quad (2.17)$$

By power counting we infer that it contains both logarithmic and linear divergences. Let us assume that $p^2 < m^2$, such that the virtual particles are necessarily off-shell.

Computation of this integral is rather similar to the vacuum polarization. This time there is no trace of gamma matrices, though, but a contraction of the two outer matrices,

to which we apply (A.11) and (A.11). We compute

$$\begin{aligned}
-i\Sigma(p) &= -e^2 \int \frac{d^dq}{(2\pi)^d} \frac{(2-d)(\not{p}+\not{q})+dm}{((p+q)^2-m^2+i\epsilon)\,(q^2+i\epsilon)} \\
&= -e^2 \int \frac{d^dq}{(2\pi)^d} \int_0^1 dx\, \frac{(2-d)(\not{p}+\not{q})+dm}{[(q+xp)^2-x(m^2-(1-x)p^2))+i\epsilon]^2} \\
&= -e^2 \int_0^1 dx \int \frac{d^dl}{(2\pi)^d} \frac{(2-d)(\not{l}+(1-x)\not{p})+dm}{(l^2-M^2+i\epsilon)^2} \\
&= -e^2 \int_0^1 dx\, [(2-d)(1-x)\not{p}+dm] \int \frac{d^dl}{(2\pi)^d} \frac{1}{(l^2-M^2+i\epsilon)^2}\,,
\end{aligned} \tag{2.18}$$

where $M^2 = xm^2 - x(1-x)p^2$. Notice that M^2 is positive for all x with $p^2 < m^2$. The momentum integral is now a scalar one and is listed in (A.21). Substituting $d = 4-2\,\varepsilon$ and $\alpha = e^2/4\pi$,

$$\begin{aligned}
-i\Sigma(p) = i\frac{\alpha}{4\pi}\left[\frac{1}{\varepsilon} - \gamma - 1 - 2\int_0^1 dx(1-x)\log\left(\frac{M^2}{4\pi\mu^2}\right)\right]\not{p} \\
-i\frac{\alpha}{\pi}\left[\frac{1}{\varepsilon} - \gamma - \frac{1}{2} - \int_0^1 dx \log\left(\frac{M^2}{4\pi\mu^2}\right)\right] m\,.
\end{aligned} \tag{2.19}$$

These expressions give the correct divergent parts.

Calculation of the Feynman parameter integrals can be done in the way that was outlined in the previous subsection. By introducing the ratio

$$r := \frac{p^2}{m^2}\,, \tag{2.20}$$

we have $M^2 = xm^2(1-(1-x)r)$. We quote two intermediate results for $r \neq 0$,

$$\int_0^1 dx\, \log\left(\frac{M^2}{4\pi\mu^2}\right) = \left[-2 + \log\left(\frac{m^2}{4\pi\mu^2}\right) + \left(1-\frac{1}{r}\right)\log(1-r)\right]\,, \tag{2.21}$$

$$\int_0^1 dx\, x \log\left(\frac{M^2}{4\pi\mu^2}\right) = \frac{1}{2}\left[-2 + \log\left(\frac{m^2}{4\pi\mu^2}\right) + \frac{1}{r} + \left(1-\frac{1}{r}\right)^2\log(1-r)\right]\,. \tag{2.22}$$

The self-energy is now given by

$$\begin{aligned}
-i\Sigma(p) = i\frac{\alpha}{4\pi}\left[\frac{1}{\varepsilon} - \gamma - \log\left(\frac{m^2}{4\pi\mu^2}\right) + 1 + \frac{1}{r} - \left(1-\frac{1}{r^2}\right)\log(1-r)\right]\not{p} \\
-i\frac{\alpha}{\pi}\left[\frac{1}{\varepsilon} - \gamma - \log\left(\frac{m^2}{4\pi\mu^2}\right) + \frac{3}{2} - \left(1-\frac{1}{r}\right)\log(1-r)\right] m\,.
\end{aligned} \tag{2.23}$$

The above solution was derived under the assumptions $r < 1$ and $r \neq 0$. We extend it to all r like was done for the vacuum polarization.

i) For $r = 0$ the integrals in (2.21)-(2.22) are trivial. We find

$$-i\Sigma(0) = i\frac{\alpha}{4\pi}\left[\frac{1}{\varepsilon} - \gamma - \log\left(\frac{m^2}{4\pi\mu^2}\right) - 1\right]\not{p} - i\frac{\alpha}{\pi}\left[\frac{1}{\varepsilon} - \gamma - \log\left(\frac{m^2}{4\pi\mu^2}\right) - \frac{1}{2}\right] m\,. \tag{2.24}$$

ii) For $r > 1$ we need to perform analytic continuation of the logarithm. Following the the prescription (A.16) we let $M^2 \to M^2 - i\epsilon$ and consequently $r \to r + i\epsilon$, which puts the logarithm just below the branch cut. So we replace $\log(1-r)$ by $\log|1-r| - i\pi\theta(r-1)$.

Finally, the solution valid for all electron momenta p, is given by

$$\begin{aligned} -i\Sigma(p) = -i\Sigma(0) &+ i\frac{\alpha}{4\pi}\left[2 + \frac{1}{r} - \left(1 - \frac{1}{r^2}\right)\Big(\log|1-r| - i\pi\theta(r-1)\Big)\right]\not{p} \\ &- i\frac{\alpha}{\pi}\left[2 - \left(1 - \frac{1}{r}\right)\Big(\log|1-r| - i\pi\theta(r-1)\Big)\right] m\,. \end{aligned} \tag{2.25}$$

2.3. Vertex Correction

$$-ie\Gamma^\mu(\bar{p},p) = (-ie)^3\int\frac{d^dq}{(2\pi)^d}\gamma^\rho\frac{i(\not{\bar{p}}+\not{q}+m)}{(\bar{p}+q)^2-m^2+i\epsilon}\gamma^\mu\frac{i(\not{p}+\not{q}+m)}{(p+q)^2-m^2+i\epsilon}\gamma^\sigma\frac{-i\eta_{\rho\sigma}}{q^2+i\epsilon}\,. \tag{2.26}$$

As usual, combine the denominators with the Feynman parameter trick (A.29). Complete the square by substituting $l = q + x\bar{p} + yp$. Then

$$\Gamma^\mu(\bar{p},p) = -4ie^2\int\frac{d^dl}{(2\pi)^d}\int_0^1 dx\int_0^{1-x} dy\frac{N^\mu}{(l^2-M^2+i\epsilon)^3}\,, \tag{2.27}$$

where, after using $p^2 = \bar{p}^2 = m^2$ and $k = \bar{p} - p$, we have $M^2 = (x+y)^2m^2 - xyk^2$ and where the numerator is given by

$$N^\mu = \tfrac{1}{2}\gamma^\rho\left(\not{l} + (1-x)\not{\bar{p}} - y\not{p} + m\right)\gamma^\mu\left(\not{l} - x\not{\bar{p}} + (1-y)\not{p} + m\right)\gamma_\rho\,. \tag{2.28}$$

Notice that for M^2 to be non-negative for all x and y in the domain, we need to have that $k^2 < 4m^2$. In other words, let us assume that the fermions in the loop are off mass-shell. Our next objective is to write the numerator in a useful form.

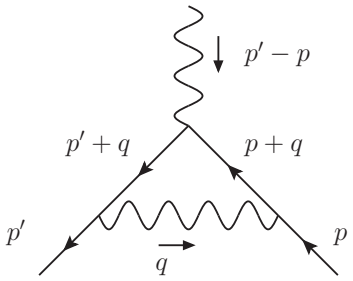

Figure 2.3.: One-loop vertex correction.

Numerator

There are few steps to simplify the numerator. First, observe that the numerator contains terms with up to two powers of the loop momentum. Applying symmetric integration, linear terms vanish, (A.23), while $l^\mu l^\nu$ can be replaced by $l^2\eta^{\mu\nu}/d$, (A.24). Second, the indices on the outer two gamma matrices are contracted, so we need the appropriate identities (A.11)-(A.14). Furthermore, in practice the vertex function gets sandwiched by Dirac spinors $\bar{u}(\bar{p})\,\Gamma^\mu(\bar{p},p)\,u(p)$. This means that we can use the Dirac equation $(\not{p}-m)u(p)=0$ and $\bar{u}(\bar{p})(\not{\bar{p}}-m)=0$, thereby removing slashed momenta. And finally, there is only one free spacetime index μ, so the numerator can be expressed as

$$N^\mu = C_1\,\gamma^\mu + C_2\bar{p}^\mu + C_3 p^\mu\,. \tag{2.29}$$

Bringing the numerator to this form can be quite tedious, making it an excellent task for a symbolic computer program. We performed the manipulations in FORM [15], see appendix B. The coefficients C_i are

$$\begin{aligned} C_1 &= l^2\,[\tfrac{2}{d}+\tfrac{d}{2}-2] - k^2\,[1-x-y+(\tfrac{d}{2}-1)xy] + m^2\,[2-4(x+y)+(\tfrac{d}{2}-1)(x+y)^2]\,,\\ C_2 &= 2m\,[y-(\tfrac{d}{2}-1)x(x+y)]\,,\\ C_3 &= 2m\,[x-(\tfrac{d}{2}-1)y(y+x)]\,. \end{aligned} \tag{2.30}$$

Inspired by the Ward identity $k_\mu\Gamma^\mu(\bar{p},p)=0$, we rewrite the numerator in terms of the linear combinations $(\bar{p}+p)^\mu$ and k^μ, giving $C_1\,\gamma^\mu+\frac{1}{2}(C_2+C_3)(\bar{p}+p)^\mu+\frac{1}{2}(C_2-C_3)k^\mu$. When contracting with k_μ, the first two terms vanish by virtue of the Dirac equation and mass-shell condition for the fermion. Since the photon is not constrained to be on mass shell, the contraction as a whole can only vanish (Ward identity) if the coefficient of the third term is zero.

We can also verify explicitly that this must be true. Interchange the dummy variables x and y. The effect is that C_2 becomes C_3 and vice versa, hence the coefficient $\frac{1}{2}(C_2-C_3)$ picks up a minus sign. Meanwhile, the domain of integration remains the same, as does the denominator. It follows that the coefficient must be zero and the k^μ term drops out.

It is conventional to further eliminate $(\bar{p}+p)^\mu$ in favor of $\sigma^{\mu\nu}k_\nu$ (with $\sigma^{\mu\nu} = \frac{i}{2}[\gamma^\mu, \gamma^\nu]$) by means of the Gordon identity

$$\bar{u}(\bar{p})\gamma^\mu u(p) = \bar{u}(\bar{p})\left(\frac{(\bar{p}+p)^\mu}{2m} + \frac{i\sigma^{\mu\nu}k_\nu}{2m}\right)u(p)\,, \tag{2.31}$$

after which

$$N^\mu = D_1\,\gamma^\mu + D_2\frac{i\sigma^{\mu\nu}k_\nu}{2m}\,, \tag{2.32}$$

with

$$D_1 = C_1 + m(C_2 + C_3)\,, \tag{2.33}$$
$$D_2 = -m(C_2 + C_3)\,. \tag{2.34}$$

Putting numerator (2.32) into the integral (2.27), we can pull the tensor structure outside the integrals.

$$\Gamma^\mu(\bar{p}, p) = F_1(k^2)\gamma^\mu + F_2(k^2)\frac{i\sigma^{\mu\nu}k_\nu}{2m}\,, \tag{2.35}$$

with *form factors* $F_{1,2}$ given by

$$F_{1,2}(k^2) = -4ie^2\int_0^1 dx\int_0^{1-x} dy\int\frac{d^dl}{(2\pi)^d}\frac{D_{1,2}}{(l^2 - M^2 + i\epsilon)^3}\,. \tag{2.36}$$

These form factors, $F_1(k^2)$ and $F_2(k^2)$, encode the coupling strength of the fermion to an electromagnetic field. In particular, $F_1(0)$ is the electric charge of the fermion and $F_2(0)$ its anomalous magnetic moment. Of course, to leading order the vertex is simply $\Gamma^\mu = \gamma^\mu$, in which case $F_1(0) = 1$ and $F_2(0) = 0$. Now let's find the next-to-leading order corrections to these form factors.

First Form Factor

Between the two form factors, F_1 is the hardest to compute, because it suffers from both UV and IR divergences. We shall regulate both divergences by dimensional regularization. Let us first define once again the ratio of the photon off-shell mass and the squared mass of two fermions,

$$r := \frac{k^2}{4m^2}\,. \tag{2.37}$$

Substituting (2.30) into (2.33) and using this ratio, D_1 reads

$$D_1 = l^2 \left[\tfrac{2}{d} + \tfrac{d}{2} - 2\right] + m^2 \left[(2-4r)(1-x-y) + \left(1-\tfrac{d}{2}\right)\left((x+y)^2 + 4rxy\right)\right] . \quad (2.38)$$

The first term is expected to give a logarithmic UV-divergence by power counting, due to the factor l^2. We apply (A.26), effectively replacing $l^2 \to d/(d-4)M^2$, which indeed produces a ε^{-1} pole as we take $d = 4 - 2\,\varepsilon$. Now

$$D_1 = -M^2 \left[\tfrac{1}{\varepsilon}\Big|_{UV} - 2 + \varepsilon\right] + m^2 \left[(2-4r)(1-x-y) + (\varepsilon - 1)\left((x+y)^2 + 4rxy\right)\right] , \quad (2.39)$$

where $M^2 = m^2\left((x+y)^2 - 4rxy\right)$ in terms of r as well. Now the momentum integral in (2.36) has attained the standard scalar form and can thus be performed. We take the result from (A.17) for the case $k = 3$.

$$\begin{aligned} F_1(k^2) &= -4ie^2 \int_0^1 dx \int_0^{1-x} dy\, D_1 \frac{-i(\mu^2)^{-1-\varepsilon}}{2(4\pi)^3}\Gamma(1+\varepsilon)\left(\frac{M^2}{4\pi\mu^2}\right)^{-1-\varepsilon} \\ &= -\frac{2\alpha\,(\mu^2)^{-1-\varepsilon}}{(4\pi)^2}\Gamma(1+\varepsilon)\int_0^1 dx \int_0^{1-x} dy\, D_1 \left(\frac{M^2}{4\pi\mu^2}\right)^{-1-\varepsilon} . \end{aligned} \quad (2.40)$$

Notice that we did not yet expand any factor around $\varepsilon = 0$. The reason is that there is an IR divergence hidden inside the Feynman parameter integrals. Only after we uncovered the divergence in the form of an ε^{-1} pole, do we start taking to make the expansion. This way we carefully retain $\varepsilon\,/\,\varepsilon$ terms.

The final task is thus to compute the two Feynman parameter integrals. We can exploit the symmetry of the domain of integration and the integrand under $x \leftrightarrow y$. After splitting D_1 into terms of zeroth, first and second degree in x and/or y,

$$D_1 = D_1^{(0)} + D_1^{(1)} + D_1^{(2)} , \quad (2.41)$$

we can apply the reparametrization (A.30), that is,

$$\int_0^1 dx \int_0^{1-x} dy\, f^{(k)}(x,y) = \int_0^1 dz\, z^{1+k} \int_0^1 dx\, f^{(k)}(x,1-x) , \quad (2.42)$$

to the functions

$$f^{(j-2-2\,\varepsilon)}(x,y) = D_1^{(j)} \left(\frac{M^2}{4\pi\mu^2}\right)^{-1-\varepsilon} , \quad (2.43)$$

for $j = 0, 1, 2$ and

$$D_1^{(0)} = m^2\,(2-4r)\,, \tag{2.44}$$

$$D_1^{(1)} = -m^2\,(2-4r)(x+y)\,, \tag{2.45}$$

$$D_1^{(2)} = -M^2\,\left(\tfrac{1}{\varepsilon}\big|_{UV} - 2 + \varepsilon\right) + m^2\,(-1+\varepsilon)((x+y)^2 + 4rxy)\,. \tag{2.46}$$

These functions are symmetric and homogeneous of degree $k = j - 2 - 2\,\varepsilon$. After reparametrization

$$\begin{aligned} F_1(k^2) = -\frac{2\alpha\,(\mu^2)^{-1-\varepsilon}}{(4\pi)^2}\Gamma(1+\varepsilon)\Big\{ &\int_0^1 dz\, z^{-1-2\,\varepsilon} \int_0^1 dx\, f^{(-2-2\,\varepsilon)}(x,1-x) \\ &+ \int_0^1 dz\, z^{-2\,\varepsilon} \int_0^1 dx\, f^{(-1-2\,\varepsilon)}(x,1-x) \\ &+ \int_0^1 dz\, z^{1-2\,\varepsilon} \int_0^1 dx\, f^{(-2\,\varepsilon)}(x,1-x)\Big\}\,. \end{aligned} \tag{2.47}$$

The trivial z-integrals decouple and contribute a factor $-\frac{1}{2}\,\varepsilon^{-1}$, $\frac{1}{2}(2+\varepsilon)$ and $\frac{1}{2}(1+\varepsilon)$ respectively. Observe the emergence of an IR divergence in the form of a ε^{-1} pole. It ultimately comes from the photon going on mass shell.

At this stage we may expand around $\varepsilon = 0$ using (A.19) and (A.20). The remaining integrals over x contain $f^{(k)}(x, 1-x)$, so we plug $y = 1-x$ into (2.44)-(2.46) and M^2. Our final result is

$$\begin{aligned} F_1(k^2) = &\frac{\alpha(\mu^2)^{-\varepsilon}}{4\pi}\left\{ \frac{1}{\varepsilon}\Big|_{UV} - \gamma - \log\left(\frac{m^2}{4\pi\mu^2}\right) - 2 + 2\,I_1 - I_2 + (4r-2)\,I_3 \right\} \\ &+ \frac{\alpha(\mu^2)^{-\varepsilon}}{4\pi}\left\{ \frac{1}{\varepsilon}\Big|_{IR} - \gamma - \log\left(\frac{m^2}{4\pi\mu^2}\right) + 2 \right\}(2-4r)\,I_1\,, \end{aligned} \tag{2.48}$$

with the following integrals for the function $f(x) = 1 - x(1-x)4r$,

$$I_1 := \int_0^1 dx\,\frac{1}{f(x)}, \quad I_2 := \int_0^1 dx\,\log(f(x)), \quad \text{and} \quad I_3 := \int_0^1 dx\,\frac{\log(f(x))}{f(x)}\,. \tag{2.49}$$

At this point one we verified agreement with the result in [14], by making the usual translation of conventions and writing $I_1 = (\frac{1}{2}\,I_2 + 1)\frac{1}{1-r}$ for the first occurrence in (2.48). They regularize the IR divergence by giving the photon a mass κ_1, which leads to a factor $\log(\kappa_1)$ instead of our $\frac{1}{\varepsilon}|_{IR} + \ldots$ in (2.48). Both diverge as ε and κ_1 tend to zero. In physical amplitudes this IR divergence is canceled by bremsstrahlung diagrams, that is, tree level vertex diagrams where either the incoming or the outgoing fermion emits a soft photon [13].

Assuming that $r \neq 0$, factorizing $f(x)$, using partial fractions and (A.35),

$$I_1 = \frac{1}{2r\beta} \log\left(\frac{\beta-1}{\beta+1}\right) , \tag{2.50}$$

$$I_2 = -2 - \beta \log\left(\frac{\beta-1}{\beta+1}\right) , \tag{2.51}$$

$$\begin{aligned} I_3 = \frac{1}{4r\beta}\Bigg\{ & 2\log(4r)\log\left(\frac{\beta-1}{\beta+1}\right) + 2\,\mathrm{Li}_2\left(\frac{1-\beta}{1+\beta}\right) - 2\,\mathrm{Li}_2\left(\frac{1+\beta}{1-\beta}\right) \\ & - \left[\log(-1-\beta) - \log(\beta-1)\right] \times \\ & \quad \left[\log(-1-\beta) + \log(-1+\beta) + \log\left(\frac{\beta}{\beta-1}\right) + \log\left(\frac{\beta}{\beta+1}\right)\right] \\ & + \left[\log(1-\beta) - \log(\beta+1)\right] \times \\ & \quad \left[\log(1+\beta) + \log(1-\beta) + \log\left(\frac{\beta}{\beta-1}\right) + \log\left(\frac{\beta}{\beta+1}\right)\right]\Bigg\} , \end{aligned} \tag{2.52}$$

in terms of $\beta = \sqrt{1-1/r}$ and the dilogarithm $\mathrm{Li}_2(x)$, defined in (A.31).

Second Form Factor

The numerator of the second form factor

$$D_2 = 2m^2[-(x+y) + (\tfrac{d}{2}-1)(x+y)^2] , \tag{2.53}$$

is independent of the loop momentum. Therefor the momentum integral is UV-convergent in four dimensions. In fact, this form factor does not suffer from an IR divergence either, so we can put $d = 4$ explicitly.

$$\begin{aligned} F_2(k^2) &= \frac{\alpha}{\pi}\int_0^1 dx \int_0^{1-x} dy \frac{(x+y)(1-(x+y))m^2}{(x+y)^2m^2 - xyk^2} \\ &= \frac{\alpha}{\pi}\int_0^1 dz \int_0^1 dx \frac{1-z}{1-x(1-x)4r} \\ &= \frac{\alpha}{2\pi}\frac{1}{4r\beta}\int_0^1 dx \left[\frac{1}{x-x_+} - \frac{1}{x-x_-}\right] \\ &= \frac{\alpha}{\pi}\frac{1}{4r\beta}\log\left(\frac{\beta-1}{\beta+1}\right) , \end{aligned} \tag{2.54}$$

where we used the reparametrization (A.30) and $x_\pm$ denote the zeros of $x^2 - x + 1/(4r)$.

The anomalous magnetic moment of the electron, $F_2(0)$, is obtained by carefully taking the limit $r \to 0$ or alternatively by straightforward calculating the original integral

over x and y for $k^2 = 0$. The result is

$$F_2(0) = \frac{\alpha}{2\pi} \approx 0.00116140973\,, \tag{2.55}$$

which was first obtained by Schwinger [1]. With this correction, theory and experiment agree to within less then one percent.

2.4. Renormalization

In the previous sections we have seen that all one-loop diagrams in QED give divergent corrections to the tree level diagrams of the same processes. At first sight this result seems to show that QED does not work as a perturbative theory. However, there is a way out.

Renormalizing the Lagrangian

The way out comes with the observation that the fields and coupling constants in the Lagrangian

$$\mathcal{L} = -\tfrac{1}{4}(F_{\mu\nu})^2 - \tfrac{1}{2}\lambda(\partial_\mu A^\mu)^2 + \bar{\psi}(i\partial\!\!\!/ - m)\psi - eA_\mu\bar{\psi}\gamma^\mu\psi\,, \tag{2.56}$$

are not physical quantities, but rather parameters of the theory. The idea is to have make the parameters divergent, such that the physical quantities calculated with the theory are finite. To do so, each parameter is rescaled by an arbitrary renormalization constant Z_i.

$$\psi \to Z_\psi^{1/2}\psi\,, \quad A_\mu \to Z_A^{1/2}A_\mu\,, \quad e \to Z_e e\,, \quad m \to Z_m m\,, \quad \lambda \to Z_\lambda\lambda\,. \tag{2.57}$$

Then the rescaled, or renormalized, Lagrangian $\mathcal{L}_\mathcal{R}$ can be written in terms of the unrenormalized Lagrangian plus counterterms.

$$\mathcal{L}_\mathcal{R} = \mathcal{L} + \mathcal{L}_\mathcal{CT}\,, \tag{2.58}$$

$$\begin{aligned}\mathcal{L}_{CT} =& -(Z_A - 1)\tfrac{1}{4}F_{\mu\nu}^2 - (Z_\lambda Z_A - 1)\tfrac{1}{2}\lambda(\partial_\mu A^\mu)^2 \\ &+ (Z_\psi - 1)\bar{\psi}(i\partial\!\!\!/)\psi - (Z_\psi Z_m - 1)m\bar{\psi}\psi - (Z_V - 1)eA_\mu\bar{\psi}\gamma^\mu\psi\,,\end{aligned} \tag{2.59}$$

where Z_V is short for $Z_\psi Z_e Z_A^{1/2}$ and V stands for vertex.

There is, however, a catch with this procedure. It only works if (i) the counterterm Lagrangian is gauge invariant, and (ii) all divergent corrections can be absorbed by the counterterm Lagrangian. A theory is called renormalizable if both these demands are satisfied.

What does it take for the counterterm Lagrangian to be gauge invariant? We know that the unrenormalized Lagrangian was made gauge invariant by replacing the ordinary derivative by a covariant derivative, $\partial_\mu \to \partial_\mu + ieA_\mu$. Hence, the counterterm Lagrangian must also contain a covariant derivative. In particular, this restricts

$$Z_\psi = Z_V \,. \tag{2.60}$$

Furthermore, the counterterm Lagrangian should contain no gauge-fixing term, so

$$Z_\lambda Z_A = 1 \,. \tag{2.61}$$

The latter two equations are referred to as renormalization constant Ward identities. In what continues, we shall not impose these identities, but rather check that they are satisfied.

To clarify the second demand, that all divergent corrections can be absorbed by the counterterm Lagrangian, let us give a hypothetical example that would violate it. We have seen that the one-loop correction to the vertex $\Gamma^\mu(k)$ contains a term of the form $\sigma^{\mu\nu}k_\nu$. If its prefactor would contain a divergence, then one would need a counterterm of the form $\kappa A_\mu \bar\psi \sigma^{\mu\nu}\partial_\nu\psi$, which is not in the Lagrangian to start with.

Renormalization to Order α

The Feynman diagrams generated by the counterterm Lagrangian are

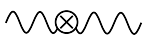

$$-i(Z_A-1)(k^2\eta^{\mu\nu}-k^\mu k^\nu) - i\lambda(Z_\lambda Z_A - 1)k^\mu k^\nu \,,$$

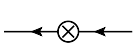

$$i(Z_\psi - 1)\not{p} - i(Z_\psi Z_m - 1)m \,,$$

$$-ie\gamma^\mu(Z_V - 1) \,.$$

We indicate the counterterms by a circled cross. These counterterms suffice to cancel the infinite contributions from the one-loop diagrams. Extracting the pole parts of (2.6), (2.19) and (2.48) we have

$$-i\frac{\alpha}{3\pi}\frac{1}{\varepsilon}(k^2\eta^{\mu\nu}-k^\mu k^\nu) \,,$$

$$i\frac{\alpha}{4\pi}\frac{1}{\varepsilon}\not{p} - i\frac{\alpha}{\pi}\frac{1}{\varepsilon}m \,,$$

$$-ie\frac{\alpha}{4\pi}\frac{1}{\varepsilon}\gamma^\mu \,.$$

A quick comparison shows that we need up to order α

$$Z_A - 1 = -\frac{\alpha}{3\pi}\left(\frac{1}{\varepsilon} + \text{finite terms}\right), \tag{2.62}$$

$$Z_\lambda Z_A - 1 = 0\,, \tag{2.63}$$

$$Z_\psi - 1 = -\frac{\alpha}{4\pi}\left(\frac{1}{\varepsilon} + \text{finite terms}\right), \tag{2.64}$$

$$Z_\psi Z_m - 1 = -\frac{\alpha}{\pi}\left(\frac{1}{\varepsilon} + \text{finite terms}\right), \tag{2.65}$$

$$Z_V - 1 = -\frac{\alpha}{4\pi}\left(\frac{1}{\varepsilon} + \text{finite terms}\right). \tag{2.66}$$

We see that up to order α the renormalization constant Ward identities $Z_\psi = Z_V$ and $Z_\lambda Z_A = 1$ hold, provided that the finite terms absorbed in Z_ψ and Z_V are equal. It is our freedom of choice to do so. A precise specification of all finite terms is subject to the particular subtraction scheme chosen. The minimal subtraction scheme dictates that no finite terms are subtracted. In the modified minimal subtraction scheme, some recurring finite terms are subtracted. A standard choice is $-\gamma + \log(4\pi)$.

Renormalization to All Orders

We will now prove that the same renormalization procedure renders also all higher order quantum corrections finite. It must be shown that, to all orders in perturbation theory, a finite number of counter terms is enough to absorb the divergences and the counterterm Lagrangian is gauge invariant.

Actually, we shall show that the counterterms from the lowest order corrections are sufficient; their coefficients Z_i just need higher order corrections. Furthermore, we shall check the renormalization constant Ward identities (2.60) and (2.61), because together they imply gauge invariance of the counterterm Lagrangian.

The proof goes by induction. Write the renormalization constants Z_i as a series in α, with a polynomial in ε^{-1} as coefficients

$$\begin{aligned} Z_i &= \sum_{n=0}^{\infty}\left(\frac{\alpha}{4\pi}\right)^n\left(\sum_{k=1}^{n} Z_i^{(n,k)}\frac{1}{\varepsilon^k} + c_i^{(n)}\right) \\ &= 1 + \frac{\alpha}{4\pi}\left(Z_i^{(1,1)}\frac{1}{\varepsilon} + c_i^{(1)}\right) + \left(\frac{\alpha}{4\pi}\right)^2\left(Z_i^{(2,2)}\frac{1}{\varepsilon^2} + Z_i^{(2,1)}\frac{1}{\varepsilon} + c_i^{(2)}\right) + \dots\,. \end{aligned} \tag{2.67}$$

Let Z_i^N denote the truncated series Z_i, such that its highest order term is α^N. Assume that the renormalization constants Z_i^N for $i \in \{\psi, A, e, m, \lambda\}$ are sufficient to cancel all divergences from diagrams of the same order. Assume also that the renormalization

constant Ward identities hold up to order N,

$$Z_\psi^N = Z_V^N\,, \qquad Z_\lambda^N Z_A^N = 1\,. \tag{2.68}$$

The problem is then to show that the latter two statements are valid for $N+1$.

The tensor structure of the vacuum polarization is completely fixed at any order. The observation that it can only be a linear combination of $\eta^{\mu\nu}$ and $k^\mu k^\nu$, together with the Ward identity $k_\mu \Pi^{\mu\nu}(k) = 0$, leads to $\Pi^{\mu\nu}(k) = \Pi(k^2\eta^{\mu\nu} - k^\mu k^\nu)$. Since this holds in particular at order $N+1$, those corrections Π are absorbed into Z_A^{N+1}. The BPH theorem implies that the counterterm is local.

For the self-energy and vertex correction the story is a bit more involved. As a consequence of the BPH theorem and Lorentz invariance, the divergent parts can be written as

$$\Sigma(p) = i\not{p}A - imB\,, \qquad \Gamma^\mu(p, p+q) = -ie\gamma^\mu C\,, \tag{2.69}$$

with the prefactors A, B and C polynomials in ε^{-1}. Referring to the counterterm diagrams in the previous subsection, we find that the constants A, B and C are absorbed by Z_ψ^{N+1}, Z_m^{N+1} and Z_V^{N+1} respectively.

With the gauge invariant Lagrangian up to order N, one can construct the fermion self-energy diagrams of one order higher. Denote the sum of non-amputated self-energy diagrams of order $N+1$ by $\Delta(p)\Sigma(p)\Delta(p)$. Now sum over all possible ways of attaching a photon with momentum q to each diagram. Denote this sum by S^μ. The photon can be attached either to one of the two external fermion propagators, or to one of the internal fermion propagators. In the former case we still have a self-energy diagram, with a disconnected tree level vertex. In the latter case the diagram has become a vertex correction of order $N+1$.

$$\begin{aligned} S^\mu = {} & \Delta(p+q)(-ie)\gamma^\mu\Delta(p)\Sigma(p)\Delta(p) \\ & + \Delta(p+q)\Sigma(p+q)\Delta(p+q)(-ie)\gamma^\mu\Delta(p) \\ & + \Delta(p+q)(-ie)\Gamma^\mu(p, p+q)\Delta(p)\,. \end{aligned} \tag{2.70}$$

The Ward identity tells us that the constructed sum, when contracted with q_μ, is equal to e times the difference of the self-energy at external momenta p resp. $p+q$,

$$q_\mu S^\mu = e[\Delta(p)\Sigma(p)\Delta(p) - \Delta(p+q)\Sigma(p+q)\Delta(p+q)]\,. \tag{2.71}$$

Here Σ and Γ^μ are all of order $N+1$, which are of the form

$$\Sigma(p) = i\not{p}A - imB\,, \qquad \Gamma^\mu(p, p+q) = -ie\gamma^\mu C\,, \tag{2.72}$$

as shown before. The expression $q_\mu S^\mu$ can then be simplified. Using the relations

$$\Delta(p+q)(-i\not{q})\Delta(p) = \Delta(p) - \Delta(p+q)\,, \qquad \Sigma(p+q) - \Sigma(p) = i\not{q}A\,, \tag{2.73}$$

the Ward identity (2.71) becomes

$$A = C\,. \tag{2.74}$$

So by choosing the finite terms equal as well, we have $Z_\psi^{N+1} = Z_V^{N+1}$. All corrections were absorbed without the using the gauge-fixing counterterm. Therefor we can drop it from the counterterm Lagrangian by setting $Z_\lambda^{N+1} Z_A^{N+1} = 1$. We have hereby completed the induction step. Because the first order corrections were explicitly renormalized, we are led to conclude that all order corrections are renormalizable. In other words, QED is a renormalizable theory.

Chapter 3.

Unitarity

In the previous chapter we computed one-loop diagrams with up to three external particles. There it became clear that the vertex diagrams is the most complicated. Calculation of one-loop n-particle scattering amplitudes is even more involved. Several methods have been constructed to address this problem.

The *unitarity* method exploits the unitarity of the scattering matrix to determine the absorptive (imaginary) part of an amplitude. In certain cases the dispersive (real) part of the amplitude can be recovered from the imaginary part by means of dispersion relations. This way the amplitude is reconstructed, with the exception of rational terms.

A different approach is to expand arbitrary one-loop integrals in terms of a basis of known scalar one-loop integrals. The *generalized unitarity* method extracts the coefficients in such an expansion by cutting diagrams and relating their discontinuities to the discontinuities of scalar integrals from the basis. The process of cutting a diagram involves putting particles propagating in the loop on shell whenever their propagator is cut.

3.1. Unitarity

The unitarity method is based on unitarity of the scattering matrix, $S^\dagger S = 1$. If we define the transition matrix T by the relation $S = 1 + iT$, then the unitarity of the scattering matrix implies the following identity for the transition matrix

$$-i(T - T^\dagger) = T^\dagger T \,. \tag{3.1}$$

By definition, the scattering amplitude $\mathcal{M}$ is related to the transition matrix by

$$(2\pi)^4 \delta^{(4)}(\sum_i p_i - \sum_j q_j)\, \mathcal{M}(a \to b) = \langle a|T|b\rangle \ , \tag{3.2}$$

for initial state $|a\rangle$ with particle momenta $\{p_i\}$ and final state $|b\rangle$ with particle momenta $\{q_j\}$. By understanding that the amplitude is to be multiplied with a momentum

conserving delta function, we abbreviate

$$\mathcal{M}(a \to b) = \langle b|T|a\rangle \ . \tag{3.3}$$

Sandwiching (3.1) between states $\langle b|\ldots|a\rangle$, inserting a complete set of states on the right hand side and using the shorthand notation from (3.3), we obtain the starting equation for the unitarity method

$$-i\left[\mathcal{M}(a \to b) - \mathcal{M}^*(b \to a)\right] = \sum_k \int d\Pi_k \mathcal{M}^*(b \to k)\mathcal{M}(a \to k)\,. \tag{3.4}$$

In words, the imaginary part of an amplitude is related to the product of the sum over all possible intermediate states of the partial amplitudes for the scattering (or decay) of the initial and final states into such intermediate state.

As an aside we remark that the famous *optical theorem* is obtained as a special case of (3.4) by setting the initial and final states equal.

$$2\ \mathrm{Im}\ \mathcal{M}(a \to a) = \sum_k \int d\Pi_k |\mathcal{M}(a \to k)|^2 \propto \sigma(a \to \text{anything})\,. \tag{3.5}$$

It states that the imaginary part of the forward scattering amplitude is proportional to the total cross section.

3.2. Cut Feynman Diagrams

3.2.1. Largest Time Equation

The scalar particle Feynman propagator is given in the spacetime representation by

$$\Delta_F(x) = \int \frac{d^4k}{(2\pi)^4} \frac{i}{k^2 - m^2 + i\,\varepsilon} e^{-ik\cdot x}\,, \tag{3.6}$$

where the argument $x = x_2 - x_1$ is a difference between spacetime points marking the end points of propagation. One can decompose this propagator into contributions from positive and negative time difference x_0,

$$\Delta_F(x) = \theta(x_0)\Delta^+(x) + \theta(-x_0)\Delta^-(x)\,, \tag{3.7}$$

with

$$\Delta^\pm(x) \equiv \int \frac{d^4k}{(2\pi)^3} \theta(\pm k_0)\delta(k^2 - m^2) e^{-ik\cdot x}\,. \tag{3.8}$$

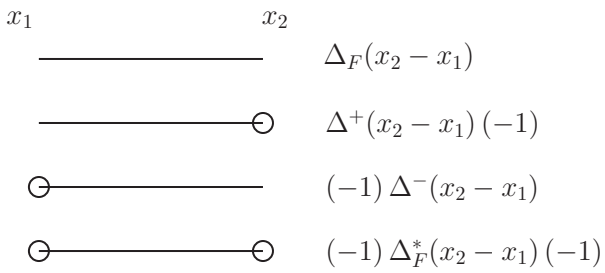

Figure 3.1.: The Feynman rules corresponding to propagator (3.7). Instead of just one, there are four different propagators, depending on which vertices are circled. Circling one vertex fixes the time ordering between the two vertices, thereby simplifying Δ_F to $\Delta^\pm$. In the case of two circled vertices, the propagator is to be complex conjugated. Finally, a circled vertex is minus an uncircled one (anticipating complex conjugation of a vertex).

Equality between (3.6) and (3.7) can be shown by integrating out k_0 in both expressions. Notice that Δ^+ and Δ^- are each others complex conjugate, so

$$\Delta_F^*(x) = \theta(x_0)\Delta^-(x) + \theta(-x_0)\Delta^+(x)\,. \tag{3.9}$$

The propagator (3.6) results in the well-known momentum space Feynman rule that assigns $i/(k^2 - m^2 + i\,\varepsilon)$ to an internal propagator for a scalar particle. Propagator (3.7), on the other hand, can be used to define an alternative set of Feynman rules. They are shown in figure 3.1.

The propagators $\Delta^\pm(x)$, connecting an uncircled vertex to a circled vertex or vice versa, give an important restriction. Looking back at the definition of $\Delta^\pm(x)$, we see that the θ-function inside is zero unless energy flows from an uncircled vertex to a circled vertex. We shall make use of this observation in the context of the cutting equation. For propagators connecting two (un)circled vertices there is no such restriction.

From this new set of Feynman rules we shall derive the largest time equation. Imagine a general connected diagram, containing n vertices of which any number are circled. Denote a completely uncircled diagram by $F(x_1, \ldots, x_n)$ and denote circling of vertices by underlining the corresponding spacetime points x_i in the argument of F. Assume that vertex x_m with $m \in \{1, \ldots n\}$ has the largest time. That is, $(x_m)_0 > (x_i)_0$ for all $i \in \{1, \ldots, m-1, m+1, \ldots, n\}$. For every propagator connected to x_m, circling the vertex x_m gives only a minus sign with respect to the uncircled case. The propagators change in principle from $\Delta_F \to \Delta^+$ or $\Delta^- \to \Delta_F^*$, but because $(x_m)_0$ is largest, those are actually equivalent. Thus

$$F(\ldots, x_m, \ldots) + F(\ldots, \underline{x_m}, \ldots) = 0\,. \tag{3.10}$$

This is called the *largest time equation*.

Consider for a moment the simplest example, $F(x_1, x_2)$. Assuming that $(x_2)_0 > (x_1)_0$, the largest time equation gives the following two identities

$$\begin{aligned} F(x_1, x_2) + F(x_1, \underline{x_2}) &= 0\,, \\ F(\underline{x_1}, x_2) + F(\underline{x_1}, \underline{x_2}) &= 0\,. \end{aligned} \tag{3.11}$$

Diagrammatically this is represented by

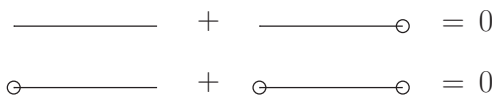

Applying the Feynman rules, the above two identities read

$$\begin{aligned} \Delta_F(x_2 - x_1) + \Delta^+(x_2 - x_1)(-1) &= 0\,, \\ \Delta_F^*(x_2 - x_1) + \Delta^-(x_2 - x_1)(-1) &= 0\,, \end{aligned} \tag{3.12}$$

for $(x_2)_0 > (x_1)_0$. Remember that the minus sign between brackets in the second term is due to circling of the vertex x_2. One can easily verify this result by looking at the Feynman propagator (3.7) and its complex conjugate (3.9).

3.2.2. Cutting Equation

In general we don't know which time $(x_i)_0$ is largest. Therefor we continue by summing all possible circlings of the vertices in a diagram. The terms in such a sum cancel pairwise.

$$\sum_{circlings} F(x_1, \ldots, x_n) = 0\,. \tag{3.13}$$

There are two extreme cases in the sum: no vertices circled and all vertices circled. From the Feynman rules we infer that the diagram with all vertices circled is the complex conjugate of the uncircled diagram: $F(\underline{x_1}, \ldots, \underline{x_n}) = F^*(x_1, \ldots, x_n)$. Singling out these two cases,

$$F(x_1, \ldots, x_n) + F^*(x_1, \ldots, x_n) = - \sum_{circlings \setminus \{0, all\}} F(x_1, \ldots, x_n)\,. \tag{3.14}$$

In general, the sum on the right hand side in contains vanishing terms. Remember the remark about the Feynman rules that we made earlier, where we concluded that energy must flow from uncircled vertices to circled vertices. Besides that we impose energy and momentum conservation at each vertex. Together they force some diagrams to be zero. Two examples are shown in figure 3.2.

The energy flow demands the central vertex to be a sink or source of energy, which it can only be without violating energy conservation, by having an external leg attached.

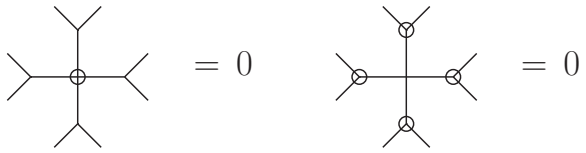

Figure 3.2.: Example of two vanishing diagrams on the right hand side of (3.14). Energy must flow from uncircled vertices to circled vertices, by construction of the Feynman rules. Imposing energy conservation at the central vertex leads to the conclusion that both diagrams vanish.

Hence the diagrams vanishes. A more algebraic way of saying the same thing is: after multiplying all internal propagators the subspace of the whole momentum space that satisfies all θ-functions and δ-functions is empty, so the integrals give zero.

The non-vanishing terms in the sum are diagrams with connected regions of circled vertices and connected regions of uncircled vertices, while each region is attached to at least one external leg. This leads to the notion of *cutting a diagram* in between the region of uncircled and the region of circled vertices. Energy can only flow through the cut in one direction, see figure 3.3. We understand that the cut propagators are put on-shell, that is, we replace

$$\frac{i}{k^2 - m^2 + i\,\varepsilon} \to 2\pi\,\theta(\pm k_0)\,\delta(k^2 - m^2)\,, \tag{3.15}$$

which follows directly from a comparison between (3.6) and (3.8). The above replacement goes under the name of Cutkosky cutting rule [16]. We also understand that on the shaded side of the cut, all standard Feynman rules are to be complex conjugated. This agrees with the rules in figure 3.1.

The largest time equation (3.14) thus reduces to the *cutting equation*,

$$F(x_1, \ldots, x_n) + F^*(x_1, \ldots, x_n) = -\sum_{cuttings} F(x_1, \ldots, x_n)\,, \tag{3.16}$$

where the sum is over all possible cuttings of the diagram $F(x_1, \ldots, x_n)$ and each cut propagator is replaced according to (3.15).

The cutting equation thus allows to calculate the real part of a diagram, which contributes by convention to the imaginary part of an amplitude. The integrals involved are greatly simplified with respect to the full calculation, thanks to the on-shell delta functions.

Fermions and Vector Bosons

The above treatment was given for a scalar particle, because its propagator allows for a clean way to introduce the new concepts. Nevertheless, the whole idea applies equally

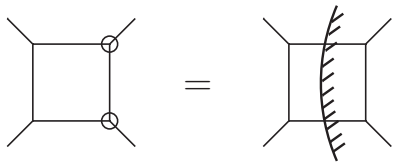

Figure 3.3.: Translation from circling vertices to cutting propagators. Like energy flows from uncircled to circled vertices, energy only flows through the cut towards the shaded side. Furthermore, the Feynman rules in figure 3.1 are replaced by the simple prescription to put cut propagators on-shell according to (3.15) and everything on the shaded side is complex conjugated.

well to fermions and vector bosons. However, for those types of particles one finds different expressions for $\Delta^{\pm}(x)$.

For the fermion propagator we can write

$$\begin{aligned} S_F(x) &= \int \frac{d^4p}{(2\pi)^4} \frac{i(\not{p}+m)}{p^2-m^2+i\,\varepsilon} e^{-ip\cdot x} \\ &= (i\not{\partial}+m)\Delta_F(x) \\ &= (i\not{\partial}+m)\left(\theta(x_0)\Delta^+(x)+\theta(-x_0)\Delta^-(x)\right) . \end{aligned}$$

The derivative of $\theta(\pm x_0)$ gives $\pm\delta(\pm x_0)$. Upon integrating $S_F(x)$ over spacetime the delta functions put $\Delta^{\pm}(x)$ at the same time $x_0 = 0$, where they are actually equal, so the two terms cancel. Hence we can define $S^{\pm}(x) \equiv (i\not{\partial}+m)\Delta^{\pm}(x)$, which are each others Hermitian conjugate, such that

$$S_F(x) = \theta(x_0)S^+(x) + \theta(-x_0)S^-(x)\,, \tag{3.17}$$

a form suitable for deriving the largest time equation and cutting equation for fermions. One obtains a cutting rule that is like (3.15), multiplied by $\not{p}+m$,

$$\frac{i(\not{p}+m)}{p^2-m^2+i\,\varepsilon} \to 2\pi\,\theta(\pm p_0)\,\delta(p^2-m^2)\,(\not{p}+m)\,. \tag{3.18}$$

Again the sign is chosen such that positive energy flows towards the shaded region.

For vector bosons a similar thing can be done, with the slight complication that we now get two derivatives acting on $\Delta_F(x)$. Whereas $\Delta^{\pm}(x)|_{x_0=0}$ are equal, the same does not hold for their derivative. Despite the arising 'contact terms', it turns out that the largest time equation can also be maintained in this case [17].

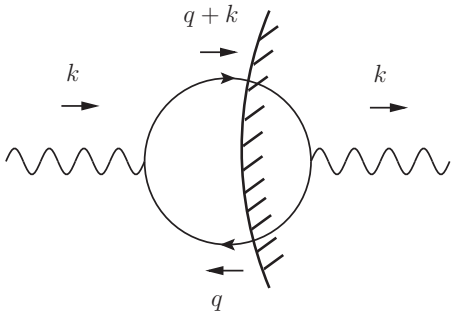

Figure 3.4.: The cut vacuum polarization diagram. Both propagators are replaced according to (3.18), with a plus sign for the top propagator and a minus sign for the other. The vertex on the right is complex conjugated.

3.2.3. Connection with Unitarity

The cutting equation (3.16) is more stringent than the unitarity equation (3.4). The reason is that the former holds for individual diagrams, while the latter holds for a scattering amplitude. But even so, for the cutting equation to imply unitarity, two conditions must be satisfied. First, diagrams in the shaded region must be equal to diagrams obtained from $S^\dagger$, and second, the $\Delta^\pm$ must be equal to a summation over intermediate states [4].

The first condition is met if the Lagrangian is its own conjugate. To clarify the second condition, it is instructive to verify it for a simple example. Consider the vacuum polarization from (2.2) contracted with polarization vectors for the external photons. We calculate both the cut diagram and the sum over intermediate states. In other words, we verify equivalence of the right hand sides of (3.16) and (3.4).

First the cut diagram. There are two internal fermion propagators which get cut according to (3.18). The propagator with momentum q becomes the negative energy solution, while the one with momentum $q+k$ becomes the positive energy solution, see figure 3.4. The vertex in the shadowed region gets a minus sign, which cancels the overall minus sign for the fermion loop. Hence we find

$$i\Pi^{\mu\nu}_{cut}(k) = (-ie)^2(2\pi)^2 \int \frac{d^4q}{(2\pi)^4}\theta(-q_0)\theta(q_0+k_0)\delta(q^2-m^2)\delta((q+k)^2-m^2)\times \\ \mathrm{tr}\left[\not\epsilon(k)\,(\not q+m)\,\not\epsilon(k)\,(\not q+\not k+m)\right]\,. \quad (3.19)$$

Next, we consider the sum over intermediate states. The expression is obtained by multiplying together the S and $S^\dagger$ diagrams and summing over spins and integrating

over the phase space.

$$\sum_{s,s'} \int d\Pi \left| \right.$$ 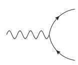 $$\left. \right|^2$$

$$= \sum_{s,s'} \int d\Pi \left[\bar{v}^{s'}(p) \, (+ie\not{\epsilon}(k)\,) \, u^s(q) \right] \left[\bar{u}^s(q) \, (-ie\not{\epsilon}(k)\,) \, v^{s'}(p) \right]$$

$$= -(-ie)^2 \int d\Pi \, \mathrm{tr} \left[\not{\epsilon}(k) \, (\not{q} + m) \, \not{\epsilon}(k) \, (\not{p} - m) \right] . \qquad (3.20)$$

Notice the minus sign in front of the mass in the antispinor spin sum. The phase space integral is explicitly [13]

$$\int d\Pi \, [\ldots] = \int \frac{d^3q}{(2\pi)^3} \frac{1}{2q_0} \int \frac{d^3p}{(2\pi)^3} \frac{1}{2p_0} (2\pi)^4 \delta^{(4)}(k - p - q) \, [\ldots] \, . \qquad (3.21)$$

Because $q_0 = \sqrt{\vec{q}^2 - m^2}$ we have

$$\int \frac{d^3q}{(2\pi)^3} \frac{1}{2q_0} [\ldots] = \int \frac{d^4q}{(2\pi)^4} \, (2\pi) \, \theta(p_0) \, \delta(p^2 - m^2) \, [\ldots] \, . \qquad (3.22)$$

Integrating out the four-momentum p, sending $q \to -q$ and pulling the overall minus sign inside the trace, one obtains precisely (3.19).

We observe that both cases, a different sign for one of the two vertices was canceled by another minus sign. In the cut diagram case that other minus sign was due to the fermion loop, while in the second case it arose from the sum over antispinor spin states.

3.3. Dispersion Relations

The unitarity method provides a way to compute the imaginary part of an amplitude, as we have witnessed in the previous sections. But of course the real part of an amplitude is of interest as well, if we want to do physically relevant computations. The idea of this section is to show how to construct the real part of an amplitude from its imaginary part by means of dispersion relations.

The use of dispersion relations goes back to Kramers and Krönig [18] in optics. Making use of the Cauchy integral formula and the optical theorem they derived [5]

$$\mathrm{Re}\ f(\omega) = \mathrm{Re}\ f(0) + \frac{\omega^2}{2\pi^2} \mathrm{P} \int_0^\infty d\omega' \frac{\sigma_{tot}(\omega')}{\omega'^2 - \omega^2} \, , \qquad (3.23)$$

to calculate the real part of the forward scattering amplitude in terms of the total cross-section. We shall derive an analogous result for a scattering amplitude.

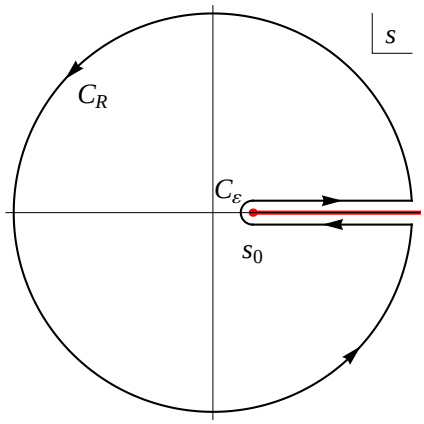

Figure 3.5.: The contour γ used in (3.26). There is a branch cut along the positive real axis, from s_0 to infinity, around which the contour is wrapped.

Consider an amplitude $\mathcal{M}(s)$ as a function of the square center-of-mass energy and suppose it has a branch cut, starting at the threshold s_0 for producing a real intermediate state, extending to infinity. We would like to apply the Cauchy integral formula

$$f(\omega) = \frac{1}{2\pi i} \oint_\gamma d\omega' \, \frac{f(\omega')}{\omega' - \omega} \,, \tag{3.24}$$

to the contour shown in figure 3.5. Below the threshold s_0 the amplitude is real, because intermediate particles cannot be produced on-shell. Assuming that $\mathcal{M}(s)$ can be defined for complex s in the upper half complex plane, the Schwartz reflection principle then allows us to extend its domain to the lower half complex plane, via $\mathcal{M}(s^*) = \mathcal{M}^*(s)$. Along the branch cut, with $s > s_0$ real, we have

$$\lim_{\varepsilon \to 0^+} \left[\mathcal{M}(s + i\,\varepsilon) - \mathcal{M}(s - i\,\varepsilon) \right] = 2i \ \mathrm{Im} \ \mathcal{M}(s) \,. \tag{3.25}$$

Then

$$\mathcal{M}(s) = \frac{1}{2\pi i} \int_{s_0}^{\infty} ds' \, \frac{\mathcal{M}(s' + i\,\varepsilon) - \mathcal{M}(s' - i\,\varepsilon)}{s' - s} + \frac{1}{2\pi i} \int_{C_R + C_\varepsilon} ds' \, \frac{\mathcal{M}(s')}{s' - s} \,, \tag{3.26}$$

for any s inside the contour. If the contributions from the circle C_R and semicircle C_ε vanish in the limits $\varepsilon \to 0$ and $R \to \infty$, we are left with

$$\mathcal{M}(s) = \frac{1}{\pi} \int_{s_0}^{\infty} ds' \, \frac{\mathrm{Im} \ \mathcal{M}(s')}{s' - s} \,. \tag{3.27}$$

If the contribution from the circle C_R does not vanish, then one can subtract $\mathcal{M}(\tilde{s})$ from $\mathcal{M}(s)$ and use partial fractions to make the integrand vanish faster at infinity by

a factor $1/s'$.

$$\begin{aligned}\mathcal{M}(s)-\mathcal{M}(\tilde{s}) &= \frac{s-\tilde{s}}{2\pi i}\int_{s_0}^{\infty} ds'\,\frac{\mathcal{M}(s'+i\,\varepsilon)-\mathcal{M}(s-i\,\varepsilon)}{(s'-s)(s'-\tilde{s})}\\ &+ \frac{s-\tilde{s}}{2\pi i}\int_{C_R+C_\varepsilon} ds'\,\frac{\mathcal{M}(s')}{(s'-s)(s'-\tilde{s})}\,.\end{aligned} \tag{3.28}$$

When the contribution from the circle vanishes due to this adjustment, then one is left with

$$\mathcal{M}(s)=\mathcal{M}(\tilde{s})+\frac{s-\tilde{s}}{\pi}\int_{s_0}^{\infty} ds'\,\frac{\text{Im}\;\mathcal{M}(s')}{(s'-s)(s'-\tilde{s})}\,. \tag{3.29}$$

As an example, one can apply (3.29) to the imaginary part of the vacuum polarization (2.15). In the current notation, that imaginary part is given by

$$\text{Im}\;\Pi(s)=-\frac{\alpha}{3}\left(1+\frac{s_0}{2s}\right)\sqrt{1-\frac{s_0}{s}} \tag{3.30}$$

for $s>s_0$, with $s=k^2$ and $s_0=4m^2$. A computation of the resulting integral can be found in [19]. The result is precisely (2.16). The precise form of $\Pi(0)$ is not recovered in this manner, however. One could say that the result is implicitly renormalized.

In conclusion, the real part of an amplitude can be calculated from the imaginary part by means of the dispersion relation (3.27) or (3.29).

3.4. Generalized Unitarity

A severe limitation of the unitarity method lies in the application of the dispersion relations. For more than two external particles the amplitude becomes a function of multiple Lorentz invariants. Consequently, the analytic structure is rather complicated and makes the contour integration a lot harder.

The generalized unitarity method is a way to circumvent the use of dispersion relations [7], [20]. A review is given in [21]. The crucial observation is that a general one-loop amplitude is decomposable into a basis of scalar integrals.

$$\mathcal{M}=\sum_i c_i B_i\,. \tag{3.31}$$

The scalar integrals B_i are up to 4-point integrals and form a finite basis. In chapter 4 we demonstrate how to determine the basis explicitly. The derivation makes use of Passarino-Veltman reduction of tensor integrals and the result [6].

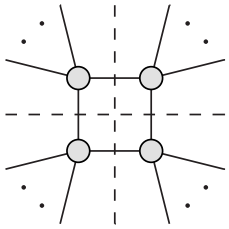

Figure 3.6.: Quadruple cut on a one-loop integral to determine its coefficient d(ijkl) in front of the corresponding scalar box integral.

In more explicit form we can write (3.34) as

$$\begin{aligned}\int \frac{d^4l}{(2\pi)^4}\frac{N(l)}{D_0 D_1 \dots D_{n-1}} \;=\; & \sum_{i_0<i_1<i_2<i_3}^{n-1} d(i_0 i_1 i_2 i_3) \int \frac{d^4l}{(2\pi)^4}\frac{1}{D_{i_0} D_{i_1} D_{i_2} D_{i3}} \\ & + \sum_{i_0<i_1<i_2}^{n-1} c(i_0 i_1 i_2) \int \frac{d^4l}{(2\pi)^4}\frac{1}{D_{i_0} D_{i_1} D_{i_2}} \\ & + \sum_{i_0<i_1}^{n-1} b(i_0 i_1) \int \frac{d^4l}{(2\pi)^4}\frac{1}{D_{i_0} D_{i_1}} \\ & + \sum_{i_0}^{n-1} a(i_0) \int \frac{d^4l}{(2\pi)^4}\frac{1}{D_{i_0}} + \mathcal{R}\,. \end{aligned} \tag{3.32}$$

The generic one-loop integral on the left hand side is expressed in terms of scalar box, triangle, bubble and tadpole integrals plus possibly a remainder $\mathcal{R}$, called a rational term. There are multiple integrals of each type (e.g. box), containing all possible subsets of (e.g. 4) denominators from the original integral. Diagrammatically (3.32) reads

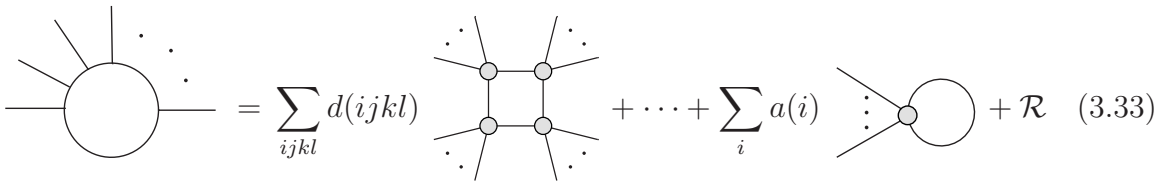

(3.33)

Once the coefficients in the expansion are known we are done, since the scalar integrals can be found in the literature, see e.g. [22]. The coefficients are the determined as follows. Making use of the Cutkosky cutting rule of unitarity (3.15) one can relate the imaginary parts of both sides of (3.34),

$$\text{Im}\ \mathcal{M} = \sum_i c_i\ \text{Im}\ B_i\,. \tag{3.34}$$

Doing so for all possible cuttings allows to read of the coefficients c_i.

In addition one performs more cuts than the standard unitarity method. There, cutting one-loop diagrams leads to precisely two cut propagators. Here double cuts are performed as well, see figure 3.6, thereby extending the original unitarity method. Actually, this method is often used the other way around. One-loop amplitudes are then constructed by 'gluing' tree amplitudes together and promoting the delta function to propagators.

Chapter 4.

OPP Reduction

In the previous chapter we introduced generalized unitarity, where a general one-loop amplitudes is expanded in a basis of known scalar integrals. The coefficients in such a basis are found by applying unitarity cuts and relating imaginary parts on both sides. This process is hard to automate, however, since the precise analytic properties of the amplitude must be known.

In this chapter we determine such coefficients using an idea by Ossola, Papadopoulos and Pittau (OPP), which is basically to expand the integrand rather than the integral. The coefficients are determined by evaluating the integrand at certain loop momenta, which is much easier to implement.

In this chapter we derive the integrand decomposition and explain how the coefficients are determined in general. We then discuss the construction of rational parts of the amplitude. As an illustration, a manageable problem is worked out in detail. In the last section we discuss implementations of the algorithm.

4.1. Integrand Decomposition

The aim of this section is to determine the form of the integrand expansion. We will first show the expansion, which is dubbed *master formula* in the OPP method, and explain some of its features. After introducing the van Neerven-Vermaseren basis, we are in the position to derive the master formula by means of tensor reduction.

4.1.1. Master Formula

Consider an amplitude for n-particle scattering at the one-loop level. The amplitude depends on the external momenta via the Lorentz invariants $s_{ij} = p_i \cdot p_j$ and also on the masses of virtual particles propagating through the loop. Any one-loop (sub)amplitude

can be written as

$$\mathcal{M}_n(s_{ij}, m_i^2) = \int \frac{d^4l}{(2\pi)^4} \frac{N(l)}{D_0 D_1 \dots D_{n-1}} \,. \tag{4.1}$$

Here, the numerator $N(l)$ represents an 'effective' numerator generated by the sum of all one-loop Feynman diagrams that contribute to the amplitude. Diagrams with fewer internal propagators are included in $N(l)$ by trivially canceling the appropriate denominators.

The inverse Feynman propagators appearing in the denominator are given by $D_i = (l + q_i)^2 - m_i^2$. In here the momenta q_i are partial sums of external momenta, although the precise relation between the two is ambiguous. Often, one chooses q_0 to be zero, thereby fixing all other q_i in terms of the external momenta: $q_i = p_1 + p_2 + \dots + p_i$, as can be verified from figure 4.1. We shall refrain from making such a choice for the time being, that is, we assume $q_0 \neq 0$. In that way all denominators D_i are treated on an equal footing. Only at the very end, when a final expression for the amplitude is obtained, do we make such a choice.

It has been shown in [23] that the numerator of the integrand in (4.1) can be decomposed into

$$\begin{aligned} N(l) \;=\; & \sum_{i_0<i_1<i_2<i_3}^{n-1} [d(i_0 i_1 i_2 i_3) + \tilde{d}(l; i_0 i_1 i_2 i_3)] \prod_{k\neq i_0,i_1,i_2,i_3}^{n-1} D_k + \\ & \sum_{i_0<i_1<i_2}^{n-1} [c(i_0 i_1 i_2) + \tilde{c}(l; i_0 i_1 i_2)] \prod_{k\neq i_0,i_1,i_2}^{n-1} D_k + \\ & \sum_{i_0<i_1}^{n-1} [b(i_0 i_1) + \tilde{b}(l; i_0 i_1)] \prod_{k\neq i_0,i_1}^{n-1} D_k + \\ & \sum_{i_0}^{n-1} [a(i_0) + \tilde{a}(l; i_0)] \prod_{k\neq i_0}^{n-1} D_k + \\ & \tilde{P}(l) \prod_{k}^{n-1} D_k \,. \end{aligned} \tag{4.2}$$

This is the master formula of the OPP reduction method. In the next two subsection we shall explain how this decomposition comes about. For now, let us inspect the contents of the given formula.

There appear two types of coefficients: the ones with a tilde, $\tilde{d}, \tilde{c}, \tilde{b}, \tilde{a}$ and $\tilde{P}$, and the ones without, d, c, b and a. The coefficients with a tilde are called *spurious terms*. They depend on the loop momentum in such a way that, after substitution of (4.2) into (4.1), they vanish upon integration over the loop momentum. The coefficients a, b, c and d then remain and multiply scalar tadpole, bubble, triangle and box diagrams. In

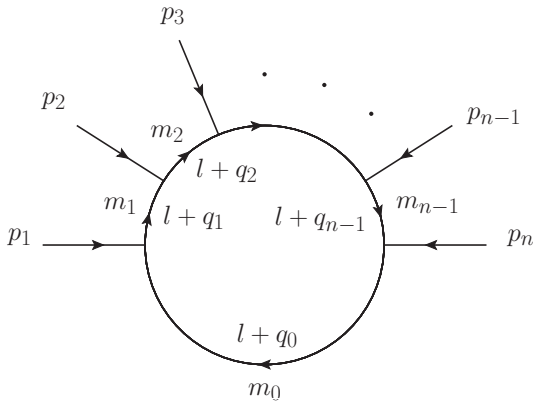

Figure 4.1.: A diagrammatic representation of the one-loop amplitude for n-particle scattering, given in (4.1).

other words, we are lead to the amplitude expansion (3.32) in the generalized unitarity method.

On a close inspection, one may observe, that the amplitude expansion is actually not entirely reproduced: the rational part is missing. This has to do with the fact that the rational part is an artifact of dimensional regularization, while we do not employ dimensional regularization at this stage. The problem of the missing rational part shall be resolved later on in section 4.3.

As a final remark we note that in a renormalizable gauge $\tilde{P}(l)$ is zero. The reason is that in such a gauge the numerator on the left hand side is at most of order $\mathcal{O}(|l|^n)$, while the term with $\tilde{P}(l)$ is the only one on the right hand side of order $\mathcal{O}(|l|^{2n})$ or higher. Since the formula holds for any l, we are led conclude that $\tilde{P}(l) = 0$.

4.1.2. The van Neerven-Vermaseren Basis

In order to derive the master formula we introduce first the van Neerven-Vermaseren basis. The basis takes its name from the first use by van Neerven and Vermaseren in [6].

In an n-particle scattering there are $n-1$ linearly independent external momenta due to momentum conservation. The same holds for the q_i in the internal propagators, since they are linear combinations of the external momenta. This notion can be expressed by shifting the loop momentum $l \to l' - q_0$ in (4.1) to obtain

$$\mathcal{M}_n = \int \frac{d^4 l'}{(2\pi)^4} \frac{N(l'-q_0)}{(l'^2 - m_0^2)((l'+k_1)^2 - m_1^2)\dots((l'+k_{n-1})^2 - m_{n-1}^2)} \,. \tag{4.3}$$

where we introduced vectors k_i defined by

$$k_i := q_i - q_0 \,. \tag{4.4}$$

Notice that whereas q_i are not unambiguously defined in terms of p_j, differences between them are. In particular we have $k_i = p_1 + \cdots + p_i$ for $i = 1, \ldots, n-1$.

The space that is spanned by the $n-1$ vectors k_i is referred to as the physical space. It has dimension $d_P = \min(4, n-1)$. We define the transverse space as the complement of the physical space in four dimensional spacetime.

For the bases of the physical and transverse space, we use the following notation. The *generalized Kronecker symbol* is defined as the determinant of a square matrix of ordinary Kronecker deltas,

$$\delta^{\mu_1\mu_2\ldots\mu_k}_{\nu_1\nu_2\ldots\nu_k} := \begin{vmatrix} \delta^{\mu_1}_{\nu_1} & \delta^{\mu_1}_{\nu_2} & \ldots & \delta^{\mu_1}_{\nu_k} \\ \delta^{\mu_2}_{\nu_1} & \delta^{\mu_2}_{\nu_2} & \ldots & \delta^{\mu_2}_{\nu_k} \\ \vdots & \vdots & & \vdots \\ \delta^{\mu_k}_{\nu_1} & \delta^{\mu_k}_{\nu_2} & \ldots & \delta^{\mu_k}_{\nu_k} \end{vmatrix} . \tag{4.5}$$

We use a compact notation where indices of the generalized Kronecker symbol are replaced by the label of the vector they are contracted with.

$$\delta^{p\mu_2\ldots\mu_k}_{\nu_1 q\ldots\nu_k} := \delta^{\mu_1\mu_2\ldots\mu_k}_{\nu_1\nu_2\ldots\nu_k} p_{\mu_1} q^{\nu_2} . \tag{4.6}$$

For $k = 1$ we can generate objects like $\delta^{\mu}_{q} = q^{\mu}$ and $\delta^{p}_{q} = p \cdot q$. For $k = 2$ we have $\delta^{p_1 p_2}_{q_1 q_2} = p_1 \cdot q_1\, p_2 \cdot q_2 - p_1 \cdot q_2\, p_2 \cdot q_1$ and so on. A special case is when the same set of vectors appears as upper and lower indices, which gives the *Gram determinant*

$$\Delta(q_1, \ldots, q_k) := \det\left(q_i \cdot q_j\right)_{k\times k} = \delta^{q_1 q_2\ldots q_k}_{q_1 q_2\ldots q_k} . \tag{4.7}$$

As a basis for the physical space we could simply use the set of vectors $\{k_i\}_{i=1,\ldots,d_P}$. However, for reasons that become clear later, we prefer to use its dual basis $\{v_i\}_{i=1,\ldots,d_P}$ defined by the condition $k_i \cdot v_j = \delta_{ij}$. Using the introduced notation, we can explicitly construct the dual basis

$$v_i^{\mu} := \frac{\delta^{k_1 \ldots \mu \ldots k_{d_P}}_{k_1 \ldots k_i \ldots k_{d_P}}}{\Delta(k_1, \ldots, k_{d_P})} . \tag{4.8}$$

Note that the vectors v_i^{μ} are not orthogonal, indeed $v_i \cdot v_j = \Delta_{ij}/\Delta(k_1, \ldots, k_{d_P})$ where Δ_{ij} is the determinant of the (i, j) cofactor of the matrix $(k_\alpha \cdot k_\beta)_{d_P\times d_P}$.

A basis $\{n_i\}_{i=d_P+1,\ldots,4}$ for the transverse space is defined to be orthonormal and orthogonal to the physical space. It can be constructed from the d_P vectors k_i and from $(4 - d_P)$ vectors a_i chosen such that all vectors are linearly independent. Then [24]

$$n_i^{\mu} := \frac{\delta^{k_1 \ldots k_{d_P}\, a_{d_P+1} \ldots \mu}_{k_1 \ldots k_{d_P}\, a_{d_P+1} \ldots a_i}}{\sqrt{\Delta(k_1, \ldots, k_{d_P}, a_{d_P+1}, \ldots, a_{i-1})}\sqrt{\Delta(k_1, \ldots, k_{d_P}, a_{d_P+1}, \ldots, a_i)}} , \tag{4.9}$$

for $i = d_P + 1, \ldots, 4$.

As an overview and reference we record the relevant dot products:

$\cdot$	k_j	v_j	n_j
k_i	$k_i \cdot k_j$	δ_{ij}	0
v_i	δ_{ij}	Δ_{ij}/Δ	0
n_i	0	0	δ_{ij}

(4.10)

where the indices on k_i and v_i run from $1, \ldots, d_P$, while those on the perpendicular vectors n_i run from $d_P + 1, \ldots, 4$.

These bases are useful to parametrize the loop momentum of the integral (4.3),

$$l'^{\,\mu} = \sum_{i=1}^{d_P} c_i v_i^\mu + \sum_{i=d_P+1}^{4} \bar{c}_i n_i^\mu \,. \tag{4.11}$$

Contracting with k_j or n_j and using the dot products given in (4.10), we find the coefficients $c_i = l' \cdot k_i$ and $\bar{c}_i = l' \cdot n_i$. Owing to the choice for a dual basis, the c_i can now be written as a difference of denominators.

$$\begin{aligned} 2\,c_i = 2\,l' \cdot k_i &= (l' + k_i)^2 - m_i^2 - (l'^{\,2} - m_0^2) - (k_i^2 - m_i^2 + m_0^2) \\ &= (l + q_i)^2 - m_i^2 - ((l + q_0)^2 - m_0^2) - (k_i^2 - m_i^2 + m_0^2) \\ &= D_i - D_0 - r_i \,. \end{aligned} \tag{4.12}$$

Notice that we reinstated the original loop momentum $l = l' - q_0$ in the second line after which we recognized the denominators D_i and D_0. In the last line we collected the last three term into

$$r_i := k_i^2 - m_i^2 + m_0^2 \,. \tag{4.13}$$

If we further define a vector w as

$$w := \tfrac{1}{2} \sum_{i=1}^{d_P} r_i v_i \,, \tag{4.14}$$

than the original loop momentum is parametrized as

$$l^\mu = -q_0^\mu - w^\mu + \tfrac{1}{2} \sum_{i=1}^{d_P} (D_i - D_0) v_i^\mu + \sum_{i=d_P+1}^{4} ((l + q_0) \cdot n_i) n_i^\mu \,. \tag{4.15}$$

This expression will play an important role in the reduction of integrals, a topic we shall now discuss.

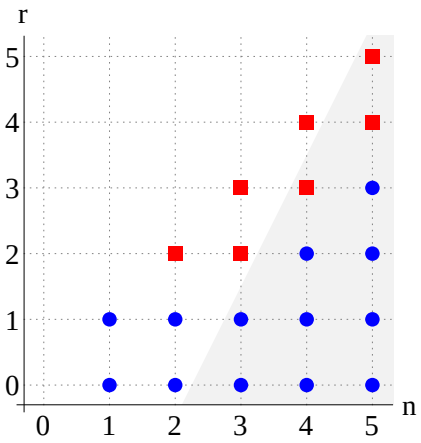

Figure 4.2.: Overview of the first n-point rank-r integrals in four dimensions. Integrals that lead to rational terms are represented by red squares, while the blue circles represent cut-constructable integrals: $r < \max(2, n-1)$. Integrals inside the shaded area are UV-finite by power counting: $r < 2n-4$

4.1.3. Tensor Reduction of One-Loop Integrals

We now use the van Neerven-Vermaseren basis to reduce tensor integrals to scalar integrals and integrals with spurious terms. We start with a five-point integral, after which the general case easily follows.

Classification of Integrals

The *rank* r of the integral in (4.1) is defined as $N(\lambda l) \propto \lambda^r$ for $\lambda \to \infty$. Together with the number of denominators n, the rank r distinguishes different types of integrals. It is convenient to represent them as points in the (n, r)-plane, as is done in figure 4.2.

In a renormalizable gauge the maximal rank of an integral is equal to n, as we mentioned before. This is why the integrals shown in figure 4.2 form a triangle on and below the line $r = n$.

The OPP method we describe assumes a four-dimensional loop momentum. Integrals that do not have a rational part can be calculated by this method and are said to be *cut-constructable*. The method does not calculate rational parts of integrals, because those are an artifact n-dimensional regularization of UV-divergent integrals. It is however not true that all UV-divergent integrals contain rational parts and all other integrals don't. In order to have a rational part an integral must at least have rank $r = 2$, which leaves a couple of UV-divergent integrals that certainly have a rational part: (2,2), (3,2), (3,3), (4,4). In the reduction scheme we employ below, we observe furthermore that UV-finite integrals can reduce to those UV-divergent integrals by the least steep reduction step $(n, r) \to (n-1, r-1)$. The condition for an integral to have a rational part (in general) is therefor $r \geq \max(2, n-1)$ [7],[22]. These facts are summarized in figure 4.2.

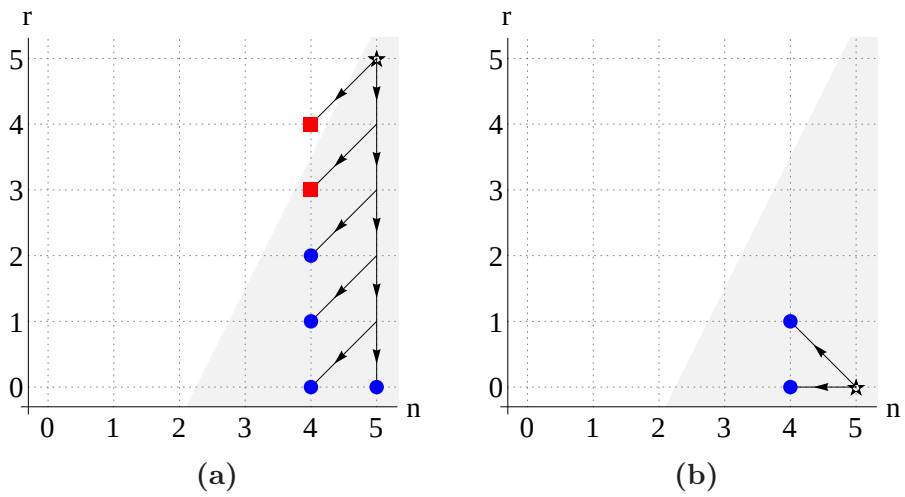

Figure 4.3.: Reduction of a general rank-five five-point integral (star) to lower point and/or rank cut-constructable integrals (blue dots) and integrals with a rational part (red squares). Step (a) is due to (4.16) and step (b) corresponds to (4.18).

Five-Point Integrals

Consider a rank-five five-point integral, that we would like to reduce to known integrals. We follow the same spirit of [25] with the difference that we present the method in four dimensions. The integrand can be written as $l^{\mu_0} \dots l^{\mu_4}/D_0 \dots D_4$. There are four reference momenta $k_1, \dots, k_4$, so the physical space has dimension four: $d_P = 4$. Hence, for the integrand of a five-point integral, (4.15) gives us

$$l^\mu = -q_0^\mu - w^\mu + \tfrac{1}{2}\sum_{i=1}^{4}(D_i - D_0)v_i^\mu \,. \tag{4.16}$$

By inserting this expression for first factor of l in the numerator of the integrand, the D_i and D_0 terms cancel against a denominator, giving rank-four four-point integrals. The first two terms give rise to rank-four five-point integrals. Schematically this is shown as the top two arrows in figure 4.3a.

The resulting five-point integrals of lower rank can be further in the same way. Whenever D_0 is canceled in the process, the loop momentum must be shifted to $l - q_1$ to bring the integral to the form where the first denominator is $l^2 - m_1^2$. Of course, shifting the loop momentum in the numerator generates new terms, but those are all at least one rank lower and can be dealt with in the next reduction steps. It should be clear that in this way the rank-five five-point integrals can be reduced to a scalar five-point integrals and a collection of four-point integrals of rank one to four, as displayed in figure 4.3a.

The scalar five-point integral can be further reduced to scalar four-point integrals. To this end, square $l + q_0$ and substitute the van Neerven-Vermaseren basis in two steps,

such that the result is at most linear in denominators.

$$\begin{aligned}(l+q_0)^2 &= (l+q_0)\cdot\left(-w+\tfrac{1}{2}\sum_{i=1}^{4}(D_i-D_0)v_i\right)\\ &= w^2+\tfrac{1}{2}\sum_{i=1}^{4}(D_i-D_0)\,(l+q_0-w)\cdot v_i\,. \end{aligned} \tag{4.17}$$

On the other hand $(l+q_0)^2 = D_0 + m_0^2$. Equating and rearranging leads to

$$m_0^2 - w^2 = \tfrac{1}{2}\sum_{i=1}^{4}(D_i-D_0)(l+q_0-w)\cdot v_i - D_0\,. \tag{4.18}$$

The left hand side is independent of the loop momentum, while all terms on the right hand side carry one inverse propagator. Dividing by $D_0D_1\dots D_4$ and integrating we find a relation between a scalar five-point integral and scalar and rank-one four-point integrals, as depicted in figure 4.3b.

In fact, the rank-one terms vanish [6] upon integration. We can understand this in the following way. The $D_i\,(l\cdot v_i)$ terms vanish because the denominator with the reference vector k_i is removed and $k_j\cdot v_i = 0$ for $j\neq i$. In the $D_0\,(l\cdot\sum_i v_i)$ term, one shifts the loop momentum to $l\to l'-q_1$. Then the reference vectors become $q_j-q_1 = (q_j-q_0)-(q_1-q_0) = k_j-k_1$ for $j=2,3,4$. Such combinations are perpendicular to the vector $\sum_i v_i$. In other words, the rank-one terms are spurious terms.

In conclusion any five-point integral is *fully reducible*, that is, reducible exclusively to lower-point integrals. It is easy to see that these reduction steps generalize to higher point integrals, because the loop momentum decomposition remains the same as $d_P = 4$ in all cases [25]. Consequently we consider all integrals with $n\geq 5$ fully reducible.

Four-Point Integrals

The highest rank integral left from the previous reduction is the four-point rank-four integral, with integrand $l^{\mu_0}l^{\mu_1}l^{\mu_2}l^{\mu_3}/D_0D_1D_2D_3$. The method of reduction is the same as before, however we cannot reduce as far because the van Neerven-Vermaseren basis is different. Indeed, now there are only three reference vectors, k_1, k_2 and k_3, so $d_P = 3$ and (4.15) gives

$$l^\mu = -q_0^\mu - w^\mu + \tfrac{1}{2}\sum_{i=1}^{3}(D_i-D_0)v_i^\mu + ((l+q_0)\cdot n_4)n_4^\mu\,. \tag{4.19}$$

By inserting this expression for l^{μ_0} in the integrand we obtain tree- and four-point integrals of one rank lower, but also a term $(l+q_0)\cdot n_4$ which is still of rank four. This first reduction step is shown by the top three arrows in figure 4.4a.

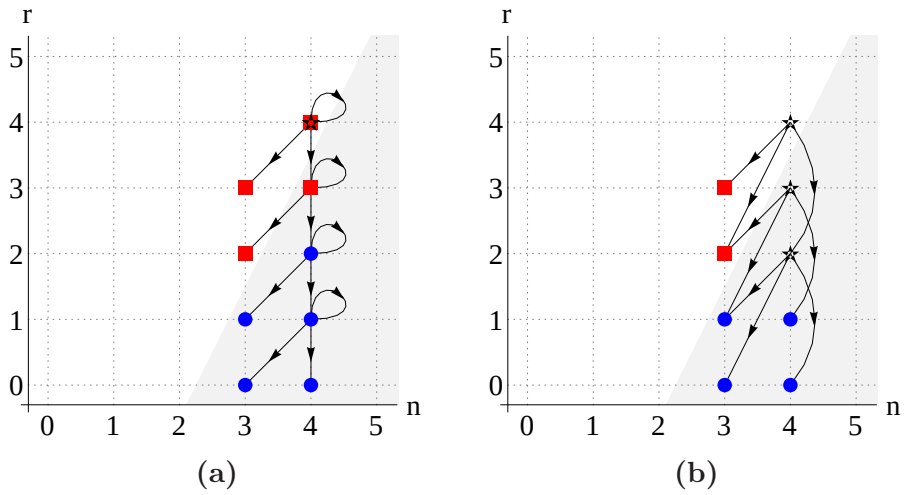

Figure 4.4.: Reduction of a general rank-four four-point integral (star) to lower point and/or rank cut-constructable integrals (blue dots) and integrals with a rational part (red squares). Step (a) is due to (4.19) and step (b) corresponds to (4.20). The more elaborate reduction path, as compared to figure 4.3, is due to the fact that the result of a scalar four-point integral can only span a three-dimensional subspace of our Minkowski spacetime.

The last terms is left unreduced, so it seems that we are stuck. However, applying the reduction once more to that term it becomes proportional to $((l+q_0)\cdot n_4)^2$. The latter can be simplified using the analog of the relation that allowed to reduce the scalar five-point integral. In the same way as (4.17)-(4.18), but this time with the decomposition (4.19), we deduce

$$((l+q_0)\cdot n_4)^2 = m_0^2 - w^2 + D_0 - \tfrac{1}{2}\sum_{i=1}^{3}(D_i - D_0)(l+q_0-w)\cdot v_i\,. \tag{4.20}$$

This equation allows us to write the unreduced integral in terms of three types of integrals, all of lower rank. This reduction is shown as the top three arrows in figure 4.4b.

Continuing in this fashion, we generate four-point integrals proportional to $((l+q_0)\cdot n_4)^r$ with ranks zero up to four. The ones with $r=2,3$ and 4 are reducible by means of (4.20). See also figure 4.4b. Two types remain, namely a scalar integral and a rank-one integral. The latter is the spurious term for the box integral

$$\tilde{d}(l;0123) = \tilde{d}_1(0123)((l+q_0)\cdot n_4)\,. \tag{4.21}$$

In the master formula (4.2) we need the general case, for indices $i_0,\ldots,i_3$. Because we are treating all denominators on equal footing (by assuming $q_0 \neq 0$), this is simply a matter of relabeling indices. The indices on the D_i and consequently on the q_i and m_i are to be mapped from $\{0,1,2,3\}$ to $\{i_0,i_1,i_2,i_3\}$.

This concludes the first step in proving the master formula for the integrand, while determining on-the-fly the explicit loop momentum dependence of the spurious term $\tilde{d}$.

Three-Point Integrals

Let us first summarize the results obtained so far. We have demonstrated that five-point integrals are fully reducible, but that four-point integrals are not. It shall come as no surprise that these are the boundary cases and that the even lower-point integrals are not fully reducible either. Following the same recipe as above one can reduce those integrals and derive the spurious terms for the triangle, bubble and tadpole coefficients.

A slight difference is that there appears freedom of choice in the form of the spurious terms. For a three-point integral there are two vectors v_1, v_2 and two vectors n_3, n_4. Reduction generates the numerators $(l' \cdot n_3)^{r_3}(l' \cdot n_4)^{r_4}$ with $r = r_3 + r_4 = 1, 2, 3$, from which one can form $2 + 3 + 4 = 9$ spurious terms [1]. However, not all of them are independent. Squaring the loop momentum we deduce this time $(l' \cdot n_3)^2 + (l' \cdot n_4)^2 = const. + \mathcal{O}(D_i)$, which can be used to eliminate three elements from the set of nine spurious terms.

i) $(l' \cdot n_3)^2$ and $(l' \cdot n_4)^2$ can be written as their difference and their sum, the latter being reducible and therefor not spurious.

ii) $(l' \cdot n_3)(l' \cdot n_4)^2$ can be written as $(l' \cdot n_3)^3$ plus reduced terms.

iii) $(l' \cdot n_3)^2(l' \cdot n_4)$ can be written as $(l' \cdot n_4)^3$ plus reduced terms.

This leaves six spurious terms for the three-point integral

$$\begin{aligned} \tilde{c}(l) &= \tilde{c}_1(l' \cdot n_3) + \tilde{c}_2(l' \cdot n_4) + \tilde{c}_3(l' \cdot n_3)(l' \cdot n_4) + \\ &\quad \tilde{c}_4[(l' \cdot n_3)^2 - (l' \cdot n_4)^2] + \tilde{c}_5(l' \cdot n_3)^3 + \tilde{c}_6(l' \cdot n_4)^3 , \end{aligned} \tag{4.22}$$

where we suppressed the indices $i_0 i_1 i_2$ and where $l' = l + q_0$.

Two- and One-Point Integrals

By now we have discussed all subtleties of the reduction of tensor integrals. The spurious terms for the two- and one-point integrals are given by

$$\begin{aligned} \tilde{b}(l) &= \tilde{b}_1(l' \cdot n_2) + \tilde{b}_2(l' \cdot n_3) + \tilde{b}_3(l' \cdot n_4) + \\ &\quad \tilde{b}_4(l' \cdot n_2)(l' \cdot n_3) + \tilde{b}_5(l' \cdot n_3)(l' \cdot n_4) + \tilde{b}_6(l' \cdot n_2)(l' \cdot n_4) + \\ &\quad \tilde{b}_7[(l' \cdot n_2)^2 - (l' \cdot n_4)^2] + \tilde{b}_8[(l' \cdot n_3)^2 - (l' \cdot n_4)^2] , \end{aligned} \tag{4.23}$$

[1] Notice that we write $l' = l + q_0$ to keep the notation compact.

and

$$\tilde{a}(l) = \tilde{a}_1(l' \cdot n_1) + \tilde{a}_2(l' \cdot n_2) + \tilde{a}_3(l' \cdot n_3) + \tilde{a}_4(l' \cdot n_4)\,. \tag{4.24}$$

4.2. Determination of Coefficients

After establishing the master formula and the explicit l-dependence of the spurious terms, we are set to further develop the OPP reduction method. The integral (4.1) for a one-loop n-particle scattering amplitude can in general not be calculated directly. Substituting the master formula in place of the numerator, reduces the integral to a set of scalar integrals multiplied by the coefficients a, b, c and d. While the scalar are known and can be looked up in the literature (see for example [22]), the coefficients are to be determined.

The idea is to evaluate both sides of the master formula at different loop momenta to obtain a system of equations that allows one to determine the coefficients. Inverting the resulting system of equations can be highly inefficient when the number of coefficients is large. For generic n, that number is $2\binom{n}{4} + 7\binom{n}{3} + 9\binom{n}{2} + 5\binom{n}{1}$. Cases of interest are typically $n = 5, 6, 7, \ldots$ for which the number of coefficients is $195, 335, 539, \ldots$. Clearly the inversion of such large systems of equations is to be avoided.

A better approach is to construct a triangular system of equations. Assume that there exist two loop momenta for which the four denominators $D_{i_0}, \ldots, D_{i_3}$ are zero. Evaluating the master formula (4.2) at those loop momenta leaves on the right hand side only the coefficients $d(i_0 i_1 i_2 i_3)$ and $\tilde{d}(1; i_0 i_1 i_2 i_3)$, since only those terms contain none of the four denominators. This then generates two equations for two unknowns. Doing so for all possible choices $i_0 < i_1 < i_2 < i_3$, one efficiently determine all d-coefficients.

After subtraction of all terms with d-coefficients on both sides of (4.2) one is in the position to repeat the procedure for the c-coefficients. This time one needs seven loop momenta, to generate as many equations for the coefficients $c(i_0 i_1 i_2)$ and $\tilde{c}(1; i_0 i_1 i_2)$ up to $\tilde{c}(6; i_0 i_1 i_2)$. Continuing in the same fashion one can also find the b- and a-coefficients.

The advantage is that one has to invert many smaller systems of equations of at most 9×9. Notice that all coefficients d must be known, including the spurious ones, before one can start to determine the c coefficients. Likewise c must be known for b and b must be known for a. The spurious terms $\tilde{a}$ don't need to be found in principle.

As a final remark, we point out that we assumed such a triangular system of equations can actually be constructed. In particular there must be enough distinct loop momenta satisfying $D_{i_0} = \cdots = D_{i_k} = 0$ for $k = 0, 1, 2, 3$ in order to generate a sufficient number of independent equations for the coefficients. We will show that this is the case by explicit construction below.

Box Coefficients

To keep the notation light we consider the determination of a specific box coefficient: $d(0123)$. Coefficients for other box integrals can be found analogously.

We must find loop momenta that satisfy $D_0 = D_1 = D_2 = D_3 = 0$. The loop momentum for a box diagram is written as defined in (4.15) with $d_P = 3$. Imposing the three conditions $D_k = D_0$ for $k = 1, 2, 3$ the third term in (4.15) vanishes. Plugging the resulting loop momentum into the remaining condition, $D_0 = 0$, we find two solutions

$$l_\pm^\mu = -q_0^\mu - w^\mu \pm \sqrt{m_0^2 - w^2}\, n_4^\mu \,. \tag{4.25}$$

At these loop momenta, most terms on the right hand side of the master formula vanish, see (4.2) with the explicit spurious terms (4.21)-(4.24). We retain

$$\begin{aligned} N(l_\pm) &= [d(0123) + \tilde{d}_1(0123)((l_\pm + q_0)\cdot n_4)] \prod_{k\neq 0,1,2,3}^{n-1} D_k(l_\pm) \\ &= [d(0123) \pm \tilde{d}_1(0123)\sqrt{m_0^2 - w^2}] \prod_{k\neq 0,1,2,3}^{n-1} D_k(l_\pm) \,. \end{aligned} \tag{4.26}$$

In terms of

$$L(l_\pm) := \frac{N(l_\pm)}{\prod_{k\neq 0,1,2,3}^{n-1} D_k(l_\pm)} \,, \qquad l_\perp := \sqrt{m_0^2 - w^2} \,, \tag{4.27}$$

the coefficients are elegantly written as

$$d(0123) = \frac{L(l_+) + L(l_-)}{2} \,, \qquad \tilde{d}_1(0123) = \frac{L(l_+) - L(l_-)}{2\, l_\perp} \,. \tag{4.28}$$

Triangle Coefficients

Assuming all d-coefficients are known, one can turn to the determination of the triangle coefficients. Again, we focus on a specific coefficient $c(012)$, together with the spurious terms $\tilde{c}_i(012)$. Applying the same approach as for the box coefficients, one finds a continuous set of solutions parametrized by an angle $\phi \in [0, 2\pi)$.

$$l_\phi^\mu = -q_0^\mu - w^\mu + \sqrt{m_0^2 - w^2}\, (\cos\phi\, n_3^\mu + \sin\phi\, n_4^\mu) \,. \tag{4.29}$$

At these loop momenta the master formula can be written as

$$L(l_\phi) = [c(012) + \tilde{c}_1(012)((l_\phi + q_0)\cdot n_3) + \cdots + \tilde{c}_6(012)((l_\phi + q_0)\cdot n_4)^3] \,, \tag{4.30}$$

where

$$L(l_\phi) = \frac{N(l_\phi) - \sum_{i=1}^{n-1}[d(012i) + \tilde{d}_1(012i)((l_\phi + q_0)\cdot n_4)]\prod_{k\neq 0,1,2,i}^{n-1} D_k(l_\phi)}{\prod_{k\neq 0,1,2}^{n-1} D_k(l_\phi)}\,. \tag{4.31}$$

The vector n_4 in the numerator of (4.31) is perpendicular to k_1, k_2 and k_i and originates from the determination of the box coefficients. It is different from the vector n_4 in (4.30), which is perpendicular to k_1, k_2 and n_3, with n_3 some vector perpendicular to k_1 and k_2.

As there are many vectors l_ϕ, there are many possible systems of equations to generate, thus leaving potential for optimization. In [26] it is suggested to make use of a discrete Fourier transform. Essentially one writes the right hand side of (4.30) in terms of $x = e^{i\phi}$ instead of $\cos\phi$ and $\sin\phi$, which then becomes $\sum_{k=-3}^{3} c_k x^k$. Performing the substitution one easily finds the new coefficients c_k in terms of the old ones. The discrete Fourier transform then gives

$$c_k = \frac{1}{7}\sum_{n=0}^{6} L(l_{\phi=2\pi n/7}) e^{-2\pi n k/7}\,. \tag{4.32}$$

Connection with Unitarity

At this stage we would like to briefly point out the connection between the OPP method and unitarity, see chapter 3. The conditions that we impose here, namely $D_i = D_j = \cdots = 0$, are nothing other than putting the corresponding particle algebraically on-shell. This is in principle the same, though different in construction, as replacing propagators by delta functions according to the Cutkosky cutting rule (3.15). Regarding the number of conditions, this method extends both unitarity and generalized unitarity. At the one-loop level the latter methods put only two or four virtual particles on-shell.

4.3. Rational Part

As was advocated in the beginning, the rational parts originate from dimensionally regulated integrals. In this section we explain how they come about and how to calculate them, originally done in [27].

Since we are ultimately interested in four-dimensional spacetime, we perform the loop momentum integration in $d = 4 + \varepsilon$ dimensions. All d-dimensional objects, such as the loop momentum and functions thereof, are denoted by a bar. The integrand of an n-point amplitude then generalizes to

$$\frac{\bar{N}(\bar{l})}{\bar{D}_0\bar{D}_1\ldots\bar{D}_{n-1}}\,, \tag{4.33}$$

with $\bar{D}_i = (\bar{l} + q_i)^2 - m_i^2$. External momenta are kept four-dimensional. Assuming that the ε-dimensional space is orthogonal to the usual four-dimensional spacetime, we can split d-dimensional objects into 4- and ε-dimensional parts

$$\bar{l}^\mu = l^\mu + \tilde{l}^\mu \,, \tag{4.34}$$
$$\bar{\gamma}^\mu = \gamma^\mu + \tilde{\gamma}^\mu \,, \tag{4.35}$$
$$\bar{g}^{\mu\nu} = g^{\mu\nu} + \tilde{g}^{\mu\nu} \,, \tag{4.36}$$

where the tilde denotes the ε-dimensional part. The orthogonality implies

$$\tilde{l} \cdot p = 0 \,, \tag{4.37}$$
$$\{\gamma^\mu, \tilde{\gamma}^\nu\} = 0 \,. \tag{4.38}$$

This means that the numerator can also be split into $\bar{N}(\bar{l}) = N(l) + \tilde{N}(\tilde{l}^2, l, \varepsilon)$. The integrand becomes

$$\underbrace{\frac{N(l)}{\bar{D}_0 \bar{D}_1 \dots \bar{D}_{n-1}}}_{4\text{dim}+\mathcal{R}_1} + \underbrace{\frac{\tilde{N}(\tilde{l}^2, l, \varepsilon)}{\bar{D}_0 \bar{D}_1 \dots \bar{D}_{n-1}}}_{\mathcal{R}_2} \,. \tag{4.39}$$

The first term gives rise to the usual four-dimensional cut constructable part, plus a rational part called $\mathcal{R}_1$. The $\mathcal{R}_1$ part arises from a lack of cancellation between the $\bar{D}_i$ in the denominator and the D_i in the numerator expansion (4.2). The second term contains the ε-dimensional part of the numerator, leading to a rational part $\mathcal{R}_2$.

Rational Part $\mathcal{R}_1$

The rational part $\mathcal{R}_1$ arises from the first term in (4.39),

$$\frac{N(l)}{\bar{D}_0 \bar{D}_1 \dots \bar{D}_{n-1}} \,, \tag{4.40}$$

as a result of a mismatch between the different dimensions of the numerator and denominator. It is actually closely related to the four-dimensional OPP method, because we can obtain it from the four-dimensional method by shifting all masses $m_i^2 \to m_i^2 - \tilde{l}^2$ because that puts $D_i \to \bar{D}_i$.

The effect of such a mass shift is that all coefficients start to depend on $\tilde{l}^2$. Due to Lorentz symmetry the spurious terms still vanish upon integration, so they don't contribute to $\mathcal{R}_1$. The coefficients of the scalar integrals can be written as polynomials

in $\tilde{l}^2$ with the maximal power of $\tilde{l}$ restricted by the maximal rank of the integral [9].

$$\begin{aligned} a(i_0;\tilde{l}^2) &= a(i_0 i_1)\,, && (4.41)\\ b(i_0 i_1;\tilde{l}^2) &= b(i_0 i_1) + b^{(2)}(i_0 i_1)\,\tilde{l}^2\,, && (4.42)\\ c(i_0 i_1 i_2;\tilde{l}^2) &= c(i_0 i_1 i_2) + c^{(2)}(i_0 i_1 i_2)\,\tilde{l}^2\,, && (4.43)\\ d(i_0 i_1 i_2 i_3;\tilde{l}^2) &= d(i_0 i_1 i_2 i_3) + d^{(2)}(i_0 i_1 i_2 i_3)\,\tilde{l}^2 + d^{(4)}(i_0 i_1 i_2 i_3)\,\tilde{l}^4\,. && (4.44) \end{aligned}$$

The newly introduced coefficients $b^{(2)}, c^{(2)}, d^{(2)}, d^{(4)}$ are the coefficients of the following integrals, which are computed in [23],

$$\begin{aligned} \int d^d\bar{l}\frac{\tilde{l}^2}{\bar{D}_{i_0}\bar{D}_{i_1}} &= -\frac{i\pi^2}{2}\left[m_{i_0}^2 + m_{i_1}^2 - \frac{(q_{i_0}-q_{i_1})^2}{3}\right] + \mathcal{O}(\varepsilon)\,, && (4.45)\\ \int d^d\bar{l}\frac{\tilde{l}^2}{\bar{D}_{i_0}\bar{D}_{i_1}\bar{D}_{i_2}} &= -\frac{i\pi^2}{2} + \mathcal{O}(\varepsilon)\,, && (4.46)\\ \int d^d\bar{l}\frac{\tilde{l}^2}{\bar{D}_{i_0}\bar{D}_{i_1}\bar{D}_{i_2}\bar{D}_{i_3}} &= \mathcal{O}(\varepsilon)\,, && (4.47)\\ \int d^d\bar{l}\frac{\tilde{l}^4}{\bar{D}_{i_0}\bar{D}_{i_1}\bar{D}_{i_2}\bar{D}_{i_3}} &= -\frac{i\pi^2}{6} + \mathcal{O}(\varepsilon)\,. && (4.48) \end{aligned}$$

In conclusion, by dividing the integrals by $(2\pi)^4$, we get an explicit formula for the rational part $\mathcal{R}_1$, namely

$$\begin{aligned} \mathcal{R}_1 &= -\frac{i}{32\pi^2}\sum_{i_0<i_1}^{n-1} b^{(2)}(i_0 i_1)\left[m_{i_0}^2 + m_{i_1}^2 - \frac{(q_{i_0}-q_{i_1})^2}{3}\right] && (4.49)\\ &\quad -\frac{i}{32\pi^2}\sum_{i_0<i_1<i_2}^{n-1} c^{(2)}(i_0 i_1 i_2) && (4.50)\\ &\quad -\frac{i}{96\pi^2}\sum_{i_0<i_1<i_2<i_3}^{n-1} d^{(4)}(i_0 i_1 i_2 i_3)\,. && (4.51) \end{aligned}$$

The coefficients can be determined either numerically, e.g.

$$d^{(4)}(i_0 i_1 i_2 i_3) = \lim_{\tilde{l}^2\to\infty}\frac{d(i_0 i_1 i_2 i_3;\tilde{l}^2)}{\tilde{l}^4}\,, \qquad (4.52)$$

or as solution to system of equations, e.g.

$$d^{(4)}(i_0 i_1 i_2 i_3) = \frac{d(i_0 i_1 i_2 i_3;1) + d(i_0 i_1 i_2 i_3;-1) - 2d(i_0 i_1 i_2 i_3)}{2}\,. \qquad (4.53)$$

Rational Part $\mathcal{R}_2$

The rational part $\mathcal{R}_2$ arises from the second term in (4.39), due to the ε-dimensional numerator and is defined as

$$\mathcal{R}_2 := \int \frac{d^d\bar{l}}{(2\pi)^4} \frac{\tilde{N}(\tilde{l}^2, l, \varepsilon)}{\bar{D}_0 \bar{D}_1 \dots \bar{D}_{n-1}} \,. \tag{4.54}$$

In [27] is was proposed to calculate this rational part once and for all for certain diagrams. The only diagrams that contribute to $\mathcal{R}_2$ are the ones with non-negative superficial degree of divergence [28]. This limits the number of external particles to four and hence severely limits the number of processes to be considered. Recording the results as Feynman rules in the form of effective vertices allows one to simply look up $\mathcal{R}_2$ for any process.

The calculation of $\mathcal{R}_2$ for a particular diagram goes as follows. Applying the splitting rules (4.34)-(4.38) to the numerator $N(l)$, one finds $\tilde{N}(\tilde{l}^2, l, \varepsilon)$. This leads to a small set of integrals, all of which can be found in [29]. The integrals range from 2- to 4-point and consist of two types: finite integrals with powers of $\tilde{l}^2$ in the numerator and UV-divergent integrals. Of the latter type one needs the pole part, which may give a rational part upon cancellation with terms $\mathcal{O}(\varepsilon)$ from the numerator.

Let us consider a small example: the fermion self-energy in QED. Its superficial degree of divergence is 1 and therefor contributes to $\mathcal{R}_2$. For this example $n = 2$, $\bar{D}_0 = \bar{l}^2$, $\bar{D}_1 = (\bar{l} + p)^2 - m^2$ and the numerator reads

$$\bar{N}(\bar{l}) = -e^2 \, \bar{\gamma}_\mu \, (\bar{\not{l}} + \not{p} + m) \, \bar{\gamma}^\mu \,. \tag{4.55}$$

Applying (4.34)-(4.38), making use of

$$\gamma_\mu \, (\dots) \, \tilde{\gamma}^\mu = 0, \qquad \gamma_\mu \gamma^\mu = 4, \qquad \tilde{\gamma}_\mu \tilde{\gamma}^\mu = \varepsilon \,, \tag{4.56}$$

and dropping terms linear in $\tilde{\not{l}}$ since those vanish upon integration, we find

$$\bar{N}(\bar{l}) = N(l) + \varepsilon \; e^2 \, (\not{l} + \not{p} - m) \,. \tag{4.57}$$

The second term is precisely the function $\tilde{N}(\tilde{l}^2, l, \varepsilon) = \bar{N}(\bar{l}) - N(l)$ according to the splitting performed in (4.39). Plugging it in the integral (4.54) allows to calculate the

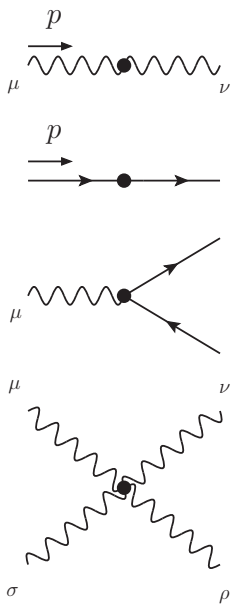

$$= -\frac{ie^2}{8\pi^2}\,\eta_{\mu\nu}(2m - p^2/3)\,,$$

$$= \frac{ie^2}{16\pi^2}(-\not{p} + 2m)\,,$$

$$= -\frac{ie^3}{8\pi^2}\gamma_\mu\,,$$

$$= \frac{ie^4}{12\pi^2}(\eta_{\mu\nu}\eta_{\rho\sigma} + \eta_{\mu\rho}\eta_{\nu\sigma} + \eta_{\mu\sigma}\eta_{\nu\rho})\,.$$

Figure 4.5.: Effective vertices in QED and their contribution to $\mathcal{R}_2$. We derived the second effective vertex in (4.58), while an explicit computation of the three-point diagram can be found in [27]. In QED the superficial degree of divergence can be computed as $D = 4 - N_\gamma - \frac{3}{2}N_e$, see [13], from which one can easily see that there are no other diagrams with $D \geq 0$.

rational part.

$$\begin{aligned}
\mathcal{R}_2 &= \int \frac{d^d\bar{l}}{(2\pi)^4} \frac{\varepsilon\, e^2\,(\not{l} + \not{p} - m)}{\bar{D}_0\bar{D}_1} \\
&= \frac{\varepsilon\, e^2}{(2\pi)^4}\Big[\gamma^\mu \underbrace{\int d^d\bar{l}\,\frac{l_\mu}{\bar{D}_0\bar{D}_1}}_{\frac{i\pi^2}{\varepsilon}\,p^\mu + \mathcal{O}(1)} + (\not{p} - m) \underbrace{\int d^d\bar{l}\,\frac{1}{\bar{D}_0\bar{D}_1}}_{-2\frac{i\pi^2}{\varepsilon} + \mathcal{O}(1)}\Big] \\
&= \frac{ie^2}{16\pi^2}(-\not{p} + 2m)\,,
\end{aligned} \tag{4.58}$$

where the two integrals from the second line can be found among the ones listed in the first appendix of [29]. Our result is in agreement with the effective vertex for a two-fermion interaction in [27]. In that paper a total of four effective vertices are listed, which suffice to determine the rational part R_2 of any QED process. We reproduce them in figure 4.5.

The $\mathcal{R}_2$ part has subsequently been calculated for the others sectors of the standard model as well. In [29] and [30] effective vertices are listed for QCD and for the electroweak sector respectively. Furthermore, in [31] the electroweak vertices were derived in the R_ξ and unitary gauge.

4.4. Application of the OPP Method

At this point we have outlined all concepts involving the OPP reduction method. Let us now apply it to a simple example to see the method in action. We decided to reduce a rank-two two-point integral in two spacetime dimensions for two reasons. First of all, the same example is worked out in [25] in a slightly different way, allowing us to compare results. The second reason is that the coefficients can be derived by hand and given in compact form, which is simply impossible for more realistic examples. We do have to start with an outline of the method in two dimensions.

Numerator Decomposition

In two dimensions any one-loop amplitude can be decomposed in terms of bubble and tadpole diagrams. This is reflected in the numerator decomposition

$$N(l) = \sum_{i<j}^{n-1} \left[\, b(ij) + \tilde{b}(l;ij) \,\right] \prod_{k\neq i,j}^{n-1} D_k + \sum_{i}^{n-1} \left[\, a(i) + \tilde{a}(l;i) \,\right] \prod_{k\neq i}^{n-1} D_k \,. \tag{4.59}$$

where $a(i)$ and $b(ij)$ are coefficients of tadpole and bubble scalar integrals respectively and n is the number of external particles of a given amplitude. The van Neerven-Vermaseren basis consists of $\{n_1, n_2\}$ for tadpoles and $\{v_1, n_2\}$ for bubbles. An explicit form of these vectors can be inferred from (4.8) and (4.9). The spurious terms depend on the loop momentum via

$$\tilde{a}(l;i) = \tilde{a}_1(i)\,((l+q_i)\cdot n_1) + \tilde{a}_2(i)\,((l+q_i)\cdot n_2)\,, \tag{4.60}$$

$$\tilde{b}(l;ij) = \tilde{b}_1(ij)\,((l+q_i)\cdot n_2)\,. \tag{4.61}$$

Of course, the same can be derived by making a Passarino-Veltman decomposition of a rank-three three-point function, just like we did in four dimensions.

As an illustration we shall now calculate a non-scalar two-point integral by computing its coefficients in terms of a scalar integral basis. That is,

$$\int \frac{d^2l}{(2\pi)^2} \frac{N(l)}{D_0\, D_1} = \int \frac{d^2l}{(2\pi)^2} \frac{b(01)}{D_0 D_1} + \int \frac{d^2l}{(2\pi)^2} \frac{a(0)}{D_1} + \int \frac{d^2l}{(2\pi)^2} \frac{a(1)}{D_0} + \mathcal{R}_1\,, \tag{4.62}$$

for $N(l) = (l\cdot n_2)^2$. The bubble coefficient $b(01)$ and the tadpole coefficients $a(i)$ are to be determined by evaluating the numerator decomposition

$$\begin{aligned}(l\cdot n_2)^2 = {} & \left[\, b(01) + \tilde{b}_1(01)\,((l+q_0)\cdot n_2) \,\right] \\ & + \left[\, a(0) + \tilde{a}_1(0)\,((l+q_0)\cdot n_1) + \tilde{a}_2(0)\,((l+q_0)\cdot n_2) \,\right] D_1 \\ & + \left[\, a(1) + \tilde{a}_1(1)\,((l+q_1)\cdot n_1) + \tilde{a}_2(1)\,((l+q_1)\cdot n_2) \,\right] D_0\,,\end{aligned} \tag{4.63}$$

at different loop momenta. The rational part $\mathcal{R}_1$ shall be explicitly found by shifting the masses, as was explained in the general four dimensional case. The rational part $\mathcal{R}_2$ is absent in $d = 2$ dimensions.

Bubble Coefficients

Let us first define some convenient variables

$$\begin{aligned} k_0 &= q_0 - q_1\,, \qquad & r_0 &= k_0^2 - m_0^2 + m_1^2\,, \\ k_1 &= q_1 - q_0\,, \qquad & r_1 &= k_1^2 - m_1^2 + m_0^2\,. \end{aligned} \tag{4.64}$$

and basis vectors

$$v_1^\mu = \frac{k_1^\mu}{k_1^2}\,, \qquad n_1^\mu = \frac{k_1^\mu}{\sqrt{k_1^2}}\,, \qquad n_2 \cdot k_1 = 0\,. \tag{4.65}$$

The loop momentum parametrization for a two-point integral, solving $D_0 = D_1 = 0$, is

$$l_\pm^\mu = -q_0 - w^\mu \pm \sqrt{m_0^2 - w^2}\, n_2^\mu\,, \qquad w^\mu = \frac{r_1}{2} v_1^\mu = \frac{r_1}{2k_1^2} k_1^\mu\,, \tag{4.66}$$

which is the two-dimensional analog of (4.29). The master formula (4.63), evaluated at these solutions, reads

$$\left(-q_0 \cdot n_2 \pm \sqrt{m_0^2 - w^2}\right)^2 = b(01) \pm \tilde{b}_1(01)\sqrt{m_0^2 - w^2}\,. \tag{4.67}$$

Setting $q_0 = 0$, it immediately follows that

$$\begin{aligned} b(01) &= m_0^2 - w^2 = m_0^2 - \frac{r_1^2}{4q_1^2}\,, \\ \tilde{b}_1(01) &= 0\,. \end{aligned} \tag{4.68}$$

Tadpole Coefficients

The loop momentum parametrization for a one-point integral, solving $D_0 = 0$ and $D_1 = 0$ respectively, are

$$l_{0,\phi}^\mu = -q_0 + m_0\left(\cos\phi\, n_1^\mu + \sin\phi\, n_2^\mu\right), \tag{4.69}$$

$$l_{1,\phi}^\mu = -q_1 + m_1\left(\cos\phi\, n_1^\mu + \sin\phi\, n_2^\mu\right), \tag{4.70}$$

for $\phi \in [0, 2\pi)$. Evaluating the master formula at solutions (4.69) and (4.70) respectively, we find

$$\begin{aligned}(-q_0 \cdot n_2 + m_0 \sin\phi)^2 - (b(01) + \tilde{b}_1(01)\, m_0 \sin\phi) \\ = (a(0) + \tilde{a}_1(0)\, m_0 \cos\phi + \tilde{a}_2(0)\, m_0 \sin\phi)\ (r_1 + 2m_0|k_1|\cos\phi)\ , \qquad (4.71)\\ (-q_1 \cdot n_2 + m_1 \sin\phi)^2 - (b(01) + \tilde{b}_1(01)\, m_1 \sin\phi) \\ = (a(1) + \tilde{a}_1(1)\, m_1 \cos\phi + \tilde{a}_2(1)\, m_1 \sin\phi)\ (r_0 - 2m_1|k_1|\cos\phi)\ , \qquad (4.72)\end{aligned}$$

where we made use of (4.64) and (4.65) to write $k_1^\mu = |k_1| n_1^\mu = -k_0^\mu$. Now that the equations are written down, we can set $q_0 = 0$, thereby breaking the symmetry in the indices 0 and 1. Evaluating the equations at angles $\phi = 0, \pi, \pi/2$ and solving for the coefficients, we determine

$$a(0) = \frac{r_1}{4\, q_1^2}\,, \qquad \tilde{a}_1(0) = -\frac{1}{2\,|q_1|}\,, \qquad \tilde{a}_2(0) = 0\,, \qquad (4.73)$$

$$a(1) = \frac{r_0}{4\, q_1^2} + \frac{1}{2}\,, \qquad \tilde{a}_1(1) = \frac{1}{2\,|q_1|}\,, \qquad \tilde{a}_2(1) = 0\,. \qquad (4.74)$$

Rational Part

According to the observation in section 4.3, the rational part $\mathcal{R}_1$ is generated by shifting all masses $m_i^2 \to m_i^2 - \tilde{l}^2$. The variables r_j clearly remain invariant under such a shift. Therefor, only the coefficient $b(01)$ is altered

$$b(01) \to b(01) - \tilde{l}^2\,, \qquad (4.75)$$

and thus we find the following rational part

$$\mathcal{R}_1 = -\int \frac{d^{2+\varepsilon}\bar{l}}{(2\pi)^2} \frac{\tilde{l}^2}{\bar{D}_0\, \bar{D}_1}\,. \qquad (4.76)$$

The result agrees with [25], where this rational part was derived as an extra coefficient $\tilde{b}_2$ from the start.

4.5. Implementation

The OPP reduction method is currently being used in practice by several frameworks. Among them are MadGraph [32], GoSam [11] and FormCalc [33]. All mentioned frameworks make use of the libraries CutTools [9],[10] and/or Samurai [34]. The latter are the numerical implementations of the OPP method.

In these programs the reduction is performed for a specific phase space point, that is, a set numerical values for the momenta of all external particles. Also the masses of

the internal particles need to be specified numerically. It fits nicely into the frameworks, where cross-sections are calculated by evaluating the amplitude at many phase space points. This means that the reduction is to be performed many times as well, somewhat of a downside. Luckily the numerical OPP reduction can be done quite fast.

We have taken a different and unique approach, by implementing an analytic OPP reduction. By this we mean that the resulting coefficients are analytic functions of the phase space variables. The upside of this approach is that the reduction has to be performed only once, after which it is simply a matter of evaluation for every phase space point. Another use could be to compare results with other methods in cases where certain limits have been taken, internal or external massless particles for example, to simplify expressions. Unavoidably, the program does not match the speed of the numerical implementations.

4.5.1. Analytic OPP Reduction in FORM

Let us outline conceptually the working of our implementation in FORM [15], see appendix C.

As input, the program only needs a numerator and the number of denominators. It starts by generating a system of equations for the box coefficients. There are only two equations and two loop momenta, which are fixed. The loop momenta are expressed in terms of the van Neerven-Vermaseren basis, which is constructed literally as (4.8) and (4.9). The determinants are constructed from squares of Levi-Civita tensors.

The system of equations is inverted by Gaussian elimination. Upon evaluating denominators at the specified loop momenta, we use the following simplification

$$\begin{aligned} D_j(l) &= (l+q_j)^2 - m_j^2 \\ &= (l+q_0+k_j)^2 - m_j^2 \\ &= m_0^2 + 2(l+q_0)\cdot k_j + k_j^2 - m_j^2 \\ &= 2(l+q_0)\cdot k_j + r_j \,, \end{aligned} \tag{4.77}$$

in the case $D_0(l) = (l+q_0)^2 - m_0^2 = 0$. The advantage is that no terms quadratic in loop momentum are left, because the loop momentum is expressed in terms of determinants.

Large expressions occurring multiple times inside the coefficients are replaced by a dummy variable and stored away to be calculated only once. They include the 3×3 and 4×4 Gram determinants for all combinations of external vectors and the length of the loop momentum in the transverse space l_p, one for every coefficient. Also coefficients entering subtraction terms are not substituted. All this contributes to a more compact output.

The number of coefficients N, including spurious terms, the number of coefficients of scalar integrals N_0 and the number of Gram determinants as a function of the number

of external particles, are given by

$$N(n) = \frac{1}{12} n(n+4)(n^2+4n+7)\,, \tag{4.78}$$

$$N_0(n) = \frac{1}{24} n(n+1)(n^2-3n+14)\,, \tag{4.79}$$

$$N_{gram}(n) = \frac{1}{24} (n-2)(n-1)n(n+1)\,. \tag{4.80}$$

There are $N_{lp} = N$ expressions l_p. The number of expressions in the output is the sum $N_{out}(n) = N_0 + N_{gram} + N_{l_p}$, since the spurious terms are discarded.

n	5	6	7	...
N_0	30	56	98	
N_{gram}	15	35	70	
N_{l_p}	195	335	539	
N_{out}	240	426	707	

(4.81)

For the triangle coefficients and beyond, the choice in loop momentum solutions increases. In order to simplify the system of equations, we chose all angles from a set of 16 values, where both the sine and the cosine take on rational values or square roots. Other angles can be chosen, but are likely to result in more dense systems of equations.

The output of the program consists of *.mx* files, to be imported in Mathematica for numerical evaluation or further simplification. A possible extension of the program is to generate Fortran code directly from FORM. This would be useful for fast numerical evaluation of amplitudes. A new optimization algorithm in FORM, described in [35], can be particularly useful for producing optimized Fortran code.

4.5.2. Results and Comparison

In this section we describe some results obtained with the FORM program, in the context a comparison and cross-check with other tools. For a cross-check, it is sufficient to compare coefficients of scalar integrals. We have performed two independent checks: analytical and numerical. The analytical check is done by comparing our expressions to the result of explicit Passarino-Veltman reduction. For the numerical comparison we found CutTools to be a convenient source of numeric values for the coefficients. Below we give explicit results for each cross-check on specific examples.

For a comparison with Passarino-Veltman reduction, consider the following integral, as part of the calculation of a five particle interaction,

$$I := \int \frac{d^4 l}{(2\pi)^4} \frac{l \cdot q_3}{D_0 D_1 D_2 D_3 D_4} \tag{4.82}$$

Performing a Passarino-Veltman reduction, we find

$$I = \frac{r_3\, w\cdot v_4}{4\, l_p^2}\, I_{0123} + \left(\frac{1}{2} + \frac{r_3\, w\cdot v_3}{4\, l_p^2}\right) I_{0124} + \frac{r_3\, w\cdot v_2}{4\, l_p^2}\, I_{0134} + \frac{r_3\, w\cdot v_1}{4\, l_p^2}\, I_{0234} - \left(\frac{1}{2} + \frac{r_3\, \left(\sum_{i=1}^4 w\cdot v_i - 1\right)}{4\, l_p^2}\right) I_{1234}\,, \tag{4.83}$$

where

$$l_p^2 = m_0^2 - w^2\,, \quad w = \tfrac{1}{2}\sum_{i=1}^4 r_i\, v_i\,, \quad r_i = q_i^2 - m_i^2 + m_0^2\,, \tag{4.84}$$

the vector v_i as defined in (4.8) and I_{ijkl} scalar four point integrals with denominators D_i, D_j, D_k and D_l. We set $q_0 = 0$, such that $q_i = \sum_{k=1}^i p_k$ for $i = 1, \ldots, 4$, and use the notation $s_{ij} = p_i \cdot p_j$. The final result then depends on the Lorentz invariants s_{ij} and the masses m_i. Expressing the coefficients of the scalar integrals in (4.82) in terms of s_{ij} and m_i is now just a matter of plugging in the definitions. We did this both in Mathematica and in FORM. The resulting expressions are rather lengthy. All coefficients considered, they contain some 4000 terms in expanded form.

We reduced the same integral (4.82) with our program in FORM. After importing the resulting expression in Mathematica, we verified equality with the expressions obtained by Passarino-Veltman reduction. The number of terms in the expressions from the OPP method is less by a factor of five, to about 700 terms, although individual terms may be larger. This translates in a smaller amount of space on disk by a factor of one-and-a-half, which is of around half a megabyte.

We also performed a numerical check with CutTools on this example. To print the coefficients in CutTools one may use the built in function *compare*. We took particles 1 and 5 to be the two incoming particles with center-of-mass energy $\sqrt{s} = 50$. The internal particles are taken massless and the external momenta

	E	p_x	p_y	p_z
p_1	25.00000000	0.00000000	0.00000000	25.00000000
p_2	−18.23423491	−15.36129843	9.32018623	0.80744155
p_3	−20.36903044	17.69218361	−3.65694432	8.80402171
p_4	−11.39673465	−2.33088518	−5.66324191	−9.61146326
p_5	25.00000000	0.00000000	0.00000000	−25.00000000

Furthermore, required input parameters are

```
rootsvalue= 50.d0
limitvalue= 1.d-2
imode   = 1
scaloop= 2
muscale= 1.d0
number_propagators= 5
```

In particular, we worked in double precision. The numerical results are

d_i	CutTools	OPP in FORM & PV in Mathematica
d_{15}	0.46959773883379685	0.46959775485191596
d_{23}	0.023234675629249163	0.023234669780819872
d_{27}	−0.0258788553625436402	−0.0258788524067555596
d_{29}	0.21717873263754892	0.21717875246313239
d_{30}	−0.7190150390949543	−0.7190150686845623

The coefficients d_i correspond to the prefactors of the scalar integrals in (4.83) in order of appearance. These indices are binomial notations for the sets of indices on the scalar integrals, e.g. $15 = 2^0 + 2^1 + 2^2 + 2^3$. Agreement is to within 10^{-7} in the worst case. The results of the OPP method in FORM and the Passarino-Veltman procedure in Mathematica returned the same values. Considering the PV reduction to give the correct answer, we conclude that the tiny differences observed are attributable to the precision in CutTools.

This is a good point to illustrate one of the possibilities of the FORM program, namely to generate analytical manageable solutions in simplifying limits. For example, in the special case $m_i = 0$ and $s_{jj} = 0$, we find

$$d_{15} = -\frac{\Sigma(-s_{14}s_{23} + s_{12}s_{34} + s_{13}(s_{24} + 2s_{34}))}{s_{34}\,\Delta}\,, \tag{4.85}$$

$$\begin{aligned} d_{23} = -\frac{1}{s_{23}s_{34}\Delta}\Big\{&\Sigma(s_{23} + s_{24})(s_{14}s_{23} - s_{13}s_{24}) + (s_{12}(s_{12} + s_{13}) - (s_{12} + 2s_{13})s_{23})s_{34}^2 \\ &- s_{23}s_{34}\left((s_{12} + s_{13})(s_{12} + 2s_{13} + s_{14}) + (s_{12} + 2s_{13} - s_{14})s_{23}\right) \\ &+ s_{24}s_{34}\left(-s_{12}^2 + s_{12}s_{23} + s_{13}(s_{13} + 3s_{23})\right)\Big\}\,, \end{aligned} \tag{4.86}$$

$$d_{27} = \frac{\Sigma(s_{14}s_{23} - s_{13}s_{24} + s_{12}s_{34})}{4s_{12}s_{23}s_{34}}\,, \tag{4.87}$$

$$\begin{aligned} d_{29} = -\frac{\Sigma}{4s_{12}s_{23}\,\Delta}\Big\{&-(s_{13} + s_{23})(-s_{14}s_{23} + s_{13}s_{24}) + s_{12}^2 s_{34} \\ &- s_{12}(s_{13}(s_{24} - s_{34}) + s_{23}(s_{14} + 2s_{24} + s_{34}))\Big\}\,, \end{aligned} \tag{4.88}$$

$$\begin{aligned} d_{30} = -\frac{1}{4s_{12}\Delta}\Big\{&(s_{13} + s_{23})(-s_{14}s_{23} + s_{13}s_{24}) + s_{12}^2(4s_{24} + 3s_{34}) \\ &+ s_{12}(-3s_{14}s_{23} + 5s_{13}s_{24} + 2s_{23}s_{24} + 3s_{13}s_{34} + s_{23}s_{34})\Big\}\,, \end{aligned} \tag{4.89}$$

with

$$\Delta = 4(-s_{14}s_{23} + (s_{12} + s_{13})(s_{24} + s_{34}))\,, \tag{4.90}$$

$$\Sigma = s_{12} + s_{13} + s_{23}\,. \tag{4.91}$$

A more difficult example is a rank-five integral like

$$\int \frac{d^4l}{(2\pi)^4} \frac{(l \cdot q_3)^5}{D_0 D_1 D_2 D_3 D_4} \tag{4.92}$$

This time not only box coefficients, but all types up to tadpoles are to be expected. For the bubble coefficients the author of CutTools implemented a different basis with random vectors [10]. We were therefor able to compare the box and triangle coefficients only. Agreement was found for various point in the phase space of the external particles and masses of the internal particles. Here we provide one example.

	E	p_x	p_y	p_z
p_1	25.00000000	0.00000000	0.00000000	25.00000000
p_2	−18.23423491	−15.36129843	9.32018623	0.80744155
p_3	−15.04397035	10.83612431	−7.793711162	−6.415412696
p_4	−21.46515062	−12.82043324	16.97994151	−2.840909856
p_5	25.00000000	0.00000000	0.00000000	−25.00000000

and non-zero internal masses $m_0^2 = 10$, $m_1^2 = 11$, $m_2^2 = 12$, $m_3^2 = 13$ and $m_4^2 = 14$.

The box coefficients are found to be

d_i	CutTools	FORM
d_{15}	28398164446.284752	28398158271.7005
d_{23}	384275484101.21271	384275410173.471
d_{27}	−116175845272.69678	−116175808930.171
d_{29}	87384507093.161591	87384482773.8572
d_{30}	−4554345610924.8574	−4554345385234.15

and the triangle coefficients evaluate to

c_i	CutTools	FORM
c_7	101087020.71750160	101087041.972901
c_{11}	$-1.809222965740\,\mathrm{E}-8$	$0.\,\mathrm{E}-52$
c_{19}	244996757.72941369	244996687.791981
c_{13}	$-1.853924040363\,\mathrm{E}-9$	$0.\,\mathrm{E}-51$
c_{21}	−173982902.35910583	−173982848.526287
c_{25}	$1.479409697457\,\mathrm{E}-8$	$0.\,\mathrm{E}-53$
c_{14}	2209468998.9249873	2209468923.02725
c_{22}	−1818576875.8090043	−1818577215.35574
c_{26}	−9790815599.0937653	−9790814257.97054
c_{28}	6977762690.0108042	6977761728.61022

There is agreement up to at least the first six digits. Any differences beyond that are attributed to the precision of CutTools, as pointed out in the previous example. The negligible imaginary parts of all coefficients were omitted in these tables.

Chapter 5.

Eikonal Approximation and Unitarity

An interesting approximation for scattering amplitudes in QCD is to take gluons soft. This is called the eikonal approximation. We describe effective Feynman rules in this approximation and present their application to a one-loop diagram. Next, we investigate how ideas from previous chapters, in particular unitarity, may be used in conjunction with eikonal approximation. The result is an alternative method to compute the imaginary part of a diagram, as demonstrated in the final section.

5.1. Eikonal Propagator

Consider a single massless quark emanating from a hard scattering process $i\mathcal{M}_0$ and assume that this quark emits a soft gluon. Such a process is depicted in figure 5.1. The assumption that the gluon is soft leads to factorization of the hard and soft parts of this process, as we shall demonstrate below. The soft part then forms an *eikonal propagator* for the quark.

We start with the standard expression

$$i\mathcal{M}^{\mu,a} = \bar{u}(p)\,(igt^a\gamma^\mu)\,\frac{i(\not{p}+\not{k})}{(p+k)^2+i\,\varepsilon}i\mathcal{M}_0\,. \tag{5.1}$$

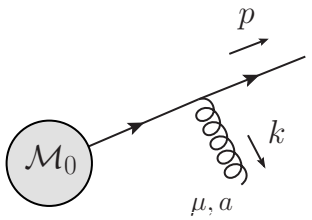

Figure 5.1.: Process under consideration in the derivation of the eikonal propagator: a final state quark that emits a soft gluon after leaving a hard scattering process $\mathcal{M}_0$.

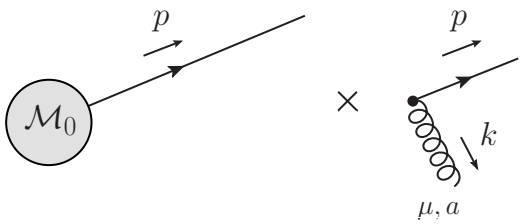

Figure 5.2.: Graphic representation of the factorization between the hard part (left) and the soft part (right) of the process in figure 5.1. The factorization is given in (5.3).

Both sides are to be contracted with $\varepsilon^*_\mu(k)$. A soft gluon has $k^\mu \to 0$, which means that we can neglect k with respect to p. Using also the fact that the quark is massless, $p^2 = 0$,

$$\frac{i(\not{p} + \not{k})}{(p+k)^2 + i\,\varepsilon} \to \frac{i\not{p}}{2p \cdot k + i\,\varepsilon}\,. \tag{5.2}$$

Now there is only a $\not{p}$ in the numerator, which we can anticommute with the gamma matrix, $\gamma^\mu \not{p} = 2p^\mu - \not{p}\gamma^\mu$. According to the Dirac equation, $\bar{u}(p)\not{p} = 0$, the second term vanishes. The first term is proportional to the identity in spinor space, so it can be pulled through the spinor. We are left with

$$i\mathcal{M}^{\mu,a} = \left(\frac{-g\,t^a p^\mu}{p \cdot k + i\,\varepsilon}\right) \bar{u}(p) i\mathcal{M}_0\,. \tag{5.3}$$

Indeed, the hard process, contained in $i\mathcal{M}_0$, factorizes from the part that describes the emission of the soft gluon. Graphically this factorization can be displayed as in figure 5.2.

There are a few remarks to be made on the above result. The factor in parenthesis in (5.3) is what we call an eikonal propagator. Notice that it is invariant under rescalings of the quark momentum p^μ and hence independent of the quarks' energy. Essentially one is neglecting the recoil of the quark from the emission of a soft gluon.

The derivation of the form $p^\mu/(p \cdot k + i\varepsilon)$ concerns an outgoing fermion and outgoing gluon. The same expression holds as long as both momenta point either away from or towards the vertex; otherwise it becomes $p^\mu/(-p \cdot k + i\varepsilon)$. In case of antifermions nothing changes. Actually for scalar particles the eikonal propagator has the very same momentum dependence. This reflects the fact that due to its infinite Compton wavelength, the gluon cannot resolve the spin of the emitting particle.

The process can be generalized by considering the emission of n soft gluons instead of one. Again the soft and hard parts are seen to factorize in the eikonal approximation [36]. This forms the basis for the derivation of *eikonal exponentiation*, a theorem stating that eikonal scattering amplitudes can be expressed in exponentiated form [12]. As a consequence, any lower-order contribution to the exponent contributes to the amplitude

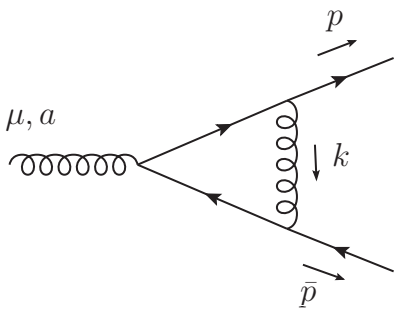

Figure 5.3.: The QCD vertex correction in eikonal approximation.

to all orders. Keeping such gain in mind, we are interested in new methods to compute one-loop contributions to the exponent.

5.2. Eikonal Vertex Correction

Our next objective is to demonstrate the use of the eikonal approximation for a one-loop QCD diagram. Consider the vertex correction in figure 5.3, where two final state quarks exchange a soft gluon. Making use of the eikonal propagator in (5.3) for the two internal quark lines, the amplitude reads

$$i\mathcal{M}^{\mu,a} = \bar{u}(p) \int \frac{d^4k}{(2\pi)^4} \frac{-g\, t^r p^\rho}{p\cdot k + i\,\varepsilon} (ig\, t^a \gamma^\mu) \frac{-g\, t^s \bar{p}^\sigma}{-\bar{p}\cdot k + i\,\varepsilon} \frac{-ig_{\rho\sigma}\delta_{rs}}{k^2 + i\,\varepsilon} v(\bar{p})\,. \tag{5.4}$$

Notice the minus sign in the denominator of the second eikonal propagator, in accordance with the discussion following (5.3). The spinor structure of the amplitude without gluon factorizes just as before. In color space we observe another factorization, owing to the standard relation $t^b t^a t^b = [C_2(r) - \frac{1}{2} C_2(G)]\, t^a$. Abbreviating this prefactor by C, we have

$$i\mathcal{M}^{\mu,a} = i\mathcal{M}_0^{\mu,a} C \int \frac{d^4k}{(2\pi)^4} \frac{gp^\rho}{p\cdot k + i\,\varepsilon} \frac{g\bar{p}^\sigma}{-\bar{p}\cdot k + i\,\varepsilon} \frac{-ig_{\rho\sigma}}{k^2 + i\,\varepsilon}\,, \tag{5.5}$$

with $i\mathcal{M}_0^{\mu,a} = \bar{u}(p)(ig\, t^a\gamma^\mu)v(\bar{p})$.

We apply a Sudakov parametrization for the soft gluon momentum, that is, we let $k^\mu = \alpha p^\mu + \beta \bar{p}^\mu + q^\mu$. Here q^μ is a spacelike vector with two degrees of freedom satisfying $p\cdot q = \bar{p}\cdot q = 0$ and $q^2 = -k_\perp^2$ by definition. A change of variables and subsequent trivial integration over the single angle dependence of q^μ yields

$$i\mathcal{M}^{\mu,a} = i\mathcal{M}_0^{\mu,a} C \frac{\alpha_s}{(2\pi)^2} \int_0^\infty dk_\perp^2 \int_{-\infty}^\infty d\alpha \int_{-\infty}^\infty d\beta\, f(\alpha,\beta)\,, \tag{5.6}$$

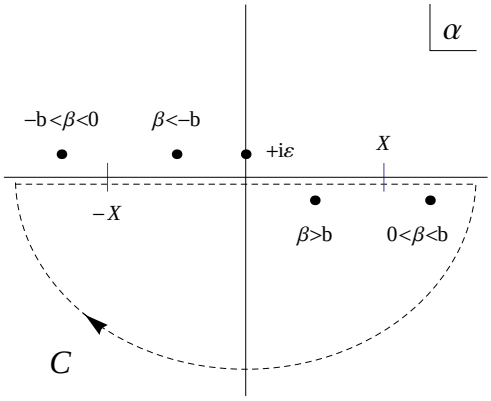

Figure 5.4.: The complex contour used in the α integration for the cases $\beta > b$ and $\beta < -b$. There is a fixed pole at $\alpha = i\,\varepsilon$ and a β-dependent pole at $\alpha = (k_\perp^2 - i\,\varepsilon)/\beta s$. The latter pole is given for different ranges of β.

which is expressed in terms of the standard variables $s = (p + \bar{p})^2 = 2p \cdot \bar{p} > 0$ and $\alpha_s = g^2/4\pi$, and we defined

$$f(\alpha, \beta) = \frac{-i}{(\beta + i\,\varepsilon)(-\alpha + i\,\varepsilon)(\alpha\beta s - k_\perp^2 + i\,\varepsilon)}\,. \tag{5.7}$$

We suppress the dependence of f on $k_\perp$ because the integration over the transverse gluon momentum is kept in the final result. So what is left to be computed are the integrals of $f(\alpha, \beta)$ over α and β.

We start with the α integration. As a function of the complex variable α, $f(\alpha, \beta)$ has two poles in the complex plane: at $+i\,\varepsilon$ and at $(k_\perp^2 - i\,\varepsilon)/\beta s$. Note that the position of the latter pole depends on the value of β. In particular it makes a jump between the second and fourth quadrant, see figure 5.4.

In order to treat things carefully, we limit the α integration to $\pm X$. Now the second pole can be outside the range of the α integral, which happens for $|\beta| < k_\perp^2/Xs$. Hence we split the β integration

$$\int_{-\infty}^{\infty} d\alpha \int_{-\infty}^{\infty} d\beta\, f(\alpha, \beta) = \lim_{X\to\infty} \int_{-X}^{X} d\alpha \left(\int_{-\infty}^{-b} d\beta + \int_{-b}^{b} d\beta + \int_{b}^{\infty} d\beta \right) f(\alpha, \beta)\,, \tag{5.8}$$

where $b = b(X) = k_\perp^2/Xs$. In the following we treat the three ranges for β separately.

Case $\beta > b$

We use the contour in figure 5.4 and subtract contributions from the semicircle SC and the pieces from $\pm X$ to infinity. Using the residue theorem, the contour integral picks up the pole at $(k_\perp^2 - i\,\varepsilon)/\beta s$. The contribution from the semicircle vanishes. For the last

two α integrals we can drop all $i\,\varepsilon$'s inside $f(\alpha,\beta)$ since there are no poles nearby.

$$\begin{aligned}
&\lim_{X\to\infty}\int_b^\infty d\beta\int_{-X}^{X} d\alpha\, f(\alpha,\beta)\\
=\;&\lim_{X\to\infty}\int_b^\infty d\beta\left(\oint_C d\alpha-\int_{SC} d\alpha-\int_{-\infty}^{-X} d\alpha-\int_X^\infty d\alpha\right) f(\alpha,\beta)\\
=\;&\lim_{X\to\infty}\int_b^\infty d\beta\,\frac{1}{\beta\,k_\perp^2}\left(2\pi+i\ln(1-\frac{b}{\beta})-i\ln(1+\frac{b}{\beta})\right)\\
=\;&\lim_{X\to\infty}\frac{1}{k_\perp^2}\left(2\pi\int_{-\infty}^{\ln(\sqrt{s/k_\perp^2}X)} dy\;-i\,\mathrm{Li}_2(1)+i\,\mathrm{Li}_2(-1)\right)\\
=\;&\frac{2\pi}{k_\perp^2}\left(\int_{-\infty}^{\infty} dy-i\frac{\pi}{8}\right)\,.
\end{aligned}\tag{5.9}$$

The second to last equality needs a bit more explanation. The first term was rewritten into a rapidity integral, $y=\frac{1}{2}\ln\frac{\alpha}{\beta}=\ln\frac{k_\perp}{\beta\sqrt{s}}$. The last two terms turned into the defining integral representation of the dilogarithm upon substitution $\gamma=\pm\frac{b}{\beta}$. See (A.31) and (A.32) for details on the dilogarithm.

Case $\beta<-b$

Use the contour in figure 5.4 again. This time both poles are above the real axis. That means no poles are inside the contour and the closed contour integral gives zero. The consequence is that there will be no rapidity integral as in the previous case. The integrations from $\pm X$ to infinity become the same as before upon $\beta\to-\beta$. Hence

$$\lim_{X\to\infty}\int_{-\infty}^{-b} d\beta\int_{-X}^{X} d\alpha\, f(\alpha,\beta)=\frac{2\pi}{k_\perp^2}\left(-i\frac{\pi}{8}\right)\,.\tag{5.10}$$

Case $-b < \beta < b$
Only the $+i\varepsilon$ pole is close to the path of integration. Symmetrize in α.

$$\begin{aligned}
&\lim_{X\to\infty}\int_{-b}^{b} d\beta \int_{-X}^{X} d\alpha\, f(\alpha,\beta) \\
=\;& \lim_{X\to\infty}\int_{-b}^{b} d\beta \int_{-X}^{X} d\alpha\, \tfrac{1}{2}\left[f(\alpha,\beta)+f(-\alpha,\beta)\right] \\
=\;& \lim_{X\to\infty}\int_{-b}^{b} d\beta \frac{1}{\beta+i\,\varepsilon} \int_{-X}^{X} d\alpha\, \frac{-\varepsilon\, k_\perp^2 + i\beta s\alpha^2}{(\alpha^2+\varepsilon^2)(\alpha^2\beta^2 s^2 - k_\perp^4)} \\
=\;& \lim_{X\to\infty}\int_{-b}^{b} d\beta \frac{1}{\beta+i\,\varepsilon} \int_{-X}^{X} d\alpha\, \left(\pi\delta(\alpha)\frac{-k_\perp^2}{\alpha^2\beta^2 s^2 - k_\perp^4} + \frac{i\beta s}{\alpha^2\beta^2 s^2 - k_\perp^4}\right) \\
=\;& \lim_{X\to\infty}\int_{-b}^{b} d\beta \frac{1}{\beta+i\,\varepsilon} \int_{-X}^{X} d\alpha\, \frac{1}{k_\perp^2}\left(\pi + i\ln(1-\frac{\beta}{b}) - i\ln(1+\frac{\beta}{b})\right) .
\end{aligned} \tag{5.11}$$

Doing the same for the β integral and recognizing the dilogarithm once again,

$$\lim_{X\to\infty}\int_{-b}^{b} d\beta \int_{-X}^{X} d\alpha\, f(\alpha,\beta) = \frac{2\pi}{k_\perp^2}\left(-i\frac{3\pi}{4}\right) . \tag{5.12}$$

Adding the three contributions (5.9), (5.10) and (5.12) according to (5.8) and plugging the result into (5.6), we finally have

$$i\mathcal{M}^{\mu,a} = i\mathcal{M}_0^{\mu,a} C\frac{\alpha_s}{2\pi}\int_0^\infty \frac{dk_\perp^2}{k_\perp^2}\left(\int_{-\infty}^{\infty} dy - i\pi\right) . \tag{5.13}$$

5.3. Cutkosky Rule in Eikonal Approximation

Looking back at previous section, we learn that computing one-loop corrections is rather tedious, even for a modest example and with the use of eikonal approximation. We stress that for other diagrams it is only likely to become much more challenging. Therefor we would like to investigate the possibility of a shortcut in the calculation, using the unitarity principles from chapter 3.

Let us first briefly return to the non-eikonal case. Recall that the imaginary part of a scattering amplitude can be obtained by summing all possible cuttings of a diagram. Cut propagators are put on shell according to Cutkosky's rule, see (3.15). For example, for a massless scalar

$$\frac{i}{p^2+i\,\varepsilon} \to 2\pi\,\theta(\pm p_0)\,\delta(p^2) . \tag{5.14}$$

The positive or negative energy solution is chosen such that the energy flows towards the shaded side of the cut. The rule for spin one-half particles is obtained by simply

multiplying both sides by $i\not{p}$. Therefor we can just as well consider the above rule as the backbone rule.

We are interested in an analogous rule for the eikonal propagator. Let C denote the traditional Cutkosky cutting rule and let E denote the eikonal approximation. Apply E to both sides of the cutting rule C for a propagator with momentum $p+k$. We induced a new cutting rule C' in the commuting diagram

$$\begin{array}{ccc} \dfrac{i}{(p+k)^2-m^2+i\,\varepsilon} & \xrightarrow{\;C\;} & 2\pi\,\theta(p_0+k_0)\,\delta((p+k)^2-m^2) \\ E\big\downarrow & & \big\downarrow E \\ \dfrac{i}{2p\cdot k+i\,\varepsilon} & \xrightarrow{\;C'\;} & 2\pi\,\theta(p_0)\,\delta(2p\cdot k) \end{array} \tag{5.15}$$

We define the rule C' to be the *eikonal cutting rule*.

$$\frac{i}{p\cdot k+i\,\varepsilon} \xrightarrow{\;C'\;} 2\pi\,\theta(\pm p_0)\,\delta(p\cdot k)\,. \tag{5.16}$$

Notice that the theta function depends only on the energy of the external particle! In terms of Sudakov parameters $p\cdot k=\beta\,p\cdot\bar{p}$ and $p\cdot\bar{p}>0$,

$$\frac{i}{\beta+i\,\varepsilon} \xrightarrow{\;C'\;} 2\pi\,\theta(\pm p_0)\,\delta(\beta)\,. \tag{5.17}$$

With this modification, a unitarity method for eikonal diagrams may be formulated. Besides the cutting rule there remains the complex conjugation rule. That is, everything on the shaded side of the cut is to be complex conjugated.

5.4. Eikonal Vertex Correction by Unitarity

Now that we have defined how to use unitarity in the eikonal approximation, we are set to revisit our QCD vertex example from section 5.2. From the final result (5.13) we obtain twice the imaginary part of the amplitude.

$$\begin{aligned} 2\ \mathrm{Im}\,[\mathcal{M}^{\mu,a}] &= 2\ \mathrm{Im}\left[\mathcal{M}_0^{\mu,a}C\frac{\alpha_s}{2\pi}\int_0^\infty\frac{dk_\perp^2}{k_\perp^2}\left(\int_{-\infty}^{\infty}dy-i\pi\right)\right] \\ &= \mathcal{M}_0^{\mu,a}\left(-C\,\alpha_s\int_0^\infty\frac{dk_\perp^2}{k_\perp^2}\right)\,. \end{aligned} \tag{5.18}$$

Notice that we factored out the overall i, which makes the difference between a Feynman diagram and its contribution to the scattering amplitude as usual.

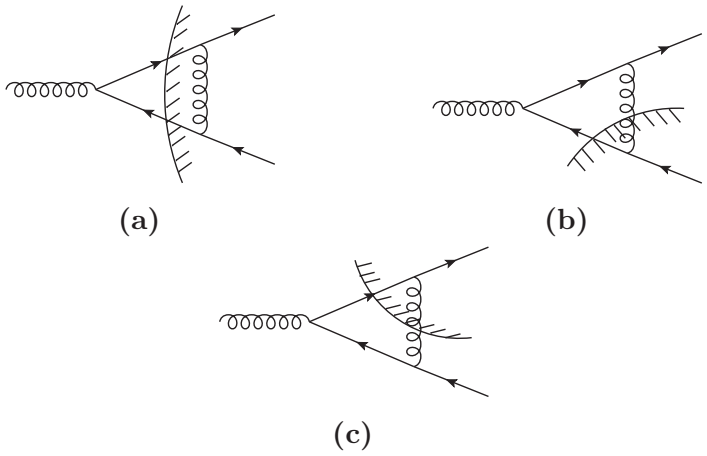

Figure 5.5.: The vertex diagram with all possible cuts. In principle there are also the cuts with the shaded side to the left, but those vanish trivially due to the energy flow from left to right.

Recall the origin of the imaginary part $-i\pi$: pieces of the contour integral around the β-dependent pole in the complex α-plane gave rise to a factor $-2i(\mathrm{Li}_2(1)-\mathrm{Li}_2(-1))/\pi = -i\pi/2$ and the double pole at $\alpha,\beta=0$ contributed another $-i\pi/2$. An indirect way to derive a relatively simple result.

We would now like to demonstrate that this imaginary part can actually be reproduced by cutting the vertex diagram, using the eikonal cutting rule C'. This should be a easier than the direct evaluation of the entire amplitude.

In order to obtain the integral over $k_\perp$ in the cut the vertex diagram we start the from Sudakov parametrized expression (5.6),

$$i\mathcal{M}^{\mu,a} = i\mathcal{M}_0^{\mu,a} C \frac{\alpha_s}{(2\pi)^2} \int_0^\infty dk_\perp^2 \int_{-\infty}^\infty d\alpha \int_{-\infty}^\infty d\beta\, f(\alpha,\beta)\,. \tag{5.19}$$

The function $f(\alpha,\beta)$, which was defined in (5.7), can be slightly rewritten as

$$f(\alpha,\beta) = \frac{i}{\beta+i\,\varepsilon}\,\frac{i}{-\alpha+i\,\varepsilon}\,\frac{i}{\alpha\beta s - k_\perp^2 + i\,\varepsilon}\,, \tag{5.20}$$

to clearly separate the three propagators in a form well suited to apply (5.17).

Consider the cut diagram in figure 5.5a. The two eikonal propagators are put on shell according to (5.17) and the gluon propagator is complex conjugated. This results in

$$f(\alpha,\beta) \xrightarrow{\text{cut } a} 2\pi\,\theta(p_0)\,\delta(\beta)\;2\pi\,\theta(\bar{p}_0)\,\delta(-\alpha)\,\left(\frac{i}{\alpha\beta s - k_\perp^2 + i\,\varepsilon}\right)^*\,. \tag{5.21}$$

The two theta functions are in fact one, because the two quarks are final state particles. Finally, the two vertices in the shaded region give an overall factor of $(-1)^2$ due to complex conjugation. With (5.21), the amplitude (5.19) becomes

$$\begin{aligned} i\mathcal{M}^{\mu,a}\big|_{\text{cut } a} &= (-1)^2\, i\mathcal{M}_0^{\mu,a} C\alpha_s \int_0^\infty dk_\perp^2 \int_{-\infty}^\infty d\alpha \int_{-\infty}^\infty d\beta\, \delta(\beta)\, \delta(-\alpha)\, \frac{-i}{\alpha\beta s - k_\perp^2 - i\,\varepsilon} \\ &= \mathcal{M}_0^{\mu,a} \left(-C\,\alpha_s \int_0^\infty \frac{dk_\perp^2}{k_\perp^2} \right) . \end{aligned} \tag{5.22}$$

Next, we look at the second cut diagram, the one in figure 5.5b. Here one eikonal propagator is cut, together with the soft gluon propagator. The gluon momentum is in the same direction as the shade on the cut, so we pick the positive energy cut.

$$f(\alpha,\beta) \xrightarrow{\text{cut } b} \frac{i}{\beta + i\,\varepsilon}\, 2\pi\, \theta(\bar{p}_0)\, \delta(-\alpha)\, 2\pi\, \theta(\alpha p_0 + \beta\bar{p}_0)\, \delta(\alpha\beta s - k_\perp^2)\,. \tag{5.23}$$

Here we used the fact that $k_0 = \alpha p_0 + \beta\bar{p}_0$. The first theta functions is trivial as before. For the single vertex in the shaded region we include a minus sign. So for (5.23), the amplitude (5.19) becomes

$$\begin{aligned} i\mathcal{M}^{\mu,a}\big|_{\text{cut } b} &= (-1)\, i\mathcal{M}_0^{\mu,a} C\alpha_s \int_0^\infty dk_\perp^2 \times \\ &\qquad \int_{-\infty}^\infty d\alpha \int_{-\infty}^\infty d\beta\, \frac{i}{\beta + i\,\varepsilon}\, \delta(-\alpha)\, \theta(\alpha p_0 + \beta\bar{p}_0)\, \delta(\alpha\beta s - k_\perp^2) \\ &= (-1)\, i\mathcal{M}_0^{\mu,a} C\alpha_s \int_0^\infty dk_\perp^2\, \delta(k_\perp^2) \int_{-\infty}^\infty d\beta\, \frac{i}{\beta + i\,\varepsilon}\, \theta(\beta\bar{p}_0) \end{aligned} \tag{5.24}$$

In the first integral we encounter the subtlety whether the delta has support inside the domain of integration. We argue that the lower bound of the integration over the squared perpendicular length of the gluon momentum, $k_\perp^2$, should strictly be 0^+. If we look back at the result of the full vertex calculation, (5.13), we see that we actually need such a lower bound in order to regularize the integral. As a consequence the first integral gives zero and we get $i\mathcal{M}^{\mu,a}|_{\text{cut } b} = 0$. An analogous computation shows that the diagram with cut c vanishes as well.

The sum of the three cut diagrams is thus equal to the expression in (5.22). Notice that it is equal to the result (5.18) for twice the imaginary part of the amplitude. In other words, we have established the cutting equation for this amplitude at order α_s:

$$2\ \text{Im}\ [\mathcal{M}^{\mu,a}] = \sum_{cut} i\mathcal{M}^{\mu,a}\big|_{cut}\,. \tag{5.25}$$

Chapter 6.

Conclusion

Theoretical high-energy particle physics aims at describing particles at the most fundamental level. In order to compare a theory with experiment, one must make definite predictions about the way particles should interact. The use of perturbation theory has enabled to make approximate predictions. Our first goal in this thesis was to review techniques for making better and better approximations. To be specific, we started by calculating one-loop diagrams in the traditional way. Several aspects have been discussed, such as dimensional regularization, Feynman parameter integration and analytic continuation. Finally we showed how to renormalize the theory of quantum-electrodynamics to all orders, by using our explicit calculations. Beyond these examples, calculations tend to become more demanding, suggesting the need for improved techniques.

Unitarity forms the heart of several such techniques. We showed how unitarity of the scattering matrix can be exploited to derive a cutting equation for Feynman diagrams, which allows easy computation of imaginary parts of diagrams. Using unitarity in conjunction with either dispersion relations or with a basis expansion for the amplitude, as in generalized unitarity, one can recover the full amplitude. Still further developments aim at bridging the gap between manual calculations and automated computer programs.

The OPP method provides the crucial step toward automated calculations. We described in detail the workings of this method and proved the basis expansion at the integrand level. In the determination of coefficients in that basis the unitarity principle pops up again, this time in the form of putting virtual particles algebraically on-shell. Particular attention was given to the rational parts of amplitude. We explained the origin of two kinds of rational part and showed how to compute them. The fact that the method works at the integrand level, such that no integration is needed whatsoever, made it suitable for numerical implementations like CutTools.

We presented a complementary program based on the same method, but performing an analytic reduction. In other words, the resulting coefficients are given in closed form in terms of the appropriate Lorentz invariants. Though very large in general, the expressions can take on manageable forms in certain points in phase space. This could provide a comparison for other analytic reduction tools. An extensive comparison with CutTools has shown excellent agreement. A possible extension of our program

includes generating Fortran code, optimized with a new FORM feature, to allow for rapid numerical evaluation.

In the final part of the thesis we discovered still another use of the unitarity principle, this time in the area of soft quantum corrections. The main result was to construct analogous cutting rules for diagrams in the eikonal approximation. We computed a vertex correction diagram in two ways and verified that the imaginary part is reproduced by the sum of all cut diagrams.

Appendix A.

Conventions and Integrals

Conventions

Natural units

$$c = \hbar = 1 \tag{A.1}$$

Fine-structure constant

$$\alpha = \frac{e^2}{4\pi} \tag{A.2}$$

Björken-Drell metric

$$\eta^{\mu\nu} = \mathrm{diag}(1, -1, -1, -1) \tag{A.3}$$

Number of spacetime dimensions

$$d = 4 - 2\,\varepsilon \tag{A.4}$$

Dirac algebra

$$\{\gamma^\mu, \gamma^\nu\} = 2\eta^{\mu\nu}\,\mathbb{1} \tag{A.5}$$

The Dirac calculus in d dimensions can be derived from (A.5), together with the choice to keep gamma matrices 4×4. This means that traces are independent of $d - 4$,

while contractions of indices do. For example [13]

$$\mathrm{tr}\,[\mathbb{1}] = 4 \tag{A.6}$$
$$\mathrm{tr}\,[\gamma^\mu] = 0 \tag{A.7}$$
$$\mathrm{tr}\,[\gamma^\mu\gamma^\nu] = 4\eta^{\mu\nu} \tag{A.8}$$
$$\mathrm{tr}\,[\gamma^\mu\gamma^\nu\gamma^\rho] = 0 \tag{A.9}$$
$$\mathrm{tr}\,[\gamma^\mu\gamma^\nu\gamma^\rho\gamma^\sigma] = 4(\eta^{\mu\nu}\eta^{\rho\sigma} - \eta^{\mu\rho}\eta^{\nu\sigma} + \eta^{\mu\sigma}\eta^{\nu\rho}) \tag{A.10}$$
$$\gamma_\mu\gamma^\mu = \eta^{\mu\nu}\eta_{\mu\nu} = \delta^\mu_\mu = d \tag{A.11}$$
$$\gamma_\mu\gamma^\rho\gamma^\mu = (2-d)\gamma^\rho \tag{A.12}$$
$$\gamma_\mu\gamma^\rho\gamma^\sigma\gamma^\mu = 4\eta^{\rho\sigma} - (4-d)\gamma^\rho\gamma^\sigma \tag{A.13}$$
$$\gamma_\mu\gamma^\rho\gamma^\sigma\gamma^\tau\gamma^\mu = -2\gamma^\tau\gamma^\sigma\gamma^\rho + (4-d)\gamma^\rho\gamma^\sigma\gamma^\tau \tag{A.14}$$

Scalar Integrals

The standard scalar integral is [13]

$$\int \frac{d^dl}{(2\pi)^d}\frac{1}{(l^2 - M^2 + i\epsilon)^k} = \frac{i(-1)^k}{(4\pi)^{d/2}}\frac{\Gamma(k-d/2)}{\Gamma(k)}(M^2)^{d/2-k} \tag{A.15}$$

with integer $k > 1$, a mass $M^2 > 0$ and $i\epsilon$ a small but positive imaginary quantity. Analytic continuation of the above result can be performed following the prescription

$$M^2 \to M^2 - i\epsilon \tag{A.16}$$

Putting $d = 4 - 2\,\varepsilon$ and introducing arbitrary reference mass μ,

$$\int \frac{d^dl}{(2\pi)^d}\frac{1}{(l^2 - M^2 + i\epsilon)^k} = \frac{i(-1)^k}{(4\pi)^k}(\mu^2)^{2-k-\varepsilon}\frac{\Gamma(k-2+\varepsilon)}{\Gamma(k)}\left(\frac{M^2}{4\pi\mu^2}\right)^{2-k-\varepsilon}. \tag{A.17}$$

In particular, we need the cases $k = 2$ and $k = 3$. Plugging in the following expansions around $\varepsilon = 0$

$$\Gamma(\varepsilon) = \frac{1}{\varepsilon} - \gamma + \mathcal{O}(\varepsilon)\,, \tag{A.18}$$
$$\Gamma(1+\varepsilon) = 1 - \gamma\,\varepsilon + \mathcal{O}(\varepsilon^2)\,, \tag{A.19}$$
$$\left(\frac{M^2}{4\pi\mu^2}\right)^{-\varepsilon} = 1 - \varepsilon\log\left(\frac{M^2}{4\pi\mu^2}\right) + \mathcal{O}(\varepsilon^2) \tag{A.20}$$

where γ is the Euler-Mascheroni constant, we find

$$\int \frac{d^dl}{(2\pi)^d}\frac{1}{(l^2-M^2+i\epsilon)^2} = \frac{i(\mu^2)^{-\varepsilon}}{(4\pi)^2}\left(\frac{1}{\varepsilon}-\gamma-\log\left(\frac{M^2}{4\pi\mu^2}\right)+\mathcal{O}(\varepsilon)\right), \quad \text{(A.21)}$$

$$\int \frac{d^dl}{(2\pi)^d}\frac{1}{(l^2-M^2+i\epsilon)^3} = \frac{-i(\mu^2)^{-1-\varepsilon}}{2(4\pi)^3}\left(\frac{M^2}{4\pi\mu^2}\right)^{-1}\times \left(1-\varepsilon\,\gamma-\varepsilon\log\left(\frac{M^2}{4\pi\mu^2}\right)+\mathcal{O}(\varepsilon^2)\right). \quad \text{(A.22)}$$

Tensor Integrals

Symmetric integration [13]

$$\int \frac{d^dl}{(2\pi)^d}\frac{l^\mu}{(l^2-M^2+i\epsilon)^k} = 0 \quad \text{(A.23)}$$

$$\int \frac{d^dl}{(2\pi)^d}\frac{l^\mu l^\nu}{(l^2-M^2+i\epsilon)^k} = \frac{\eta^{\mu\nu}}{d}\int \frac{d^dl}{(2\pi)^d}\frac{l^2}{(l^2-M^2+i\epsilon)^k} \quad \text{(A.24)}$$

Application of [14]

$$\begin{aligned} 0 &= \int \frac{d^dl}{(2\pi)^d}\frac{\partial}{\partial l_\mu}\Big(l_\mu f(l)\Big) \\ &= n\int \frac{d^dl}{(2\pi)^d}\,f(l)+\int \frac{d^dl}{(2\pi)^d}\,l_\mu\left(\frac{\partial f(l)}{\partial l_\mu}\right) \end{aligned} \quad \text{(A.25)}$$

to $f(l)=(l^2+m^2-i\epsilon)^{-k}$ leads to

$$\int \frac{d^dl}{(2\pi)^d}\frac{l^2}{(l^2-M^2+i\epsilon)^{k+1}} = \frac{d}{d-2k}\int \frac{d^dl}{(2\pi)^d}\frac{M^2}{(l^2-M^2+i\epsilon)^{k+1}} \quad \text{(A.26)}$$

Feynman Parameter Integrals

The general identity is [13]

$$\frac{1}{\prod_i D_i} = \left(\prod_i \int_0^1 dx_i\right)\frac{(n-1)!\,\delta(1-\sum_i x_i)}{(\sum_i x_i D_i)^n}, \quad \text{(A.27)}$$

where i runs from 1 to n. We use the cases $n = 1$ and $n = 2$,

$$\frac{1}{D_1 D_2} = \int_0^1 dx \frac{1}{(xD_1 + (1-x)D_2)^2} \tag{A.28}$$

$$\frac{1}{D_1 D_2 D_3} = \int_0^1 dx \int_0^{1-x} dy \frac{2}{(xD_1 + yD_2 + (1-x-y)D_3)^3} \tag{A.29}$$

In the latter integral we can exploit the symmetry of the integration domain. Let $f^{(k)}(x,y)$ be a symmetric homogeneous polynomial of degree k. That is, $f^{(k)}(x,y) = f^{(k)}(y,x)$ and $f^{(k)}(c\,x, c\,y) = c^k f^{(k)}(x,y)$. Then [37]

$$\begin{aligned} \int_0^1 dx \int_0^{1-x} dy\, f^{(k)}(x,y) &= \int_0^1 dz\, z^{1+k} \int_0^1 d(\tfrac{x}{z}) \int_0^1 d(\tfrac{y}{z})\, \delta(1 - \tfrac{x}{z} - \tfrac{y}{z}) f^{(k)}(\tfrac{x}{z}, \tfrac{y}{z}) \\ &= \int_0^1 dz\, z^{1+k} \int_0^1 dx'\, f^{(k)}(x', 1-x') \end{aligned} \tag{A.30}$$

The first equality may be shown by integrating out z on the right hand side. A divergence (typically IR) arises from the first integral when $k < -1$.

Dilogarithm

Definition of the dilogarithm for complex argument [38]

$$\mathrm{Li}_2(z) := -\int_0^z dt\, \frac{\log(1-t)}{t} \quad \text{for } z \in \mathbb{C}\backslash[1,\infty) \tag{A.31}$$

It has very few special values - as far as anyone knows there are eight - including

$$\mathrm{Li}_2(0) = 0\,, \quad \mathrm{Li}_2(1) = \frac{\pi^2}{6}\,, \quad \mathrm{Li}_2(-1) = -\frac{\pi^2}{12} \tag{A.32}$$

The dilogarithm has a branch cut for real $z > 1$. Making use of the reflection property

$$\mathrm{Li}_2(-1/z) + \mathrm{Li}_2(-z) = 2\,\mathrm{Li}_2(-1) - \tfrac{1}{2}\log^2(z) \tag{A.33}$$

we have the following analytic continuation for real $r > 1$

$$\mathrm{Li}_2(r \pm i\,\varepsilon) = -\,\mathrm{Li}_2(1/r) - \tfrac{1}{2}\log^2(r) + \frac{\pi^2}{3} \pm i\pi \log(r) \tag{A.34}$$

A particularly useful variation on (A.31) is [39]

$$\int_0^1 dx\,\frac{\log(x-a)}{x-b} = \Bigg[-\operatorname{Li}_2\left(\frac{x-a}{x-b}\right) + \frac{1}{2}\log^2(x-b) + \left[\log(x-b) - \log(x-a)\right]\log\left(\frac{a-b}{x-b}\right)\Bigg]_0^1 \tag{A.35}$$

Appendix B.

Dirac Algebra with FORM

For the Dirac algebra involved with the vertex calculation in section 2.3, we wrote the following FORM code.

```
Symbol      d;
Dimension   d;
Function    g;
Vector      P, p, l, k, sum, sigma;
Symbol      x, y, m;
Index       i, j;
Off Statistics;
#include gammaproduct.h
*           |   k = P - p
*           |
*           |                 q                     loop momentum
*          / \                l = q + x*P + y*p     after Feynman parameter trick
*     P+q /   \ p+q
*        /     \              p and k incoming
*       /~~~~~~~\             P outgoing
*    P /    q    \ p
*     /           \
Local Numerator = g( Lr, l +(1-x)*P -y*p, Um, l -x*P +(1-y)*p, Ur ) +
                  m * g( Lr, l +(1-x)*P -y*p, Um, Ur ) +
                  m * g( Lr,                  Um, l -x*P +(1-y)*p, Ur ) +
                m^2 * g( Lr,                  Um, Ur );
* Call gammaproduct procedure with contraction identities, such as
* gamma_mu  gamma^nu  gamma^mu  =  (2-d) * gamma^nu
#call gammaproduct
.sort
* Symmetric integration
id g(l) * l(Um) = 1/d * l.l * g(Um);
id g(?a,l,?b) = 0;
id l(Um) = 0;
id l.p?!{l} = 0;
.sort
* Split products of gamma matrices
repeat id g(?a, i?, j?, ?b) = g(?a, i) * g(j, ?b);
.sort
```

```
* Anticommute g(P) to left, and use Dirac equation
repeat id g(i?) * g(P) = - g(P) * g(i) + 2 * P(i);
id g(P) = m;
.sort
* Anticommute g(p) to right and use Dirac equation
repeat id g(p) * g(i?) = - g(i) * g(p) + 2 * p(i);
id g(p) = m;
.sort
* Put external fermions on mass shell
id P.P = m^2;
id P.p = m^2 - 1/2 * k^2;
id p.p = m^2;
.sort
* N^mu = C1 gamma^mu + C2 P^mu + C3 p^mu
Bracket g,P,p;
.sort
Local C1 = Numerator[g(Um)];
Local C2 = Numerator[P(Um)];
Local C3 = Numerator[p(Um)];
AntiBracket x, y, d;
Print C1, C2, C3;
.sort

C1 =
   + m^2 * ( 4 - 8*y - 2*y^2 - 8*x - 4*x*y - 2*x^2 + d*y^2 + 2*d*x*y + d*x^2 )
   + l.l * (  - 4 + 4*d^-1 + d )
   + k*k * (  - 2 + 2*y + 2*x + 2*x*y - d*x*y );
C2 =
   + m * ( 4*y + 4*x*y + 4*x^2 - 2*d*x*y - 2*d*x^2 );
C3 =
   + m * ( 4*y^2 + 4*x + 4*x*y - 2*d*y^2 - 2*d*x*y );

* N = D1 gamma^mu + D2 i sigma^munu k_nu/(2m)
Local D1 = C1 + m*(C2+C3);
Local D2 = - m*(C2+C3);
AntiBracket x, y, d;
Print D1, D2;
.end

D1 =
   + m^2 * ( 4 - 4*y + 2*y^2 - 4*x + 4*x*y + 2*x^2 - d*y^2 - 2*d*x*y - d*x^2 )
   + l.l * (  - 4 + 4*d^-1 + d )
   + k*k * (  - 2 + 2*y + 2*x + 2*x*y - d*x*y );
D2 =
   + m^2 * (  - 4*y - 4*y^2 - 4*x - 8*x*y - 4*x^2 + 2*d*y^2 + 4*d*x*y + 2*d*x^2 );

0.00 sec out of 0.00 sec
```

The procedure gammaproduct is largely based on code for gamma matrix manipulations in the FORM tutorial *FORM for Pedestrians* by André Heck.

Appendix C.

Analytic OPP Reduction in FORM

In this appendix we show the FORM program written to perform an analytic OPP reduction. Let us start by looking at the first lines of code.

```
*************************************************************************
*   Automated reduction of (n>4)-point function in four dimensions
*************************************************************************
*   Conventions
*           p3 \
*               \
*                \--------------
*                /                .
*            m2 /                  .
*   --------- / l+q2                .
*   p2        |                      |
*         m1  |  l+q1                |
*   ---------|                       |-----------
*   p1         \  l+q0     l+q{n-2} /      p{n-2}
*            m0 \                    / m{n-2}
*               \--l+q{n-1}----/
*                /   m{n-1}      \
*               /                 \
*              / p{n}              \ p{n-1}
*
*   With q0 = 0
V   l;
V   q0, ..., q10;
S   m0, ..., m10;
V   p1, ..., p10;

*************************************************************************
*   Free parameters
*************************************************************************
* Numerator in terms of momenta l and q
#$numerator = l.q3^5;
* Number of propagators in loop
#$n = 5;
```

Here we have listed our conventions and allow the user to set free parameters. After this follow some more declarations and we include a file header.h, which contains useful procedures. Then we are ready to calculation box coefficients.

```
*************************************************************************
*   BOX coefficients [d(l,ijkl)]
*************************************************************************
* Number of coefficients
#$ncoef = 2;
* Number of externel legs
#$point = 4;
#define letter "d";
* Generating sets of indices
#include codeA.h
* Loop over permutations of indices
#do p = 1, `$nperm'
* Define permutation dependent variables
#include codeB.h
* Build system of equations L = C.x
Local [c(1,`indi')] = <C11 * x1> + ... + <C1`$ncoef' * x`$ncoef'>;
#do j = 1, `$ncoef'
  Local   Z`j' = L`j' - ( <C`j'1 * x1> + ... + <C`j'`$ncoef' * x`$ncoef'> );
  Local   X`j' = x`j';
#enddo
* Specify matrix C
#do j = 1, `$ncoef'
  #$C`j'1 = 1;
  #$C`j'2 = l`j'.n4;
  #$l`j' = - q`i0' - w + lp`letter'`$bin' * ( Cos(phi`j') * n4 );
#enddo
* Specify w
#$w = 1/2 * ( r(`i1',`i0') * v1 + r(`i2',`i0') * v2 + r(`i3',`i0') * v3);
* Specify angles phi of solutions li
#$phi1 = 0;
#$phi2 = pi;
* Solve system of equations
#include codeC.h
* Specify left hand side
#include codeD.h
* Define vectors v and n
argument pow,2;
  id v1.v1 = gram(k`i2', k`i3') * invgram(k`i1', k`i2', k`i3');
  id v2.v2 = gram(k`i1', k`i3') * invgram(k`i1', k`i2', k`i3');
  id v3.v3 = gram(k`i1', k`i2') * invgram(k`i1', k`i2', k`i3');
  id v1.v2 = (-1)^(1+2) * del(k`i2', k`i3',   k`i1', k`i3') * invgram(k`i1', k`i2', k
      `i3');
  id v1.v3 = (-1)^(1+3) * del(k`i2', k`i3',   k`i1', k`i2') * invgram(k`i1', k`i2', k
      `i3');
  id v2.v3 = (-1)^(2+3) * del(k`i1', k`i3',   k`i1', k`i2') * invgram(k`i1', k`i2', k
      `i3');
  id v1.vec? = del(vec  , k`i2', k`i3',   k`i1', k`i2', k`i3') * invgram(k`i1', k`i2
      ', k`i3');
  id v2.vec? = del(k`i1', vec  , k`i3',   k`i1', k`i2', k`i3') * invgram(k`i1', k`i2
      ', k`i3');
```

```
  id v3.vec? = del(k`i1', k`i2', vec   ,   k`i1', k`i2', k`i3') * invgram(k`i1', k`i2
      ', k`i3');
  id n4.vec? = del(k`i1', k`i2', k`i3', vec   ,   k`i1', k`i2', k`i3', k`i4')
             * pow(-1/2, gram(k`i1', k`i2', k`i3', k`i4') )
             * pow(-1/2, gram(k`i1', k`i2', k`i3') );
endargument;
.sort
* Simplify solutions
#include codeE.h
* Store coefficients
#include codeF.h
* Ending loop over permutations of indices
#enddo
.sort
```

We deferred code that is being used multiple times (for solving the lower point coefficients as well) as much as possible to external files. They are typically denoted by code*.h. One of the most important procedures that is used above, is the one that solves the system of equations.

```
#procedure solveEqns(ncoef)
* Solves system of `ncoef' equations L = C.x for x
B x1, ..., x`ncoef';
.sort
* Solve for x
#do i = 1,`ncoef'
  #$x`i' = FirstBracket_(Z`i');
  #$c`i' = Z`i'[`$x`i''];
  #message $c`i' = `$c`i''
  #$rhs = `$x`i'' - Z`i'/(`$c`i'');
  id `$x`i'' = $rhs;
  #message Solving for `$x`i''
  id Sqrt(sym1?) / Sqrt(sym1?) = 1;
  B x1, ..., x`ncoef';
  .sort
#enddo
* Check that Z1, ..., Z`ncoef' are indeed zero
#do i = 1,`ncoef'
  #$test`i' = Z`i';
  #if(`$test`i'' != 0)
    #message Z`i' != 0, system of eqns is not solved properly
    .end
  #endif
#enddo
#message System of equations succesfully solved
Drop Z1, ..., Z`ncoef';
.sort
#endprocedure
```

Another important part involves calculations with the van Neerven-Vermaseren vectors.

```
* Write gram, invgram and del in terms of Levi-Civita
argument pow,2;
```

```
  argument pow,2;
    id gram(?a) = e_(?a)^2;
  endargument;
  id del(vec1?,       vec2?) = pow(1, e_(vec1           ) * e_(vec2           ) );
  id del(vec1?, ..., vec4?) = pow(1, e_(vec1,       vec2) * e_(vec3,       vec4) );
  id del(vec1?, ..., vec6?) = pow(1, e_(vec1, ..., vec3) * e_(vec4, ..., vec6) );
  id del(vec1?, ..., vec8?) = pow(1, e_(vec1, ..., vec4) * e_(vec5, ..., vec8) );
  id gram(?a) = pow(1, e_(?a)^2);
  id invgram(?a) = pow(-1, e_(?a)^2);
  repeat;
    id pow(sym1?, e_(?a)*e_(?b)) * pow(sym2?, e_(?a)*e_(?b)) = pow(sym1 + sym2, e_(?a
        )*e_(?b));
  endrepeat;
endargument;
.sort

(...)

* Contracting Levi-Civita
if( expression( [c(l,'indi')] ) != 1 );
  argument pow,2;
  argument pow,2;
    contract;
  endargument;
    contract;
  endargument;
endif;
.sort
```

At this stage all box coefficients have been computed and stored in .mx files, using

```
Format mathematica;
* Store coefficients
#do j = 1, `$ncoef'
  #write <`outputfolder'`letter'coeff`j'_`$bin'.mx> "`letter'coeff[{`j'-1},`$bin'] =
      %E", X`j'
  #message Wrote `outputfolder'`letter'coeff`j'_`$bin'.mx
#enddo
* Store lp
#write <`outputfolder'lp`letter'`$bin'.mx> "lp`letter'`$bin' = %E", [lp`letter'`$bin
    ']
#message Wrote `outputfolder'lp`letter'`$bin'.mx
.sort
```

For the triangle coefficients there are a couple of changes. First of all, the system of equations is larger; we have to pick seven angles. More importantly, we need to subtract the box coefficients from the numerator. How this works is shown below.

```
*************************************************************************
*   TRIANGLE coefficients [c(l,ijk)]
*************************************************************************
* Number of coefficients
#$ncoef = 7;
* Number of externel legs
```

```
#$point = 3;
#define letter "c";
* Generating sets of indices
#include codeA.h
* Loop over permutations of indices
#do p = 1, `$nperm'
*#do p = `$nperm'-2, `$nperm'
* Define permutation dependent variables
#include codeB.h
* Build system of equations L = C.x
Local [c(1,`indi')] = <C11 * x1> + ... + <C1`$ncoef' * x`$ncoef'>;
#do j = 1, `$ncoef'
  Local   Z`j' = L`j' - ( <C`j'1 * x1> + ... + <C`j'`$ncoef' * x`$ncoef'> );
  Local   X`j' = x`j';
#enddo
* Specify matrix C
#do j = 1, `$ncoef'
  #$C`j'1 = 1;
  #$C`j'2 = l`j'.n3;
  #$C`j'3 = l`j'.n4;
  #$C`j'4 = l`j'.n3^2 - l`j'.n4^2;
  #$C`j'5 = l`j'.n3 * l`j'.n4;
  #$C`j'6 = l`j'.n3^3;
  #$C`j'7 = l`j'.n4^3;
  #$l`j' = - q`i0' - w + lp`letter'`$bin' * ( Cos(phi`j') * n3 + Sin(phi`j') * n4 );
  #message $l`j' = '$l`j''
#enddo
* Specify w
#$w = 1/2 * ( r('i1','i0') * v1 + r('i2','i0') * v2 );
* Specify angles phi of solutions li
#$phi1 = 0;
#$phi2 = 1/2*pi;
#$phi3 = pi;
#$phi4 = 3/2*pi;
#$phi5 = 1/4*pi;
#$phi6 = 3/4*pi;
#$phi7 = 5/4*pi;
* Solve system of equations
#include codeC.h
* Subtract coefficients from numerator
* > generate BOX subtraction terms
  #$Ln = 0;
  #do i = `setNR'
  #if(`i' != )
    #$Ln = `$Ln' + c(1,`indi',`i') * D(1, ..., `$n');
  #endif
  #enddo
  #message $Ln = `$Ln';
  #inside $Ln
    Symmetrize c 2,3,4,5;
    Chainout D;
    id D(0) = 1;
    repeat id c(1,?a,sym?,?b)*D(sym?) = c(1,?a,sym,?b);
    id D(sym?) = pow(1, D(sym,1));
    #do j = 1, `$npermBox'
```

```
      id c(l,`$iBox`j'') = [c(l,`$iBox`j'')];
    #enddo
  #endinside
  #message $Ln = `$Ln';
* > subtract from numerator
  id Ln(l?) = Ln(l) - (`$Ln');
  .sort
* Specify left hand side
#include codeD.h
* Define vectors v and n
argument pow,2;
  id v1.v1 = gram(k`i2') * invgram(k`i1', k`i2');
  id v2.v2 = gram(k`i1') * invgram(k`i1', k`i2');
  id v1.v2 = (-1)^(1+2) * del(k`i2',   k`i1') * invgram(k`i1', k`i2');
  id v1.vec? = del(vec  , k`i2',   k`i1', k`i2') * invgram(k`i1', k`i2');
  id v2.vec? = del(k`i1', vec  ,   k`i1', k`i2') * invgram(k`i1', k`i2');
  id n3.vec? = del(k`i1', k`i2', vec  ,   k`i1', k`i2', k`i3')
             * pow(-1/2, gram(k`i1', k`i2', k`i3') )
             * pow(-1/2, gram(k`i1', k`i2') );
  id n4.vec? = del(k`i1', k`i2', k`i3', vec  ,   k`i1', k`i2', k`i3', k`i4')
             * pow(-1/2, gram(k`i1', k`i2', k`i3', k`i4') )
             * pow(-1/2, gram(k`i1', k`i2', k`i3') );
  id v1 = del(k`i2',  k`i2') * invgram(k`i1', k`i2') * k`i1' - del(k`i2', k`i1') *
      invgram(k`i1', k`i2') * k`i2';
  id v2 = del(k`i1',  k`i1') * invgram(k`i1', k`i2') * k`i2' - del(k`i1', k`i2') *
      invgram(k`i1', k`i2') * k`i1';
  id n3 = del(k`i1', k`i2',  k`i1', k`i2') * pow(-1/2, gram(k`i1', k`i2', k`i3') ) *
      pow(-1/2, gram(k`i1', k`i2') ) * k`i3'
        - del(k`i1', k`i2',  k`i1', k`i3') * pow(-1/2, gram(k`i1', k`i2', k`i3') ) *
            pow(-1/2, gram(k`i1', k`i2') ) * k`i2'
        + del(k`i1', k`i2',  k`i2', k`i3') * pow(-1/2, gram(k`i1', k`i2', k`i3') ) *
            pow(-1/2, gram(k`i1', k`i2') ) * k`i1';
  id n4 = del(k`i1', k`i2', k`i3',  k`i1', k`i2', k`i3') * pow(-1/2, gram(k`i1', k`i2
      ', k`i3', k`i4') ) * pow(-1/2, gram(k`i1', k`i2', k`i3') ) * k`i4'
        - del(k`i1', k`i2', k`i3',  k`i1', k`i2', k`i4') * pow(-1/2, gram(k`i1', k`i2
            ', k`i3', k`i4') ) * pow(-1/2, gram(k`i1', k`i2', k`i3') ) * k`i3'
        + del(k`i1', k`i2', k`i3',  k`i1', k`i3', k`i4') * pow(-1/2, gram(k`i1', k`i2
            ', k`i3', k`i4') ) * pow(-1/2, gram(k`i1', k`i2', k`i3') ) * k`i2'
        - del(k`i1', k`i2', k`i3',  k`i2', k`i3', k`i4') * pow(-1/2, gram(k`i1', k`i2
            ', k`i3', k`i4') ) * pow(-1/2, gram(k`i1', k`i2', k`i3') ) * k`i1';
endargument;
.sort
* Simplify solutions
#include codeE.h
* Store coefficients
#include codeF.h
* Ending loop over permutations of indices
#enddo
.sort
```

Notice also the difference in the van Neerven-Vermaseren vectors, with respect to the box case. In a similar fashion also the bubble and tadpole coefficients are computed. Finally we merge the *.mx* outputfiles into a few files, for importing into Mathematica.

```
*************************************************************************
*   Merge outputfiles
*************************************************************************
#system ./mergeformoutput `outputfolder' gram
#system ./mergeformoutput `outputfolder' lp
#system ./mergeformoutput `outputfolder' dcoeff
#system ./mergeformoutput `outputfolder' ccoeff
#system ./mergeformoutput `outputfolder' bcoeff
#system ./mergeformoutput `outputfolder' acoeff
.end
```

Bibliography

[1] J. Schwinger, *On quantum-electrodynamics and the magnetic moment of the electron*, *Phys. Rev.* **73** (Feb, 1948) 416–417.

[2] G. 't Hooft and M. Veltman, *Scalar One Loop Integrals*, *Nucl.Phys.* **B153** (1979) 365–401.

[3] G. Passarino and M. Veltman, *One Loop Corrections for e+ e- Annihilation Into mu+ mu- in the Weinberg Model*, *Nucl.Phys.* **B160** (1979) 151.

[4] G. 't Hooft and M. J. G. Veltman, *Diagrammar*. CERN, Geneva, 1973.

[5] J. Bjorken and S. Drell, *Relativistic quantum mechanics*. International series in pure and applied physics. McGraw-Hill, 1964.

[6] W. L. van Neerven and J. A. M. Vermaseren, *LARGE LOOP INTEGRALS*, *Phys. Lett.* **B137** (1984) 241.

[7] Z. Bern, L. J. Dixon, D. C. Dunbar and D. A. Kosower, *Fusing gauge theory tree amplitudes into loop amplitudes*, *Nucl.Phys.* **B435** (1995) 59–101 [hep-ph/9409265].

[8] Z. Bern and A. Morgan, *Massive loop amplitudes from unitarity*, *Nucl.Phys.* **B467** (1996) 479–509 [hep-ph/9511336].

[9] G. Ossola, C. G. Papadopoulos and R. Pittau, *Reducing full one-loop amplitudes to scalar integrals at the integrand level*, *Nucl.Phys.* **B763** (2007) 147–169 [hep-ph/0609007].

[10] G. Ossola, C. G. Papadopoulos and R. Pittau, *CutTools: A Program implementing the OPP reduction method to compute one-loop amplitudes*, *JHEP* **0803** (2008) 042 [0711.3596].

[11] G. Cullen, N. Greiner, G. Heinrich, G. Luisoni, P. Mastrolia *et. al.*, *Automated One-Loop Calculations with GoSam*, *Eur.Phys.J.* **C72** (2012) 1889 [1111.2034].

[12] J. Gatheral, *EXPONENTIATION OF EIKONAL CROSS-SECTIONS IN NONABELIAN GAUGE THEORIES*, *Phys.Lett.* **B133** (1983) 90.

[13] M. Peskin and D. Schroeder, *Introduction to quantum field theory*. Advanced Book Program. Addison-Wesley Pub. Co., 1995.

[14] B. de Wit and J. Smith, *Field theory in particle physics*. No. v. 1 in

North-Holland Personal Library. North-Holland, 1986.

[15] J. Kuipers, T. Ueda, J. A. M. Vermaseren and J. Vollinga, *FORM version 4.0*, *ArXiv e-prints* (Mar., 2012) [1203.6543].

[16] R. Cutkosky, *Singularities and discontinuities of Feynman amplitudes*, *J.Math.Phys.* **1** (1960) 429–433.

[17] M. Veltman, *Diagrammatica: the path to Feynman rules*. Cambridge lecture notes in physics. Cambridge University Press, 1994.

[18] R. D. L. KRONIG, *On the theory of dispersion of x-rays*, *J. Opt. Soc. Am.* **12** (Jun, 1926) 547–556.

[19] O. Yudilevich, *Calculating massive one-loop amplitudes*, Master's thesis, Utrecht University, 2009.

[20] Z. Bern, L. J. Dixon, D. C. Dunbar and D. A. Kosower, *One loop n point gauge theory amplitudes, unitarity and collinear limits*, *Nucl.Phys.* **B425** (1994) 217–260 [hep-ph/9403226].

[21] Z. Bern, L. J. Dixon and D. A. Kosower, *On-Shell Methods in Perturbative QCD*, *Annals Phys.* **322** (2007) 1587–1634 [0704.2798].

[22] R. K. Ellis and G. Zanderighi, *Scalar one-loop integrals for QCD*, *JHEP* **0802** (2008) 002 [0712.1851].

[23] F. del Aguila and R. Pittau, *Recursive numerical calculus of one-loop tensor integrals*, *JHEP* **0407** (2004) 017 [hep-ph/0404120].

[24] W. Giele and G. Zanderighi, *On the Numerical Evaluation of One-Loop Amplitudes: The Gluonic Case*, *JHEP* **0806** (2008) 038 [0805.2152].

[25] R. K. Ellis, Z. Kunszt, K. Melnikov and G. Zanderighi, *One-loop calculations in quantum field theory: from Feynman diagrams to unitarity cuts*, 1105.4319.

[26] P. Mastrolia, G. Ossola, C. Papadopoulos and R. Pittau, *Optimizing the Reduction of One-Loop Amplitudes*, *JHEP* **0806** (2008) 030 [0803.3964].

[27] G. Ossola, C. G. Papadopoulos and R. Pittau, *On the Rational Terms of the one-loop amplitudes*, *JHEP* **0805** (2008) 004 [0802.1876].

[28] T. Binoth, J. P. Guillet and G. Heinrich, *Algebraic evaluation of rational polynomials in one-loop amplitudes*, *JHEP* **0702** (2007) 013 [hep-ph/0609054].

[29] P. Draggiotis, M. Garzelli, C. Papadopoulos and R. Pittau, *Feynman Rules for the Rational Part of the QCD 1-loop amplitudes*, *JHEP* **0904** (2009) 072 [0903.0356].

[30] M. Garzelli, I. Malamos and R. Pittau, *Feynman rules for the rational part of the Electroweak 1-loop amplitudes*, *JHEP* **1001** (2010) 040 [0910.3130].

[31] M. Garzelli, I. Malamos and R. Pittau, *Feynman rules for the rational part of the*

Electroweak 1-loop amplitudes in the $R_x i$ gauge and in the Unitary gauge, *JHEP* **1101** (2011) 029 [1009.4302].

[32] J. Alwall, M. Herquet, F. Maltoni, O. Mattelaer and T. Stelzer, *MadGraph 5 : Going Beyond*, *JHEP* **1106** (2011) 128 [1106.0522].

[33] S. Agrawal, T. Hahn and E. Mirabella, *FormCalc 7*, 1112.0124.

[34] P. Mastrolia, G. Ossola, T. Reiter and F. Tramontano, *Scattering AMplitudes from Unitarity-based Reduction Algorithm at the Integrand-level*, *JHEP* **1008** (2010) 080 [1006.0710].

[35] J. Kuipers, J. A. M. Vermaseren, A. Plaat and H. J. van den Herik, *Improving multivariate Horner schemes with Monte Carlo tree search*, *ArXiv e-prints* (July, 2012) [1207.7079].

[36] E. Laenen, L. Magnea, G. Stavenga and C. D. White, *Next-to-eikonal corrections to soft gluon radiation: a diagrammatic approach*, *JHEP* **1101** (2011) 141 [1010.1860].

[37] G. Sterman, *An introduction to quantum field theory*. Cambridge University Press, 1993.

[38] L. Lewin, *Polylogarithms and associated functions*. North Holland, 1981.

[39] W. Beenakker and A. Denner, *Infrared divergent scalar box integrals with applications in the electroweak standard model*, *Nuclear Physics B* **338** (1990), no. 2 349 – 370.